1993

Balanced and unbalanced welds for angle compression members.

Sherief Sharl Shukry. Sakla
University of Windsor

BALANCED AND UNBALANCED WELDS FOR ANGLE COMPRESSION MEMBERS

by
Sherief Sharl Shukry Sakla

A Thesis
submitted to the Faculty of Graduate Studies and Research
through the Department of Civil and Environmental Engineering
in Partial Fulfillment
of the Requirements for the degree of
Master of Applied Science
at the University of Windsor

Windsor, Ontario, Canada
1992

ISBN 0-315-83072-7

I hereby declare that I am the sole author of this document.

I authorize the University of Windsor to lend this document to other institutions or individuals for the purpose of scholarly research.

Sherief Sharl Shukry Sakla

I further authorize the University of Windsor to reproduce the document by photocopying or by other means, in total or in part, at the request of other institutions or individuals for the purpose of scholarly research.

Sherief Sharl Shukry Sakla

ABSTRACT

It is common practice, in Canada, to balance fillet welds on angle members about the projection of the centroidal axis on the welded leg. Such a balanced weld causes the forces at the connection of the angle to be balanced about the centroidal axis through the distribution of the fillet welds. In some instances, however, due to certain design restrictions, there is no room to place a balanced weld and the designer is forced to use an unbalanced weld. It is not known what effect such unbalanced welds have on the compressive load carrying capacity of the angle. The Canadian Standards Association, as well as the American Specification and the British Standard, has approved this type of unbalanced connections. This approval was based on research carried out on tension members by Gibson and Wake in 1942. As a result of this research it has been assumed that the same conclusion applies to compression members. No experimental verification was done to determine the effect of such unbalanced weld connections on angle compression members.

In order to determine the effects of the weld patterns on the behaviour of angle compression members, a series of ultimate compression tests and finite element analysis were performed.

The experimental procedure consisted of applying a compressive load on two 50.8 x 50.8 x 6.35 mm (i.e. 2 x 2 x 1/4 in.) angle members connected at the ends to HSS's

with balanced and unbalanced weld patterns. Two different column heights were used which resulted in slenderness ratios that fall in the "slender" and "intermediate" range. The load was applied gradually until failure occurred in the specimen.

The effect of unbalanced welds seems to be beneficial for slender angles but has a detrimental effect on the load carrying capacity of intermediate range angles. As the weld pattern changes from balanced to an unbalanced weld, the flexibility of the angle increases. The experimental failure loads are compared with the results from a finite element model. The welded angles were also designed as beam-columns according to CAN/CSA S16.1-M89 and the results were compared with the experimental failure loads.

To My Father

ACKNOWLEDGEMENTS

The author wishes to express his sincere gratitude to his advisor Dr. Murray C. Temple, who most helpfully supervised the research for this thesis, and also for his guidance, effort, patience, and encouragement during the development of this research.

The author would also like to thank the faculty and staff of the Department of Civil and Environmental Engineering, as well as the computer consultants of the Computing Services at the University of Windsor for their assistance during the development of this research. Special thanks are also due to Mr. Frank Kiss, Mr. Dieter Liebsch, Mr. Richard Clark, and the members of the Technical Support Centre for their assistance in the preparation of the test specimens and experimental setup.

The author wishes to acknowledge the financial support provided by the Natural Sciences and Engineering Research Council of Canada.

Finally, the author is grateful to his family for their support and encouragement.

TABLE OF CONTENTS

LIST OF TABLES

LIST OF FIGURES

NOMENCLATURE

A	nominal area of the angle cross section.
b	width of the angle.
C_e	Euler's Load.
C_r	compressive resistance calculated in accordance with CAN/CSA-S16.1-M89.
E	modulus of elasticity.
e	eccentricity of the applied load in beam-column modelling.
e_u, e_v	co-ordinates of point of application of the external load with reference to the centroidal principal axes.
F_y	yield stress of steel.
I_u, I_v	moment of inertia of an angle about u and v axes, respectively.
K	effective length factor.
L	length of the angle used in the specimen.
M_u, M_v	moment produced about u and v axis, respectively, by the eccentric force in beam-column modelling.
r_u, r_v	radii of gyration about the u and v axis, respectively, for flexural buckling for the angle.
S_u, S_v	the elastic section moduli of the angle section about the u and v axis, respectively.
t	thickness of the angle.
x,y,u,v	co-ordinate axes for the individual angle.
ϕ	resistance factor in CAN/CSA-S16.1-M89.

CHAPTER 1

INTRODUCTION

1.1 General

Angle compression members are commonly used in building structures in Canada as web members in trusses and as bracing members. They are typically joined at their ends to gusset plates, webs of tees, or HSS sections which are usually sandwiched between double angles. Currently, these joints are shop welded and field bolted.

Welding is often used more than bolts in making joints between angle members and other members. Welding has become more popular recently because it is faster, cheaper and better than any other method of making joints. Welded design and construction offers the opportunity to achieve more efficient use of materials. The speed of fabrication and erection can help compress production schedules.

Welded connections save steel since for tension members no reduction in the cross-sectional area is required for holes in the members which means that the gross section is effective in carrying the load. Welds offer the best method of making rigid connections resulting in reduced member depth and weight.

In many instances, double angles are connected at the ends with welds which are unbalanced about the centroidal axis of the member. Engineers are forced to use this type of unbalanced connections in many cases because there is no room to place a balanced weld.

The Canadian Standards Association has approved this type of connection. CAN/CSA-S16.1-M89, "Limit States Design of Steel Structures" [7], Clause 21.7 states that "Except in members subject to repeated loads, disposition of fillet welds to balance the forces about the neutral axis or axes for end connections of single-angle, double-angle, or similar type of axially loaded members is not required".

A general description of what exactly a balanced weld is on an angle member may be in order here. Such a weld on an angle member is one in which the forces at the connection of the angle are balanced about the centroidal axis through the distribution of the fillet welds (Figure 1.1). In other words, when a load is applied to the member, the sum of the moments at the connection about the centroidal axis is equal to zero. An unbalanced weld therefore is one that is distributed in such a manner that the fillet weld causes an induced moment about the centroidal axis when a compressive load is applied.

1.2 Justification of The Need

In many trusses there is no need for gusset plates. The simplest type of truss construction is made of angle shapes and tees or HSS's. The top and bottom chords are made of tee's and HSS's with angle sections for diagonals, as shown in Figure 1.2. This is easy to fabricate, as no joint preparation is required, and weld because the sections lap each other and fillet welds are used. In trusses where the chords are HSS's or tees and the webs are double angles it is impossible, in some cases, to balance the welds. This is particularly true with diagonals at an angle of 45 degrees to the chords. A commonly used HSS for the chords of trusses has a wall height of 76.2 mm. When the corner radii are subtracted a flat wall height of 50 mm remains. If the angle framing into the chord at a 45 degree angle has a 55 mm leg, a balanced weld cannot be achieved (Figure 1.3). If the leg of the angle has a 65 mm width, the weld can be only deposited at the end and along one side. Thus unbalanced welds are inevitable under these circumstances but it is not known what effect such unbalanced welds have on the compressive load carrying capacity of the angle.

The Canadian Standards Association's approval of unbalanced welds is based on a paper by Gibson and Wake entitled "An Investigation of Welded Connections of Angle Tension Members" published in 1942 [9]. As a result of this research it has been assumed that the same conclusions apply to compression members, but this has not been demonstrated. Before this research the designing and detailing of welded structures with angle members was complicated by the conventional practice of connecting such members with balanced welds. Such a balanced design requires approximately twice as much weld along the heel of the angle as is placed along the toe of the angle and it is often difficult or expensive to provide space for such connections.

With the effects of these unbalanced welds unknown for angle compression members, such members cannot be properly designed until information about the effect of the different weld patterns becomes available.

1.3 Objective

Since no published research had been found on balanced welds for angle compression members, other than Gibson and Wake which was carried out on angle tension members, the objective of this thesis was to carry out an experimental investigation which would be verified through a finite element analysis to determine the effect of the balanced and unbalanced weld conditions on

1) the ultimate load carrying capacity, and

2) the load-deflection behaviour under different weld conditions.

Then, a suitable weld arrangement can be recommended for use to connect angles with compressive loads to other members.

1.4 Research Program

An experimental program was carried out. It consisted of the testing of 18 specimens, of which nine were 1900 mm long and the other nine 1000 mm in length, which can be classified as slender and of intermediate length, respectively.

A commercial finite element analysis package ABAQUS [1] was used to predict the behaviour of these columns and the buckling loads.

CHAPTER II

LITERATURE REVIEW

2.1 Previous Work

A literature survey, to determine the extent of the published research on balanced and unbalanced welds for angle compression members, revealed nothing related to this subject except a paper by Gibson and Wake entitled "An Investigation of Welded Connections for Angle Tension Members" published in 1942 [9]. In this investigation, fifty-four ultimate strength tension tests of welded connections of angles to flat plates were carried out. The specimens were designed to fail in the welds themselves. Fifteen different arrangements of welds which comprise most of the types of joints commonly used for angle connections were investigated. Eccentric single angle tests as well as double angle tests were carried out.

This research indicated that the arrangement of the welds in the connection of an angle tension member has very little effect on its behaviour at working loads. It also showed that the eccentricity normal to the plane of welds has a major effect on the behaviour of the welded angle.

The main conclusion of this research was that the strength of the common type of connections which have only one leg of the angle connected show little difference (about 3%) between balanced and unbalanced connections. The conventional theory that the working strengths of the welds connecting an angle member must be balanced about the projection of the center of gravity of the angle on the connected leg is not essential to the design of adequate connections for angle tension members.

2.2 Standards and Specifications

Before the Gibson and Wake research, the designing and detailing of welded structures with angle members was often complicated by the conventional practice of connecting such members with balanced weld.

The following paragraphs show the related clauses of the steel standards and specifications. Two steel standards, the Canadian and British standards, and one specification, the American, were studied. It can be seen that the two standards and the one specification have made use of the Gibson and Wake research.

2.2.1 Canadian Standard, CAN/CSA-S16.1-M89. "Limit States Design of Steel Structures". [7]

Clause 21.7 covers this subject and states that "Except for members subject to repeated loads, disposition of fillet welds to balance the forces about the neutral axis or axes for end connections of single-angle, double-angle, or similar types of axially loaded members is not required".

2.2.2 American Specification, AISC

"Load and Resistance Factor Design Specification for Structural Steel Buildings",1986. [2]

Clause J1.6 requires that "Groups of welds or bolts at the ends of any member which transmit axial force into that member shall be sized so that the center of gravity of the group coincides with the center of gravity of the member, unless provision is made for the eccentricity. The foregoing provision is not applicable to end connections of statically-loaded single angles, double angles and similar members".

2.2.3 British Standard, BS 5950 1985,

"Code of Practice for Design in Simple and Continuous Construction : Hot Rolled Sections", [5]

Clause 4.7.6.C states that "Angles, channels and T-sections for discontinuous members, the effect of eccentric end connections may be neglected and the strut is designed as an axially loaded member".

2.3 Comparison

In the Gibson and Wake research [9] the specimens were designed to break in the weld. In this research the connections were designed according to the Canadian Standard taking the loads as that for pin-ended columns. The members failed by buckling and the connections did not fail. Thus the ultimate behaviour of the angles could be studied under different weld conditions.

CHAPTER III

EXPERIMENTAL PROCEDURE

3.1 General

An experimental program was carried out to get data to determine the effect of balanced and unbalanced welds on the behaviour of angle compression members. The program consisted of eighteen ultimate strength tests of welded connections of angles to hollow sections. The angles were designed according to CAN/CSA-S16.1-M89, "Limit States Design of Steel Structures" [7]. In order to reduce the number of variables in this research the same size of angles, 51 x 51 x 6.35 mm (i.e. 2 x 2 x 1/4 in.), were used for all tests. Two column lengths were used in this investigation which resulted in slenderness ratios that fall in the "slender" and "intermediate" range.

For each column length, three different arrangements of weld were investigated. The arrangements where:

(1) a weld balanced about the centroid of the angle,

(2) a weld balanced about the centre of the leg, which will be referred to as an equal weld, and

(3) a weld that is unbalanced about the centroid of the angle or the leg.

An effective length factor of 1.0 was used to predict the compressive resistance of the angles according to CAN/CSA-S16.1-M89 [7]. This is a common design practice. Weld lengths were calculated based on that compressive resistance. That means the welds were designed as if the angles were pin-ended. As explained later in Section 5.3.1.1, the minimum length of fillet welds, as given by CAN/CSA-W59-M1989 [8], was not used. The weld patterns used in the specimens are shown in Figures 3.1 and 3.2.

In practical applications the gusset plates and webs of tee sections as used in truss construction offer bending restraint to single angle members. Trying to simulate this situation in the laboratory, the angle members were welded to a hollow section at their ends.

3.2 Test Specimens

Two different lengths of angle members, 1900 and 1000 mm, were used. These specimens had an L/r_z ratios of 192 and 101 which means that the two types could be classified as "slender" and as of "intermediate" length, respectively.

The typical specimens, as shown in Figures 3.3 and 3.4, consisted of two angle members welded to a HSS at the top and bottom. The compression members were 50.8 x 50.8 x 6.35 mm (i.e. 2 x 2 x 1/4 in.) angles and the HSS's were 152 x 102 x 9.5 mm (i.e. 6 x 4 x 3/8 in.). The total length of the slender specimen was 1970 mm with the compression members themselves being 1900 mm long. For the intermediate length specimens, the total length was 1050 mm with the compression members themselves being 1000 mm long.

The centroidal axis of the angles coincided with the centroidal axis of the hollow sections. Details of the specimens ends are shown in Figures 3.5 and 3.6.

The two angles of each specimen were not interconnected to each other at any point, except at the ends. In other words, two single angles were tested at the same time but the double angle arrangement was used for simplicity of loading the specimens and to minimize the effect of eccentric loading.

3.3 Preparation of Test Specimens

The angle members and the HSS blocks were prepared and cut to the proper length. The HSS blocks were then machined at both ends to ensure that all of them were identical. Then four guiding holes of 12.7 mm diameter were drilled on one side of the blocks. Exact measurements were made for the alignment of these holes because they were then used to guide the specimen into the upper and lower bases of the testing frame to ensure that the centroid of the specimen coincided with the force applied to the specimen by the jack.

All the pieces of the slender specimens were clamped together and then welded in a horizontal position to form the specimen. The welding was done by an experienced certified welder using E480XX electrodes and a temperature of AC High 145. Flux and slag were removed from all welds after welding. The ends of the welded specimen were then machined in the Technical Support Centre to ensure that both ends of the specimen were precisely parallel to each other and perpendicular to the longitudinal axis of the specimen. The machined surface can be seen in Figure 3.7. Machining the ends of the specimens after welding was a tedious and time consuming process and it took about two hours for each specimen. Therefore a different procedure was suggested for the intermediate length specimens.

For intermediate length specimens, the ends of the specimens were machined before welding and then attached to the upper and lower plates of the testing frame and held in position by clamps. The angles were then welded to them. The last procedure was closer to what happens in the practical construction of trusses. A close-up look at one end of an intermediate length specimen right after welding is shown in Figure 3.7.

3.4 Test Setup

All the tests were carried out in the Civil Engineering Structural laboratory at the University of Windsor. A testing frame was built to accommodate the test specimens of variable length. This section describes the setup and pieces of equipment used to carry out the experiments.

3.4.1 End Conditions and Fixtures

Fixed end conditions were created using a special arrangement at the base and top ends of the specimens. These specially constructed end fixtures were designed to prevent displacements and rotations about the three global axes at the ends of the specimen, the HSS section.

At the base, where the load was applied by the hydraulic hand jack, a bottom plate

304.8 x 203.2 x 25.4 mm was placed directly on and fitted to the loading jack. This bottom plate was guided by a frame so that it could move only in the vertical direction. This frame was welded to a steel plate in the concrete floor of the laboratory thus preventing any displacement in the horizontal plane. The angle sides of this frame prevented the rotation of the specimen about its longitudinal axis. To minimize the restraint in the vertical directions, the sides of frame where there was contact between the bottom plate and the frame angles were lubricated. Details of the setup at the bottom are shown in Figure 3.8.

At the top, a prefabricated bracket was used and was fastened to an existing frame at a height suitable for the specimen height. The upper plate, 203.2 x 203.2 x 25.4 mm, was screwed to the load cell which, in turn, was bolted to the top bracket. This arrangement prevented both displacements and rotations of the upper plate. Details at the top of the setup are shown in Figures 3.9 and 3.10.

Each of the upper and lower plates had four studs 12.7 mm in diameter and 25 mm long as shown in Figure 3.11. These studs were used to facilitate the alignment of the specimen and to prevent the ends of the specimens from slipping or kicking out during loading. These studs guided the specimens while being placed in between the two end plates of the test frame so that the centroidal axis of the specimen coincided with that of the applied load.

This arrangement gave complete fixity at the top end of the specimen but at the base a maximum rotation of 0.36 degrees was observed during the loading of the specimens. This rotation could not be prevented from taking place because of the small space that existed between the base plate, which fit as a cap on the loading jack, and the loading jack.

3.4.1.1 Loading Jack

At the base, the load was applied on the specimens through a hydraulic hand jack having a capacity of 267 kN (60 kips), as shown in Figure 3.8.

3.4.1.2 The Load Cell

A universal flat load cell with a 448 kN (100 kips) capacity was used for the testing of all the specimens and was placed at the top of the setup, as shown in Figure 3.10. The load cell was connected to a strain indicator.

The load cell was attached to a prefabricated bracket at the top of the column. This bracket was fastened to an existing frame at a height which would accommodate the column. Another plate, similar to the lower one, was screwed to the load cell.

3.4.1.3 Test Frame

The specimen to be tested was placed in between the upper and lower plates of the test frame. The upper bracket was used as the upper support for the specimen. The lower plate resting on the loading jack was used as the lower support. Figures 3.12 and 3.13 show the complete setup of mechanical jack, lower plate, specimen, upper plate, load cell and the top bracket. This setup was used for both the intermediate length and slender specimens.

3.4.2 Instrumentation

The most critical aspect of the experiment was to acquire sufficient data so that the behaviour of the angle compression member under balanced and unbalanced weld conditions could be accurately studied and then compared to the finite element model results.

Due to the simple buckled shape of the single angle columns, obtaining data for lateral displacements was not complicated. Four dial gauges were placed at the mid-height of the specimen at the centre of each angle leg as shown in Figures 3.14 and 3.15.

The purpose of the dial gauges was to measure the lateral deflection in the X and Y directions for each angle so that it was possible to determine the effect of balanced and unbalanced weld patterns on both the magnitude of the deflection and the position of the failure axis of each angle member.

3.5 Test Procedure

First, the specimens were measured to determine their out-of-straightness. Two steel blocks, with known dimensions, wire and calliper were used. The steel blocks were clamped at the ends of the angle leg and a wire was firmly stretched between them as shown in Figure 3.16. A calliper was then used to measure the distance between the leg of the angle and the wire at mid-height and the two quarter points of the angle. This procedure was repeated for the four legs of the two angles of each specimen. The steel block thickness was then deducted from the distance measured between the wire and the leg of the angle to give the initial out-of-straightness of the angles in both X and Y directions.

The specimen was now ready to be placed in the test frame. A small load of approximately 8 kN was applied to the specimen at the beginning to ensure that the top and lower plates were in complete contact with the ends of the specimen and to eliminate any gap between them that might exist due to the friction between the guiding studs and the holes in the end blocks of the specimen. The preload was then released to almost zero. Dial gauges were now positioned and set to zero before loading started.

The load on the specimens was applied slowly in increments of 5 kN for slender specimens and 10 kN for intermediate range specimens. This load increment was then reduced to 2 kN for slender specimens and 3 kN for intermediate length specimens after reaching 70% of the expected failure load.

In all cases, the system was allowed to reach equilibrium, the point at which the lateral displacements had stopped increasing at a given load, prior to reading the dial gauges.

In all tests, the failure point was the point where a small increment of applied load caused large displacements and the load remained at the same value. A typical test took an average of two hours to complete.

3.6 Data Reduction

3.6.1 Load

The results of the calibration tests for the flat load cell were used to convert the microstrain readings of the strain indicator into a load in kN. The calibration curve for the 448 kN load cell is plotted in Figure 3.17.

The variation in the calibration factor, within a short period of time, was found, from previous experience, to be extremely small.

3.6.2 Displacement

Only the lateral displacements of each angle in both X and Y directions were recorded and analyzed. In fact, the major displacement occurred in the X direction, perpendicular to the plane of the welded leg. The ratio between the displacements in both X and Y was used to determine the axis about which the angle buckled so that the effect of the weld pattern on the position of this axis could be determined.

The rotation of the individual angles was not considered because the torsional-flexural buckling load is much higher than the flexural buckling load for the slender and intermediate length columns. From previous studies, the rotation of the individual angles was checked and was found to be very small. The displacements versus the corresponding load were plotted for all the tested specimens.

3.6.3 Out-of-Straightness

The measured out-of-straightness was used to describe the geometry of the test specimens in the iterative-incremental procedure to predict the theoretical load-deflection curves.

The measured out-of-straightness varied from L/500 to L/1000 where L is the length of the angle member. In these tests no limits were placed on the out-of-straightness.

3.7 Ancillary Tests

3.7.1 Tension Test

Three tension tests were conducted on specimens taken from the same stock as that of test specimens in order to determine the yield stress and Young's modulus of elasticity. Three tension test specimens were prepared, each one was cut from a different length of angle. The specimens were prepared according to the ASTM Standards [3], designation :E8-89, but their dimensions were adapted to suit the dimensions of the angles and the grips of the testing machine. The thickness of the specimen was that of the angle. The dimensions of these specimens are shown in Figure 3.18.

In order to determine Young's modulus, two electric resistance strain gauges were used to determine the strain in the specimen, one on each side at the centre of the reduced section.

The tension tests were carried out in the universal testing machine. The strain was measured by a strain indicator which was connected to a switch and a balance unit. Average values of yield stress were used in the computations.

3.7.2 Calibration Test

A calibration test was carried out for the 448 kN load cell used in the compression tests. This test was also carried out in the universal testing machine. The calibration test results were then plotted to be used. The curve is shown in Figure 3.17.

CHAPTER IV

THEORETICAL ANALYSIS

4.1 Introduction

It would be desirable to be able to predict the load carrying capacities of angles under balanced and unbalanced weld patterns. Thus, the experimental and theoretical results could be compared.

Although a single angle member could be considered a very simple member, the complexity of determining its strength by either experimental investigation or finite element method should not be underestimated if the angle is under compressive loads. Angle members are sensitive to the loading position and the end conditions.

A commercial finite element package ABAQUS [1] has been used to perform a nonlinear static analysis. Both material and geometric nonlinearity were considered in the analysis of both slender and intermediate length specimens. Residual stresses due to the manufacturing process of the angles or due to the welding of the specimen were excluded from the analysis due to the difficulty of determining such stresses. The steel was modelled as a linear elastic, perfectly plastic material. Different weld patterns were modelled by changing the boundary conditions and the applied loads at the welded nodes.

4.2 Finite Element Program

The commercial finite element package used for the analysis, ABAQUS [1], is a batch program. In order to use ABAQUS to analyze a member, a data deck describing the problem has to be prepared. The data deck consists of two parts : the model data and the history data. The model data describes the nodes, elements, nodal constraints, elements properties, material description and the data required to specify the model itself. ABAQUS also has a large library of elements of which plate elements and truss elements were used in the analysis process. Two different nodal constraints were used:

(1) Boundary constraints: in which a specific boundary condition is defined for the node, and

(2) Equations: which are linear relationships between certain degrees of freedom of certain nodes.

The history data defines what happens to the model, in other words, the sequence of loading for which the model's response is sought. This history is divided into steps. In this problem, static loads are applied and the nonlinear static response was computed. The applied loads were assigned up to fifty increments, as an upper bound, to reach the ultimate load. Each increment was assigned up to 15 iterations to converge or the increment was automatically reduced.

4.3 Finite Element Procedure

In the next two sections, a brief discussion of the finite element analysis of structures and the incremental-iterative procedure is described. This method gives the theoretical load-deflection curves which in turn can be used to determine the buckling load.

4.3.1 Basics of Finite Element Analysis

A three-dimensional nonlinear finite element analysis was used to study the ultimate load of the tested angles using eight-node plate elements.

From the potential energy formulation, the following is obtained:

$$\Pi_p = \frac{1}{2}\{U\}^T\ [K_e]\ \{U\} + \frac{1}{2}\{U\}^T\ [K_G]\ \{U\} - \{U\}^T\{P\} \qquad (4\text{-}1)$$

where Π_p is the potential energy of the system; $\{U\}$ is the global displacement vector; $\{P\}$ is the global load vector; $[K_e]$ is the global elastic stiffness matrix; and $[K_G]$ is the global geometric stiffness matrix. The geometric stiffness matrix is included in the analysis to account for the deformed geometry of the elements in the equilibrium equations since the problem of angle members under a compressive load is a large deflection problem.

Differentiating with respect to the displacement and equating the result to zero to determine the minimum potential energy of the system results in the following:

$$[K_e]\{U\} - [K_G]\{U\} = \{P\} \tag{4-2}$$

Which can be simplified to the following form

$$[K]\{U\} = \{P\} \tag{4-3}$$

where $\mathbf{K} = \mathbf{K}_e + \mathbf{K}_G$

4.3.2 Nonlinear Iterative-Incremental Analysis

Nonlinearity of structural members may arise from large displacement effects, material nonlinearity and boundary nonlinearity.

In a linear problem, loads are applied to a model and the response can be obtained directly. Nonlinear finite element problems are usually solved by taking several linear steps because the stiffness matrix itself is a function of displacements and the displacements are unknown which makes the one step solution of the nonlinear structure impossible.

Geometric nonlinearity is caused by the difference between the stiffness matrix of the reference structure and that of the deformed structure under a load increment. Many solution procedures have been proposed to solve nonlinear problems. ABAQUS uses the well known Newton's method as a numerical technique for solving the nonlinear equilibrium equations.

The nonlinear solution of the problem is obtained iteratively by solving a series of linear problems. For any displaced state of the structure, let **u** be the vector of nodal displacements; $\mathbf{R}_i$ the vector of internal resisting loads (i.e. the vector of loads in equilibrium with the internal forces of the structure); $\mathbf{K}_T$ the current tangent stiffness matrix of the structure. The vector of unbalanced loads is given by

$$R_u = R_e - R_i \tag{3-4}$$

and provides a measure of the solution error.

The iterative sequence for Newton-Raphson iteration is as follows :

$$R_u^j = R_e - R_i^j \tag{3-5}$$

$$\Delta r^j = (k_T^j)^{-1} R_u^j \tag{3-6}$$

$$r^{(j+1)} = r^j + \Delta r^j \tag{3-7}$$

$$R_i^{(j+1)} = function \ (r^{(j+1)}) \tag{3-8}$$

The loading is divided into several increments and at each load increment the nonlinear equations are solved using either Newton's method or variations of it which are referred to as quasi-Newtonian techniques.

Using an estimated load, as an upper load limit, automatic load increments were applied. The automatic scheme for the procedure is based on the convergence of the iteration process of each increment, until the specified load tolerance in $\mathbf{R}_u^j$ was achieved.

If the number of iterations exceeded the maximum allowed, the increment size was reduced by a factor of four. If this resulted in a smaller increment than was specified as a minimum in the input, the run was terminated.

4.4 The Finite Element Model

In the following sections, the steps and assumptions in the modelling are reviewed. The review includes considerations in choosing the mesh, the verification problem used, material modelling, modelling of the initial imperfection, and the most difficult aspect of the modelling which is the boundary conditions.

4.4.1 Choice of Mesh

The finite element mesh is usually chosen based on pilot runs and is a compromise between economy and accuracy. Several element types were tested in the pilot runs. The number of elements used in the angle mesh was varied as well. Finally, it was decided to use an eight-node plate element with six degrees of freedom assigned to each node.

As the load transfers first through the welded leg and then through the whole cross section, the overwhelming factor in the final choice of the mesh was to have a finer mesh at the ends of the angle so that the exact weld lengths could be modelled. Refinement of the mesh at the ends was also necessary due to the fact that the distribution of stresses takes place at this zone. The global axes were taken such that the cross-section of the angles was in the x-y plane.

4.4.2 Verification of the Mesh

In order to get confidence in the program and the chosen mesh, a verification problem was used. The verification problem consisted of an angle member connected by single bolts at the ends, in the middle of the bolted leg. The member was 1676 mm in length, and the angle size was 76.2 x 76.2 x 6.35 mm. Both the experimental results and the nonlinear finite element analysis by a different program were available [11]. ABAQUS results for this verification problem were in a good agreement with the other results.

The procedure followed to choose the relevant mesh for this problem was as follows: first, a convergence test was carried out for the regular mesh and then the appropriate number of elements was selected. Then, more refined meshes were created at the end elements of the angle to make it possible to model the exact lengths of the welds. Thus the new mesh, with the refined ends, was checked against the verification problem to make sure that the results were still very close after making the refinement.

4.4.3 Material Modelling

The steel was modelled as a linear elastic, perfectly plastic material by specifying both Young's modulus of elasticity and the yield stress obtained from the tension tests.

However, as the plate elements cannot have in-plane load except in the form of concentrated loads at the nodes, it was noted that for intermediate length columns the failure load is much smaller than that of the verification problem. This can be explained by the fact that concentrated nodal loads at the edges of the angle caused the material to yield first at these loading points where the concentrated loads were applied. This problem was overcome by changing the properties of the material used for the end elements to be fully linear elastic.

4.4.4 Initial Out-of-Straightness

The coordinates of the nodes of the model were defined taking into consideration the initial out-of-straightness of the angle. The assumed ideal initial imperfection has a parabolic shape with maximum imperfection of L/1000 at the mid-height of the angle.

4.4.5 Boundary Conditions

The real problem encountered in the modelling of the welded angles was the modelling of the weld itself as a boundary condition applied at the welded nodes. It can be seen from the verification test that the problem is a boundary condition problem. A literature survey to find any published research in which a finite element model of a weld subjected to both shear forces and bending moments perpendicular to the plane of weld was used and revealed that the weld is either neglected and the material is considered to be continuous or the weld material is assumed to be very rigid.

The first trials for the modelling assumed that the weld material is very rigid so that the welded points can be assigned zero displacements in order to simulate rigid support of the welded leg near the weld (see Figures 4.1 and 4.2). This assumption was used by Lipson and Haque [10] in the modelling of a single-angle bolted-welded connection. The second trial was done by assuming that the welded leg was assigned zero displacements at the end points of the edge of the welded leg (see Figures 4.3 and 4.4). The third trial was performed by placing springs at the welded nodes. The stiffness of the springs was proportional to the length of the weld represented by each node. Elastic springs were tried as well as elastic-plastic springs. Several spring stiffnesses were tried in order to pick the one that gives an ultimate load close to that obtained from the laboratory. All these different modelling assumptions and their results are reviewed and compared to the experimental results in the following chapter.

4.5 Analytical Modelling As a Beam-Column

In angles welded along one leg only, the applied load is transferred to the angle member, at its ends, through the welded leg. As the two angle members used in each specimen were not connected together, except at the ends, it can be seen that the load is always applied at the end with an eccentricity e_y with respect to the y-axis. As the weld pattern changes from balanced to unbalanced weld, the eccentricity with respect to the x-axis changes from zero to e_x.

As demonstrated in statics, the load applied at the welded leg can be replaced with a load at the centroid of the angle and a couple of bending moments at the ends. Such a column, subjected to both axial compression force and bending moments are called beam-columns.

In Appendix B, the angle member under balanced and unbalanced weld patterns are analyzed as a beam-column problem according to the design procedure prescribed by CAN/CSA-S16.1-M89 [7]. This design procedure is based on interaction expressions accounting for the following:

(1) a laterally supported member fails when it reaches its in-plane moment strength reduced for the presence of axial load;

(2) a laterally unsupported member may fail by lateral-torsional buckling or a combination of weak axis buckling and lateral buckling;

(3) a relatively short column can reach its full cross-sectional strength whether it is laterally supported or not;

(4) when subjected to axial load only, the axial compressive resistance depends on the maximum slenderness ratio;

(5) members bent about the weak axis do not exhibit out-of-plane behaviour;

(6) a constant moment has the most severe effect on in-plane behaviour;

(7) a constant moment has the most severe effect on the lateral-torsional buckling behaviour. This effect disappears if the member is short enough, in which case, cross-sectional strength controls; and

(8) moment may be amplified by axial loads increasing the deflections [6].

Four modes of failure are tested in the proposed solution procedure. They include local buckling of an element, strength of the full cross section, overall member strength and lateral-torsional buckling strength. Results from this analysis are given and compared with the experimental results to check whether these members can be designed as beam-columns or not. The idealized rectangular cross-section used in the analysis is shown in Figure 4.5.

CHAPTER V

RESULTS AND DISCUSSION

5.1 General

This chapter focuses on the results of the experimental investigation to show the effect of balanced and unbalanced welds on the load carrying capacity of welded angles. The finite element modelling of the problem is then discussed and both the experimental and theoretical results are compared. A beam-column design approach according to CAN/CSA-S16.1-M89 is used to predict the ultimate failure load and is then compared with the experimental failure loads. First, the geometric and mechanical properties of the test specimens are determined. The values obtained are then used to calculate the theoretical failure loads and interpret the experimental data.

5.2 Properties

5.2.1 Geometric Properties

The specimens used were all made from structural steel angles of nominal dimensions 50.8 x 50.8 x 6.35 mm in SI units, that is 2 x 2 x 1/4 in. in U.S. customary units. The computations of the geometric properties of angles are based on the idealized rectangular cross section in which the toe and the fillet radii are omitted (see Figure 4.5). The geometric properties can easily be calculated using values that are tabulated in the CISC Handbook.

$$I_{xy} = -bt(\frac{b}{2}-y)(x-\frac{t}{2}) - t(b-t)(y-\frac{t}{2})(\frac{b+t}{2}-x) \tag{5-1}$$

$$I_v = \frac{I_x + I_y}{2} - \sqrt{\frac{(I_x + I_y)^2}{4} + I_{xy}^2} \tag{5-2}$$

$$I_u = \frac{I_x+I_y}{2} + \sqrt{\frac{(I_x + I_y)^2}{4} + I_{xy}^2} \tag{5-3}$$

$$r_v = \sqrt{\frac{I_v}{A}} \tag{5-4}$$

$$r_u = \sqrt{\frac{I_u}{A}} \tag{5-5}$$

$$J = \frac{t^3}{3}(2b-t) \tag{5-6}$$

where b,t = the width and the thickness of the angle leg, respectively; A= the total area; I= moment of inertia; r= radius of gyration; and J= torsional constant of the angle. The nominal geometric properties of the angle cross section are listed in Table 1.

For convenience, the nominal properties listed in the Handbook of Steel

Construction, which are also listed in Table 1, were used for the theoretical calculations. The actual dimensions of the angles varied from the nominal dimensions by -0.3 to 1.6%.

5.2.2 Mechanical Properties

To obtain the mechanical properties of the angles, three tension tests were carried out. These tests were conducted on three specimens taken randomly from the steel angles used to construct the compression angle specimens. The tension specimens were cut from the steel angles and prepared according to ASTM A370-77 [3]. The dimensions of the tension test specimens are given in Figure 3.18. Two strain gauges were used, one on each side of the specimen to measure the elongation of the specimen during the testing process. The actual cross section dimensions of the specimens were measured before testing and were used to calculate the properties of the angles.

The test data for each specimen are shown in Table 2. It can be seen that the average yield stress and Young's modulus of elasticity are 366 MPa and 195 000 MPa, respectively. These values were used in all the theoretical calculations and the finite element analysis.

The mechanical properties of the HSS's were not determined because they do not have any significant effect on the load carrying capacities of the specimens.

5.3 Experimental Results

5.3.1 Failure Loads

The experimental failure loads for all the test specimens are tabulated in Tables

3 and 4 for both slender and intermediate length columns, respectively. At the top of each table, the predicted compressive resistance, calculated according to CAN/CSA-S16.1-M89 [7], is given. The calculation of this value is based on taking the resistance factor equal to 1.0. The effective length factor was taken as 1.0 which means that the specimens were designed as if they were pin-ended. This compressive resistance for the pin-ended column was used for the design of the weld. It can be seen that the experimental failure loads were quite consistent with each other for each weld group which gives confidence in these experimental results.

5.3.1.1. Failure Loads of Slender Specimens

It can be seen from Table 3 that as the weld pattern goes from one that is balanced about the centroid of the angle to one that is balanced about the centre of the leg, the failure loads increase by as much as 25%. The failure loads increase by as much as 33% when the weld is grossly unbalanced about the centre of gravity of the angle when compared to the failure loads when welds balanced about the centroid are used.

It should be mentioned that when designing the welds, the minimum weld length as given by the CAN/CSA-W59-M1989 [8], which is 40 mm in this case, was not used. This requirement was neglected in this research so that the behaviour of angles under balanced and unbalanced welds for both slender and intermediate length columns could be assessed when both of them are designed on the same basis. A 40 mm weld is very long compared to the weld required from the design equations for the small sized angles used in the tests. Thus, the use of such a weld would have resulted in the use of so much weld that any difference between balanced and unbalanced welds would not have been evident. For larger angles the use of the minimum weld length would not have been a problem.

All the angles failed by flexural buckling about an axis falling between the y and v axes (see Figure 4.5 and Tables 11 and 12). The welds did not fail. In one case only, the weld of one angle in Specimen No.2 failed before the angles buckled and the Specimen was re-welded and tested again. In both specimens No.1 and No.5, one of the 10 mm welds failed after excessive large deformations took place in the angles. The load at which these welds failed was considered to be the failure load because the load-deflection curve was almost flat at that load.

5.3.1.2. Failure Loads of Intermediate Length Specimens

The failure loads for intermediate length specimens are tabulated in Table 4. It can be seen that the use of unbalanced welds resulted in reduced load carrying capacities with respect to the same column with balanced welds. The load carrying capacity is reduced by 5% when a weld balanced about the centre of the leg is used as opposed to one balanced about the centroidal axis, and by 10% when a grossly unbalanced weld is used. This is due to the orientation of the bending axis of failure.

In all tests, the angles failed by flexural buckling and the welds did not fail. The rotation of the angle was not measured because it was mentioned in previous research that this angle is very small and can be neglected. However, it was noticed that there was a small rotation at the cross-section of the specimens with balanced welds. It is believed that this did not significantly affect the load carrying capacity of those specimens. The load-deflection curves of intermediate length specimens are given in Appendix A (Figures A.10 to A.12). Specimens with equal and unbalanced welds failed by flexural buckling like slender specimens.

5.3.2 Load-Deflection Curves

The experimental load-deflection curves of all the specimens are shown in Appendix A. These curves are drawn for the deflections at the mid-height of the specimens. The positive directions for the deflections are shown on every graph.

5.3.2.1 Slender Specimens Load-Deflection Curves

Figures A.1 to A.9 show the load-deflection curves for slender specimens. At the failure load, all specimens had a deflection perpendicular to the plane of weld (u_1) about 2.5 to 5 times the deflection parallel to the plane of weld (u_2). This means that all the specimens failed by flexural buckling about an axis falling between the y and v axes (see Figure 4.5 and Table 11). This location of the bending axis between these two axes is expected because near the ends the weld is restraining the cross section against rotation while near the middle of the column the cross section can rotate more freely.

Table 5 shows the average displacements u_1 and u_2 for each specimen and then for each group of specimens at a load equal to the compressive resistance according to CAN/CSA-S16.1-M89 assuming an effective length factor of 1.0. It can be seen that the failure axis is always closer to the x-axis than to the v-axis.

Figures 5.1 and 5.2 show a comparison between the load-deflection curves for three specimens representing the three different weld patterns used in this research.

It should be noted from these curves and from the average deflections given in Table 5 that as the weld pattern changes from a balanced to unbalanced weld, the flexibility of the angle increases. That means that at a certain load the lateral deflection of an angle with an unbalanced weld is greater than that of an angle with an equal weld, which in turn is greater than that of an angle with a weld balanced about the centroid.

5.3.2.2 Intermediate Length Specimens Load-Deflection Curves

Figures A.10 to A.18 show the load-deflection curves for intermediate length specimens. Like slender specimens, the deflection was predominately in the u_1 direction (perpendicular to the plane of weld) where u_1 varied from 1.8 to 5.7 times the deflection in the u_2 direction (parallel to the plane of weld), as shown in Table 6.

Intermediate length specimens behaved in a manner similar to that of slender specimens in that a change in the weld pattern from balanced to an unbalanced weld increases the flexibility of the angle. Hence the lateral deflection becomes greater at the same load. The failure axis also falls between the y and v-axis and is always closer to the y-axis. A comparison between the load-deflection curves for three specimens representing the three different weld patterns are shown in Figure 5.3 and 5.4.

It was observed during the experiments, and it can be concluded from the load-deflection curves of the intermediate length specimens, that there was a small rotation of the cross-section of the specimens with a weld pattern that was balanced about the centroid of the angle. This rotation of the cross section about the longitudinal axis was not measured because it was reported from previous research that this angle is small. It is believed that this rotation did not significantly affect the load carrying capacity.

5.3.3 Initial Imperfection

Tables 7 and 8 show the measured initial imperfection of the angles for slender and intermediate length specimens, respectively. The initial imperfection was measured as indicated in Chapter 3 (see Figure 3.16). It can be seen from these tables that the initial imperfection ranged from L/500 to L/1300 for slender specimens except for specimen No.2 where the weld at one angle failed at first and it was re-welded and tested again. The values shown in Table 7 are those obtained after re-welding. For intermediate length specimens, the initial imperfection ranged from L/500 to L/1000 except for Specimen No.2. It can be seen also from both tables that, in some cases, the initial imperfection of one angle is significantly greater than the other one in the same specimen. That happened due to the welding process, since the shrinkage of the weld due to the cooling process which caused the second welded end of the second welded angle to move away from the HSS and it had to be forced into the proper position by clamps, thus, causing additional initial imperfection to occur in the angle. It can be seen from Tables 7 and 8 that the initial imperfection of the tested angles has a very small effect on the failure loads and this conclusion is verified by the finite element analysis as will be shown later in this chapter (see Figures 5.5 and 5.6).

5.3.4 Effective Length Factor

The buckling axis of a welded angle is not the same along its length. At the ends of the angle, where the weld is restraining the cross section, the angle buckles about the y-axis (parallel to the welded leg). At the middle of the specimen, where the cross section has more freedom to deflect, the buckling axis falls between the y-axis and the v-axis (where the v-axis is the weakest axis).

In practical design of angles as compression members, the weakest axis is often used as a base for the calculation of the load carrying capacity. The experimental average effective length factor for the different weld patterns for both intermediate length and slender specimens is shown in Tables 3 and 4, respectively.

It can be seen from Table 3 that for slender welded angles, an effective length factor of 0.85 is considered appropriate for design purposes. The average effective length factor when the weld pattern is one balanced about the centroid axis, which is 0.94, probably would not have been the same if the minimum length weld had been used (40 mm in this case).

For intermediate length columns, as seen in Table 4, angles with welds balanced about the centroid should be designed for an effective length factor of 0.85. In cases where equal and unbalanced welds are used, a reduction factor or a different effective length factor should be used in the calculations of the ultimate load.

5.4 Finite element Modelling

As mentioned in Chapter IV, a finite element program, ABAQUS, was used for the analysis of the specimens which were tested in the laboratory. ABAQUS was tested using an angle hinged at the end of the angle in the middle of the leg, for which the results were known, and the ABAQUS results were close to those obtained from both the laboratory and from another finite element program. Several approaches were tried for both slender and intermediate length specimens to determine the model that will give results which are the closest one to the experimental results.

The first trials for the modelling of the weld assumed that the weld material is very rigid so that at the welds the displacements are zero with respect to the HSS (see Figures 4.1 and 4.2). This approach was used by Lipson and Haque [10] in the modelling of single-angle bolted-welded connections. Actually, trying to model the weld as hinges at the weld points resulted in a failure loads and buckling shapes of a fixed ends angle, which does not agree with the experimental results where all the failure loads were very close to those of pin-ended angles. This means that the modelling of the welded angle is a boundary condition problem.

5.4.1 Finite Element Modelling of Slender Specimens

For slender specimens, the model which gives results which are the closest to the experimental results is when the angle is assumed to have double hinges at the ends of the welded leg (see Figure 4.3). Table 9 shows the results of this model compared with the experimental results. It can be seen that the failure loads are within 10% of the experimental failure loads. The trend of having higher failure loads as the weld pattern changes from balanced to unbalanced is verified using this model. The deformed shape for a slender specimen with a weld balanced about the centroid as obtained from this model is shown in Figure 5.7.

The results of this model are close to the experimental results because the average weld length on each side of the welded angle is 21 mm which is only about 1% of the total length of the angle. Thus, it can be assumed that the weld is behaving like a hinge at the ends of the angles.

5.4.2 Finite Element Modelling of Intermediate Length Specimens

For intermediate length specimens, the assumptions made for the slender columns did not give relevant results. This can be explained by the fact that the average weld length on each side of the welded leg is about 60 mm which is 6% of the total length of the angle. Table 10 shows the results from a model where the angle was double hinged at the ends (see Figure 4.4) and the results of the intermediate length angle using hinges at all the weld points are compared with the experimental results.

Another modelling trial was performed by placing springs at the welded nodes. The stiffness of the springs were proportional to the length of the weld represented by each node. Elastic springs were tried as well as elastic-plastic springs. Several spring stiffnesses were tried in order to determine the one that gives an ultimate load close to the experimental failure loads for specimens with welds balanced about the centroid. However, the failure loads for the other weld patterns did not agree with what was obtained from the experimental investigation. In addition, the stiffness of weld is not known and was chosen arbitrarily.

5.4.3 Finite Element Results for Initial Imperfection

For both intermediate length and slender columns, the double hinged angle model shown in Figures 4.3 and 4.4, was again used to determine the effect of initial imperfection on the failure loads of angles. Initial imperfection were taken in both the x and y directions and the resultant of them were used in the comparison. Figures 5.5 and 5.6 show the ultimate load carrying capacities versus the initial imperfection. It can be shown that going from L/1000 to L/500 affects the load carrying capacities by only 5% which can be neglected. This is the range which covers all the initial imperfections measured in the laboratory.

5.5 Discussion of the Results

There are two factors controlling the ultimate failure load of a column which are:

(a) The eccentricity of the loading, and

(b) The end conditions which includes hinged verses fixed end conditions and torsional restraint.

Eccentricity does not have a significant effect on slender columns but the end conditions do. Both of the two stated factors affect the load carrying capacities of short columns.

The effect of unbalanced welds seems to be beneficial for slender angles but has a detrimental effect on the load carrying capacity of intermediate length angles. The use of unbalanced welds in intermediate length columns reduces the load carrying capacity by about 10% when compared to the load carrying capacity of intermediate length columns with balanced welds. This may be due to the change in the orientation of the bending axis of failure. As shown in Table 11, as the weld pattern changes from unbalanced to balanced weld, the failure axis at mid-height of the specimen is closer to the y-axis increasing the moment of inertia about the failure axis, and hence the failure load increases.

The unexpected results are for slender columns where using unbalanced welds increased the failure load by about 33%. This happens because in an unbalanced weld, more weld is being deposited on the weak edge of the angle thus providing more support for this edge. This changes the orientation of the failure axis to one that is closer to the y-axis, thus increasing the failure load (see Table 12).

In all the tests, although welded connections were used and fixed end conditions were created at the ends of the specimens, all the failure loads were very close to those of pin-ended angles. That means, if an angle is welded to a very stiff member with a weld designed according for a pin-ended angle, the failure load will be still very close to those of a pin-ended column.

A comparison between all results obtained for the load carrying capacities of slender and intermediate length specimens are shown in Tables 13 and 14.

Due to the fact that the angle is eccentrically loaded through the welded leg, causing greater bending to take place about the y-axis, displacement u_1 (perpendicular to plane of weld) is in all cases greater than displacement u_2 (parallel to the weld pattern).

The effect of the initial imperfection on the failure loads of angles loaded through one leg is not significant as indicated in the previous section because it adds a small eccentricity to the already eccentrically loaded angle and thus its effects can be neglected.

5.6 Standards and Experimental Results

As indicated in Chapter II, the Canadian Standard states that the disposition of the fillet welds to balance the forces about the neutral axis for end connections of single-angle, double-angle of axially loaded members is not required. The American Specification and the British Standard have basically the same statement.

As can be shown from the experimental results, the effect of unbalanced welds has a detrimental effect on the load carrying capacity of intermediate length columns. For a slenderness ratio of 100, an angle with grossly unbalanced weld has a failure load 10% less than the same angle with a weld balanced about the centre of gravity. An angle with weld balanced about the centre of the leg has a load carrying capacity that is 5% less than an angle with balanced weld.

This statement has to be changed for angle compression members to force the use of balanced welds for intermediate and short columns unless a reduction factor is taken into considerations when unbalanced are used.

5.7 Design as Beam-Columns

In Appendix B, welded angles under balanced and unbalanced welds were analyzed as beam-columns according to the procedure given by CAN/CSA-S16.1-M89 Clause 13.8 [7]. The analysis was based on the assumption that the load is transmitted to the welded angle through the centre of gravity of the weld group.

It can be shown from Appendix B that for slender specimens, a failure load of 18.3 kN is obtained for an angle with balanced welds when analyzed as a beam-column. The average of the experimental failure load for this specimen is 33.9 kN. The beam-column analysis underestimates the ultimate load carrying capacity by 47-61% for slender columns.

Like slender columns, beam-column analysis underestimates the ultimate load carrying capacities of intermediate length specimens by 53-67%. From Appendix B and the experimental results, It can be deduced that the procedure given in Clause 13.8 produces a very conservative solution and underestimates the ultimate load carrying capacity single angles welded along one leg by more than 50%. This conservatism in the ultimate load carrying capacity is due to the end fixity which reduces the end moments used in the calculations and the conservatism in the C_r value given in CAN/CSA-S16.1-M89 Clause 13.8.

CHAPTER VI

CONCLUSIONS AND RECOMMENDATIONS

6.1 Conclusions

Based on the theoretical and experimental results, the following conclusions can be drawn from this research:

(1) The effect of unbalanced welds seems to be beneficial for slender angles but has a detrimental effect on the load carrying capacity of intermediate length angles. The use of unbalanced welds in intermediate length columns reduces the load carrying capacity by about 10% when compared to the load carrying capacity of intermediate length columns with balanced welds.

(2) As the weld pattern changes from balanced to an unbalanced weld, the flexibility of the angle increases. That means that at a certain load, the lateral deflection of an angle with an unbalanced weld is greater than that of an angle with an equal weld, which in turn is greater than that of an angle with a weld balanced about the centroid.

(3) The initial imperfection of the tested angles has a very small effect on the failure

loads and that was verified also by the finite element program used for the theoretical analysis.

(4) Although welded connections were used to weld the angles to the HSS and the HSS was not free to rotate, all of the failure loads were very close to those predicted for

(5) pin-ended angles.

An effective length factor of 0.85 is considered appropriate for the design of slender columns with any weld pattern. For intermediate length columns, the same effective length factor 0.85 is appropriate for angles with balanced welds.

(6) Analysis of welded angles as beam-columns according to CSA-S16.1-M89 Clause 13.8 produces an invalid solution and cannot be applied to the problem of single angles welded through on leg.

6.2 Recommendations

(1) Balanced welds should be used for both short and intermediate length angle compression members unless a reduction factor is used to account for low load carrying capacity obtained when using unbalanced welds.

(2) It is recommended that an effective length factor of 0.85 be used for angles with welded connections.

6.3 Further Research

Further research is required to determine the effect of balanced and unbalanced welds on double-angles, effect of balanced and unbalanced welds on short columns, effect of weld length on the failure load and buckling shape of angles, and to determine a method for modelling the weld.

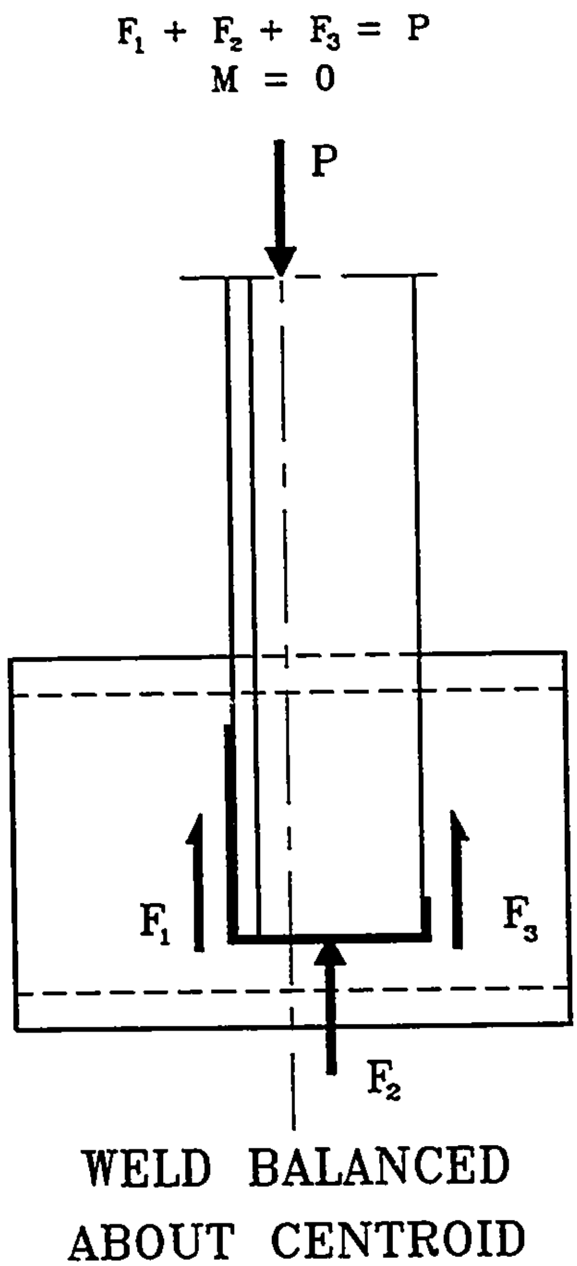

FIGURE 1.1

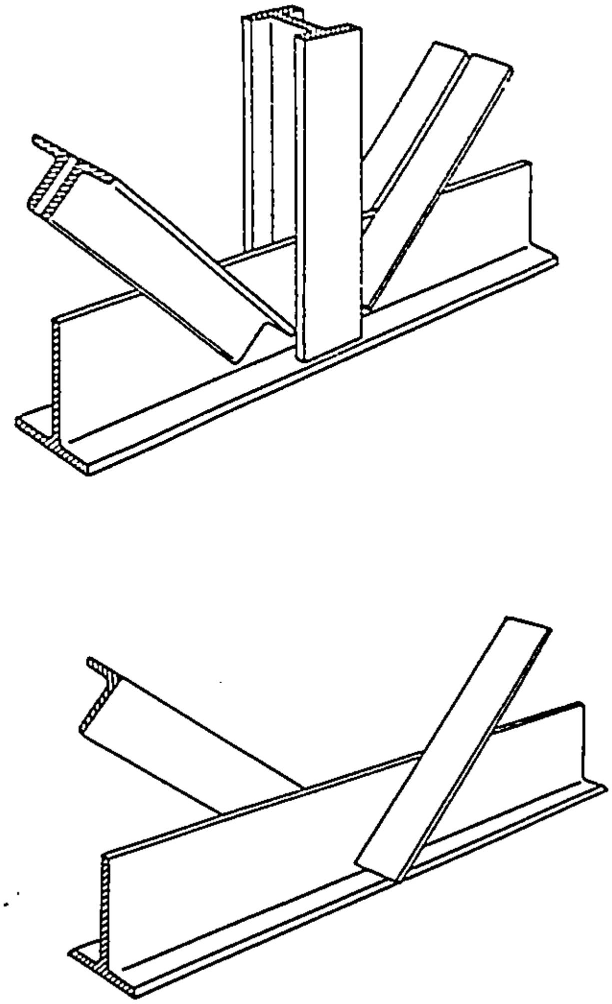

SIMPLEST TYPES OF TRUSS CONSTRUCTION
(After Blodgett, O. W. [4])

FIGURE 1.2

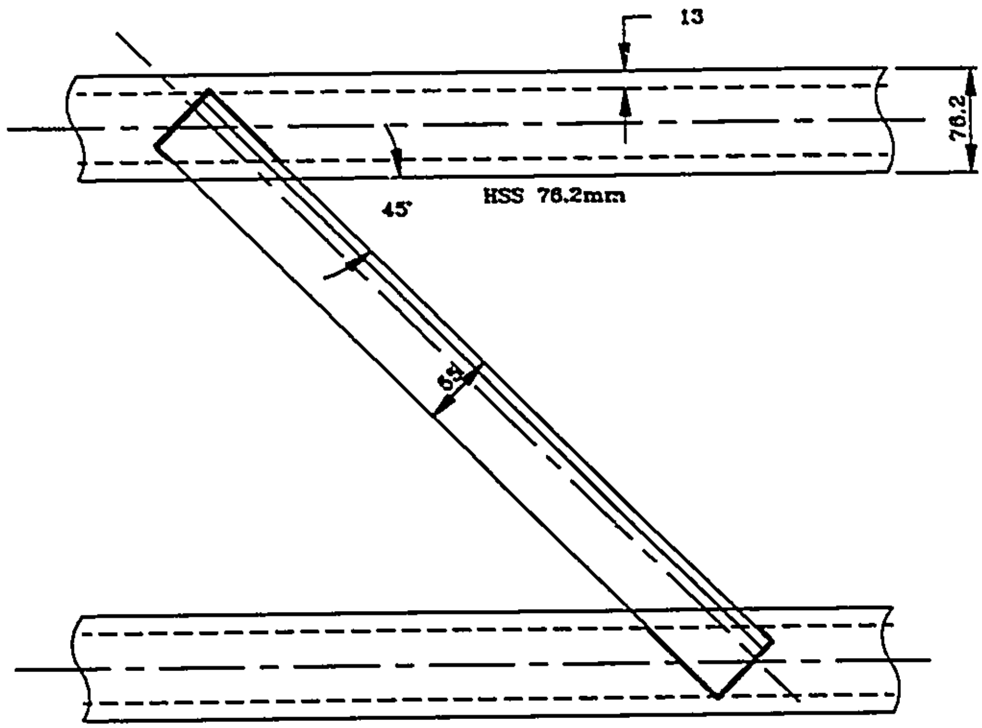

ANGLE WELDED TO HSS WITH

BALANCED AND UNBALANCED WELDS

FIGURE 1.3

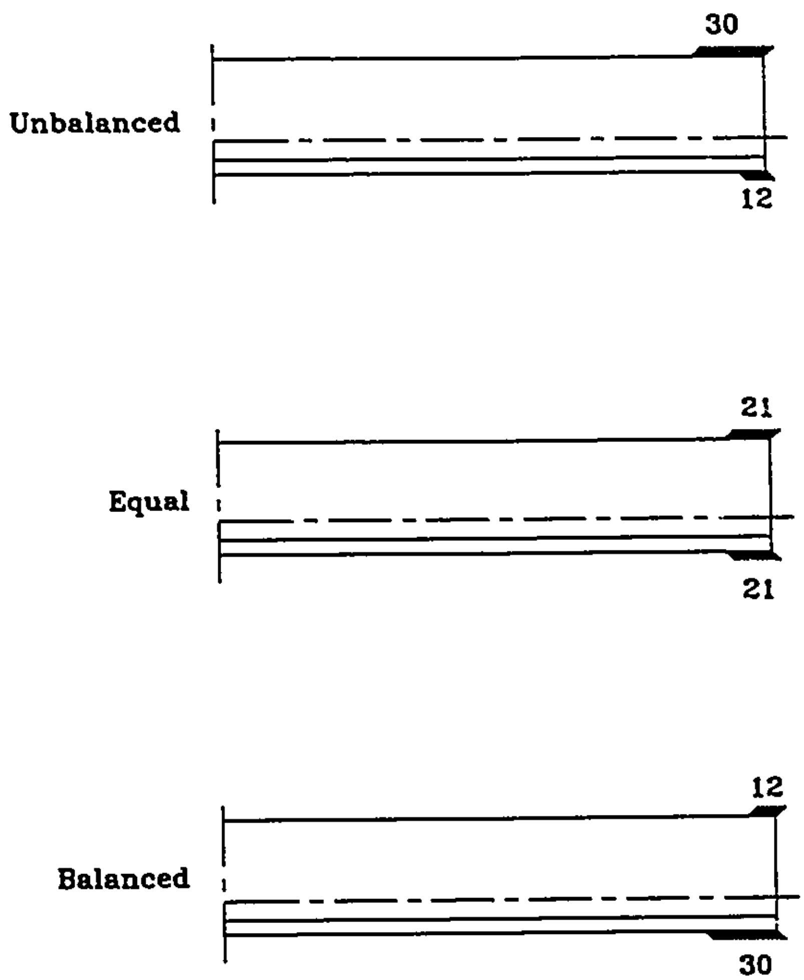

WELD PATTERNS

FOR SLENDER SPECIMENS

FIGURE 3.1

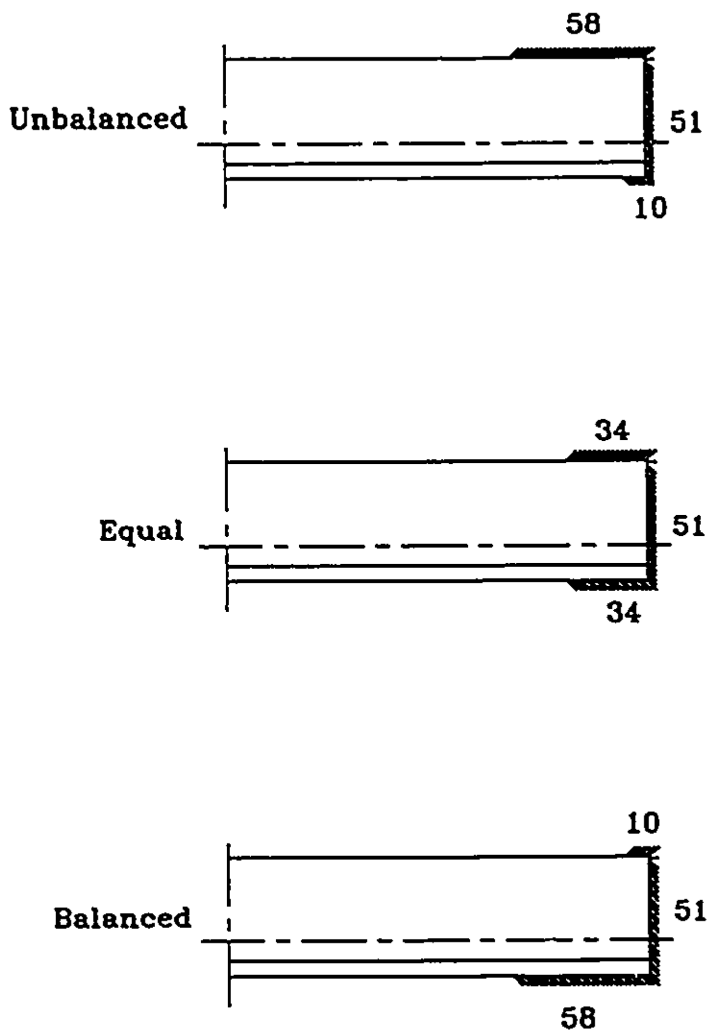

WELD PATTERNS

FOR INTERMEDIATE LENGTH SPECIMENS

FIGURE 3.2

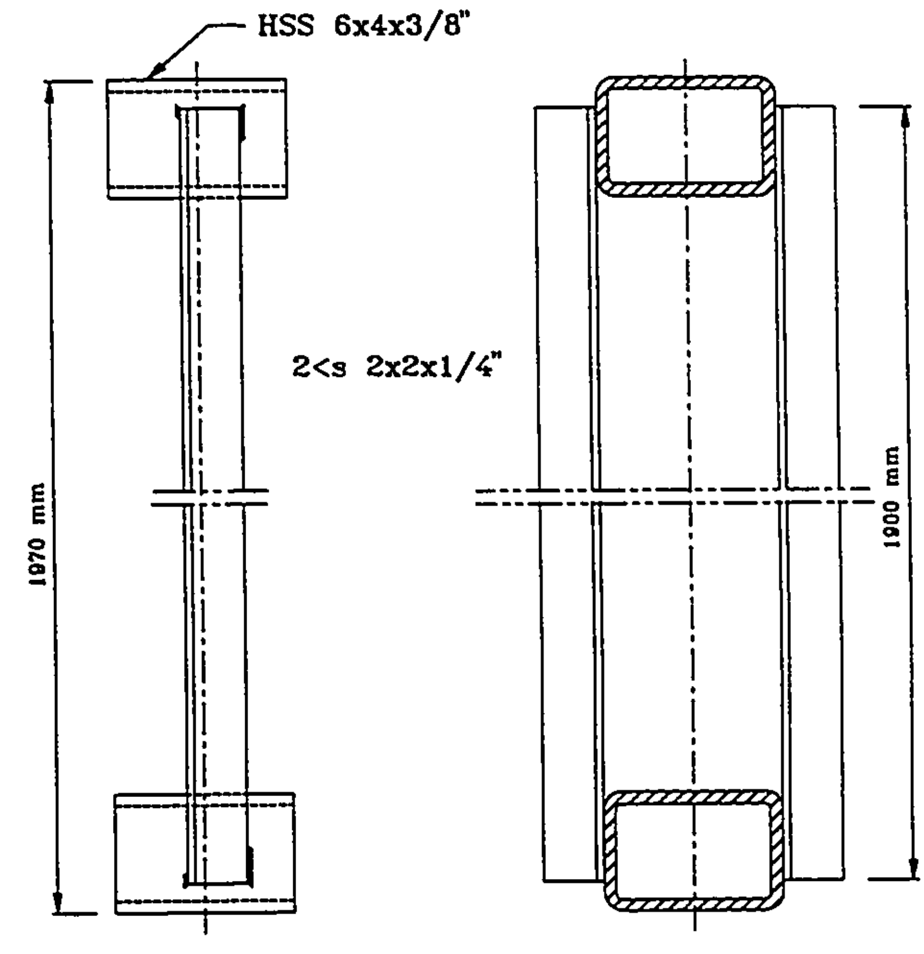

SLENDER SPECIMEN

FIGURE 3.3

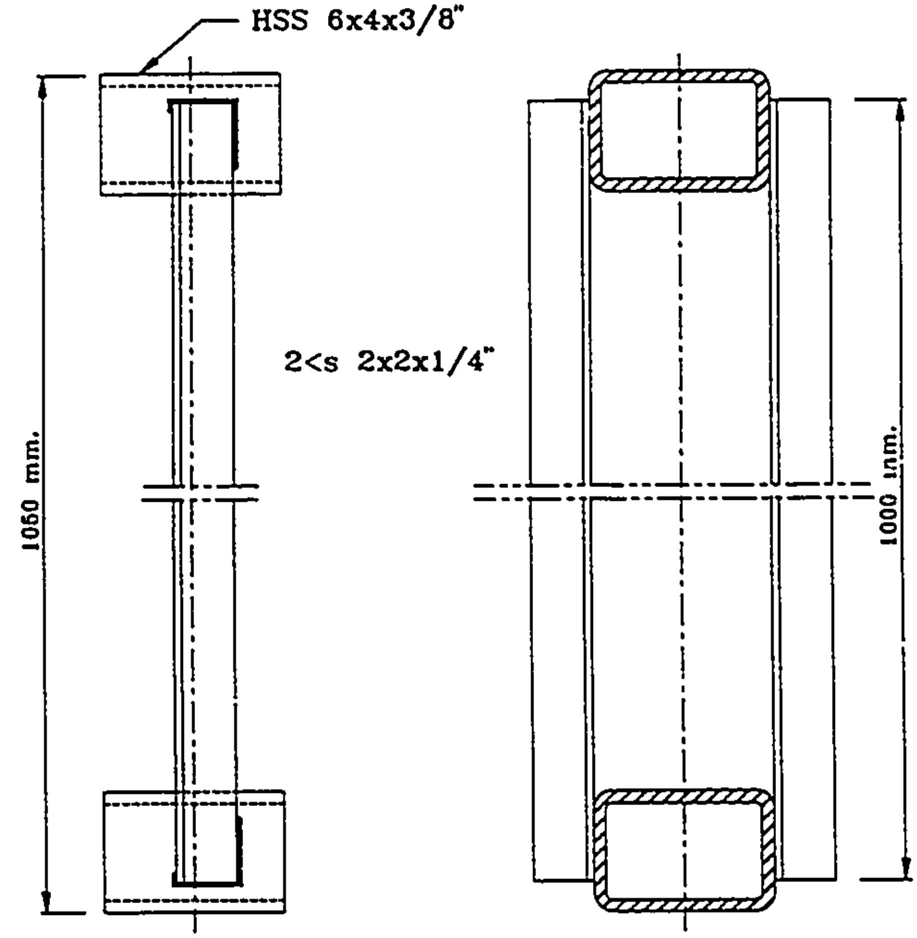

INTERMEDIATE LENGTH SPECIMEN

FIGURE 3.4

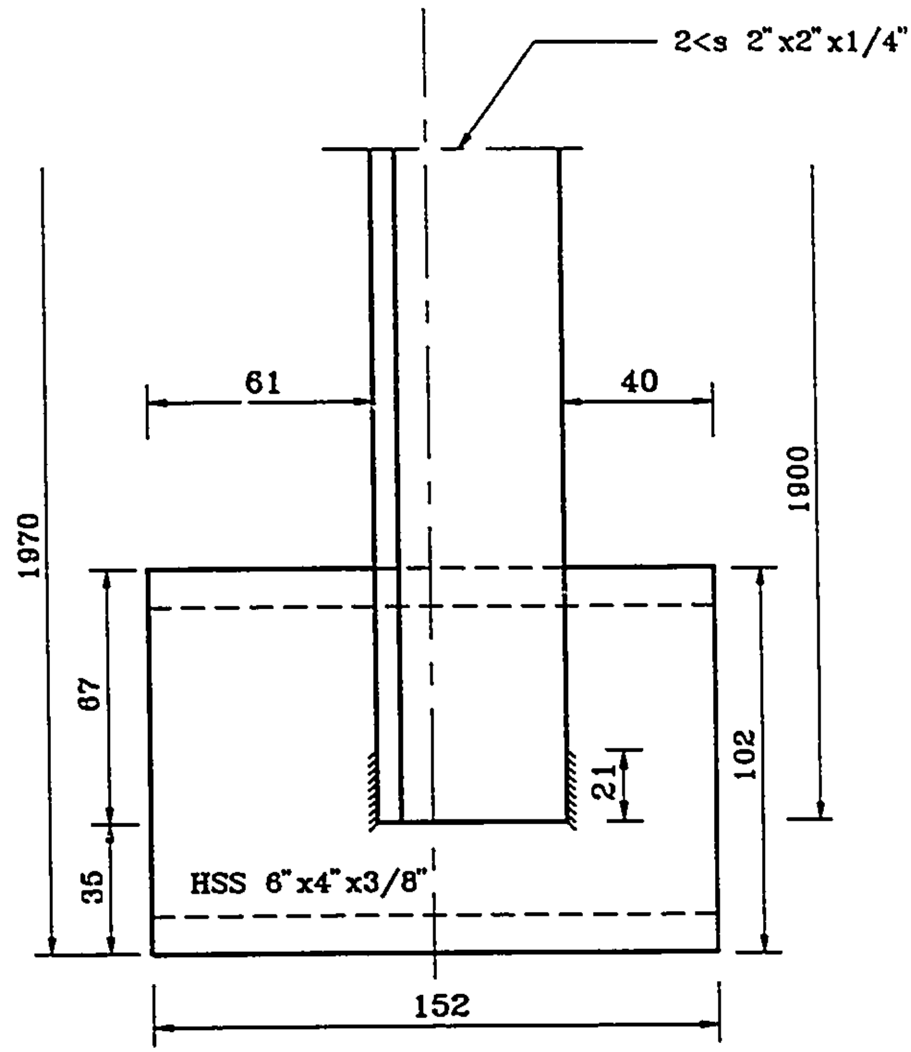

DETAILS OF A LONG SPECIMEN WITH WELD
BALANCED ABOUT THE CENTER OF THE LEG

FIGURE 3.5

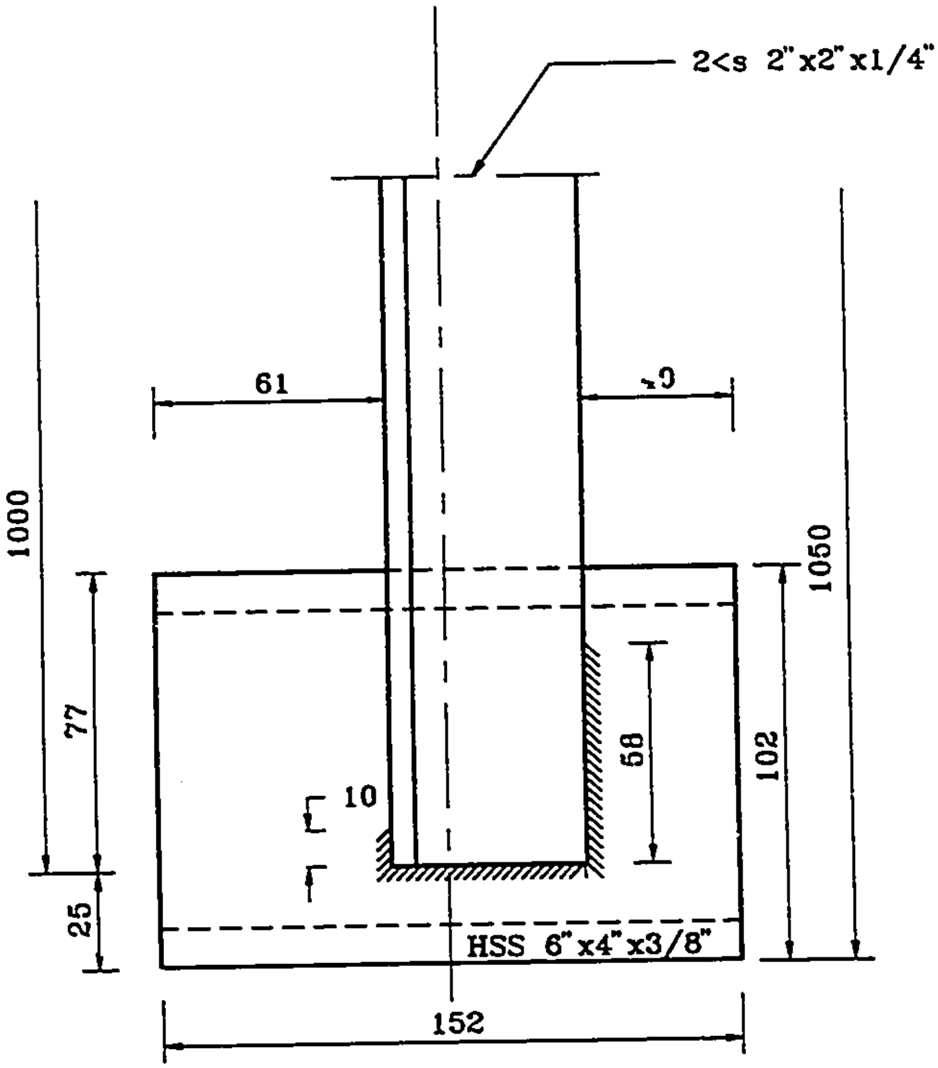

DETAILS OF AN INTERMEDIATE LENGTH SPECIMEN

WITH AN UNBALANCED WELD

FIGURE 3.6

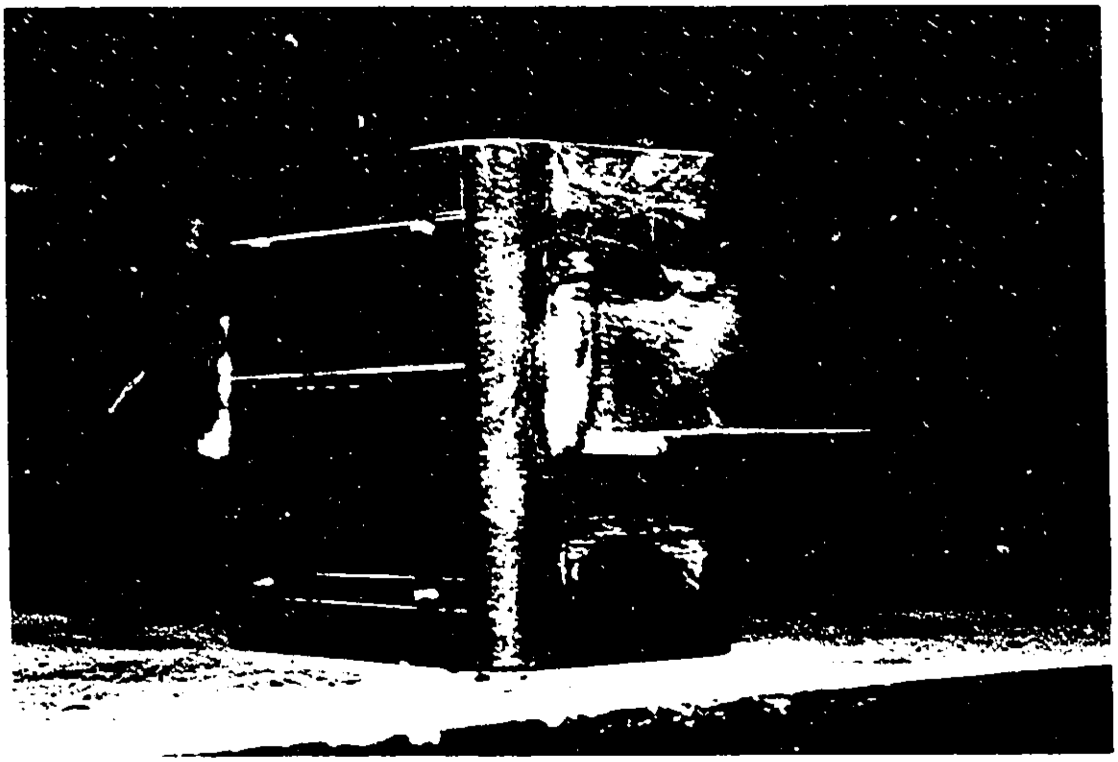

A CLOSE-UP LOOK AT ONE END OF

AN INTERMEDIATE LENGTH SPECIMEN BEFORE BEING TESTED

SHOWING THE UNBALANCED WELD AND THE GUIDING HOLES

FIGURE 3.7

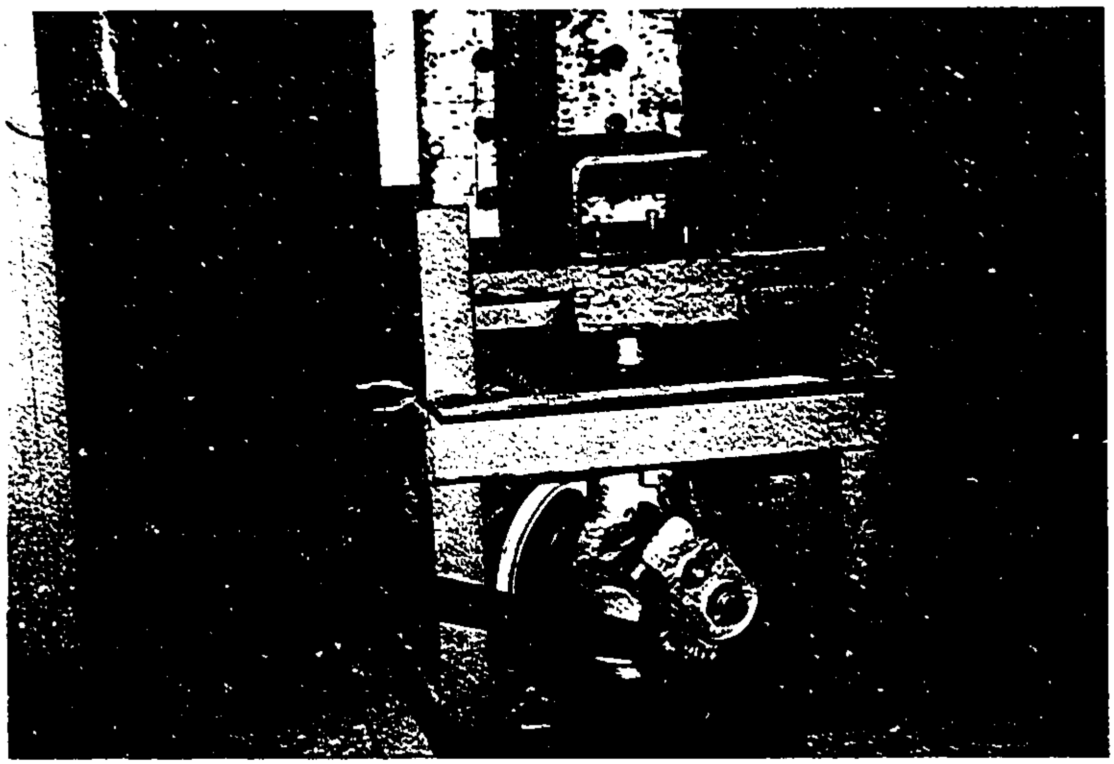

BOTTOM END FIXTURES FOR SLENDER SPECIMENS

FIGURE 3.8

TOP END FIXTURES FOR INTERMEDIATE LENGTH SPECIMENS

WITH 444 kN CAPACITY LOAD CELL

FIGURE 3.9

A CLOSE-UP LOOK AT THE TOP OF A

SLENDER SPECIMEN SHOWING THE UPPER PLATE,

LOAD CELL, AND STEEL BRACKET

FIGURE 3.10

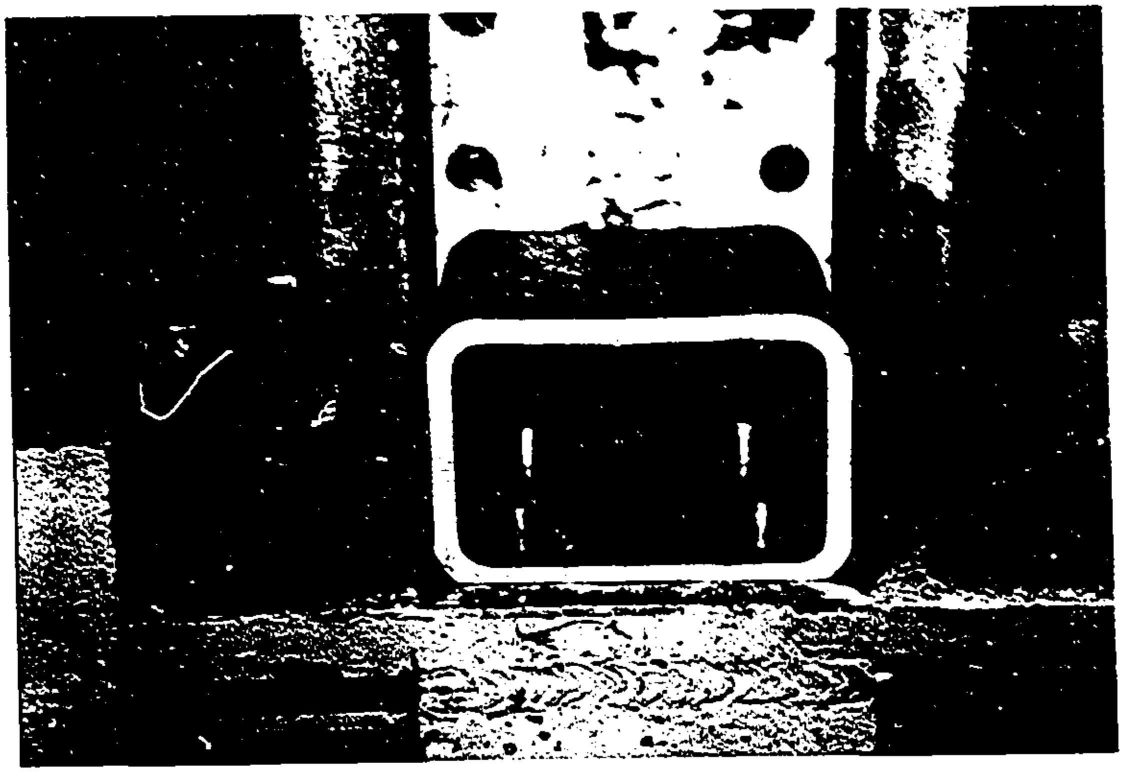

A CLOSE-UP LOOK AT THE BOTTOM OF

A SLENDER SPECIMEN

SHOWING THE GUIDING STUDS IN THE LOWER PLATE

FIGURE 3.11

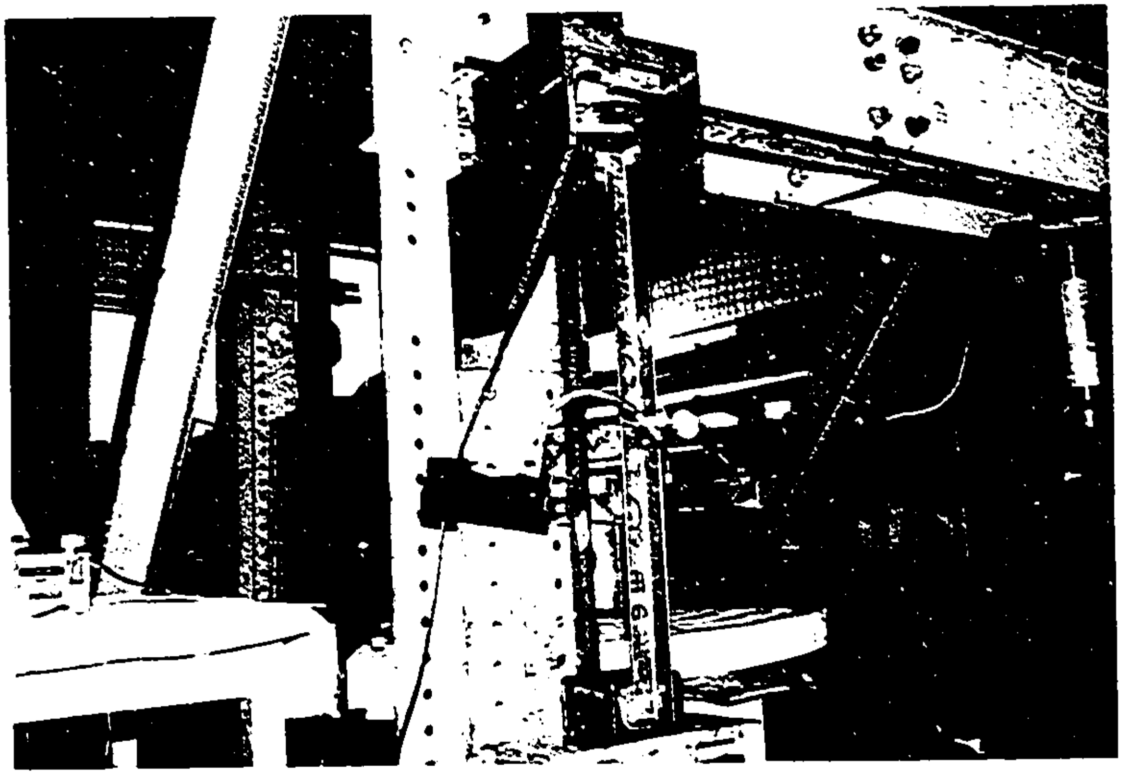

COMPLETE SETUP FOR INTERMEDIATE LENGTH SPECIMENS

FIGURE 3.12

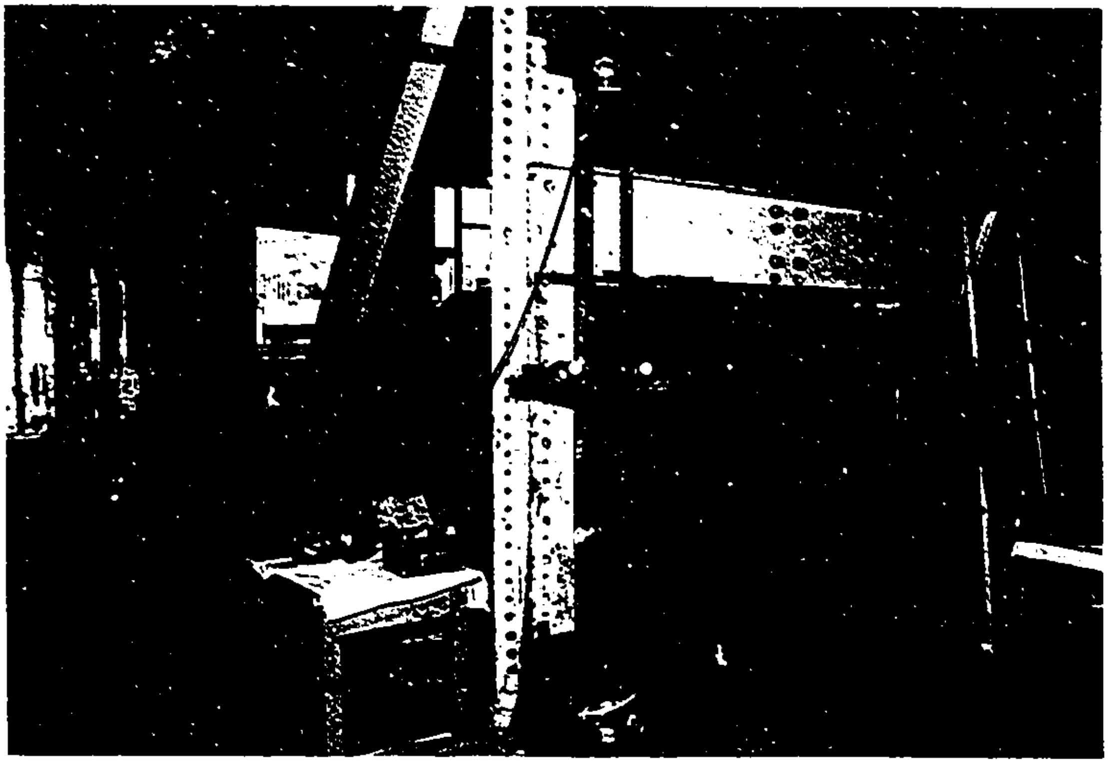

COMPLETE SETUP FOR SLENDER SPECIMENS

FIGURE 3.13

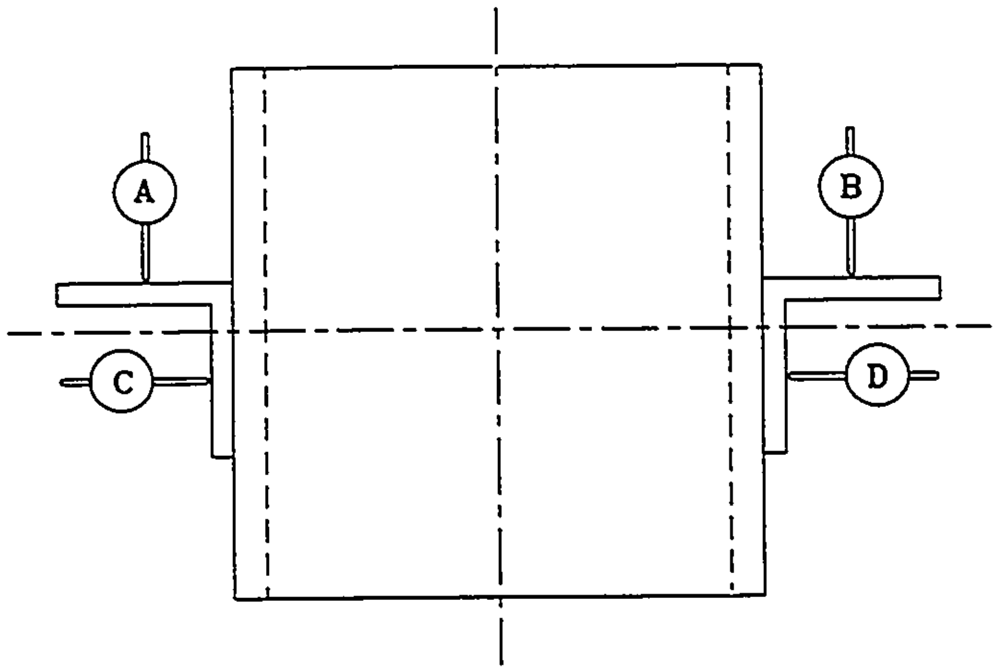

SCHEMATIC OF DIAL GAUGES
AT MID-HEIGHT
OF THE SPECIMENS

FIGURE 3.14

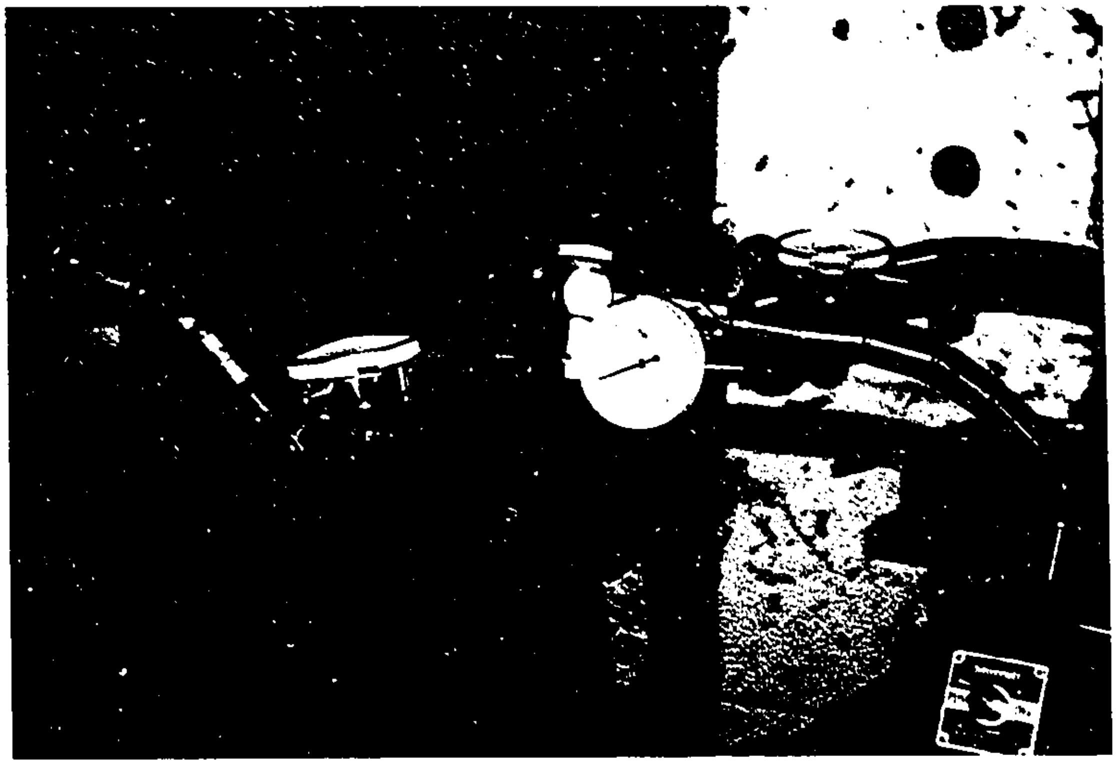

THE ARRANGEMENT OF DIAL GAUGES

AT MID-HEIGHT OF INTERMEDIATE LENGTH SPECIMENS

FIGURE 3.15

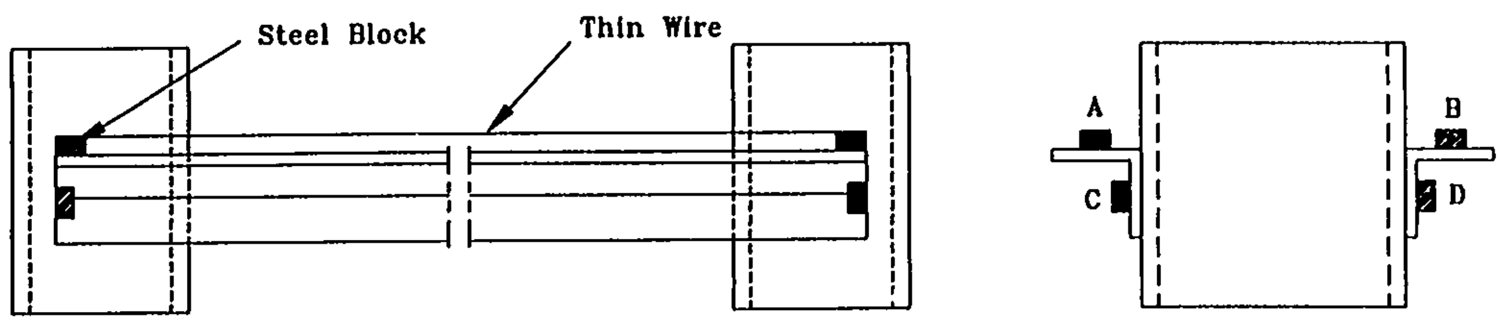

SETUP FOR MEASURING
INITIAL OUT-OF-STRAIGHTNESS

FIGURE 3.16

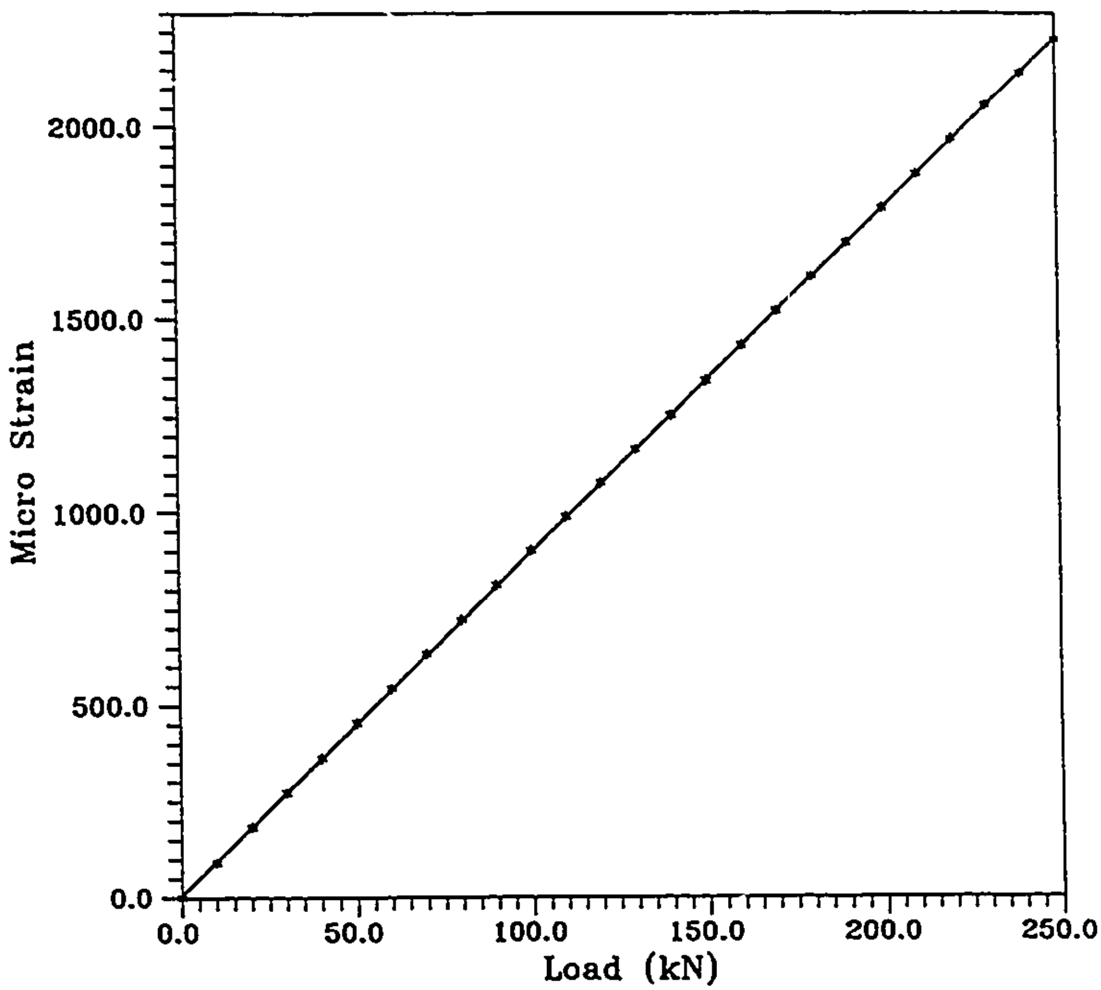

CALIBRATION CURVE FOR
THE 448 kN CAPACITY LOAD CELL

FIGURE 3.17

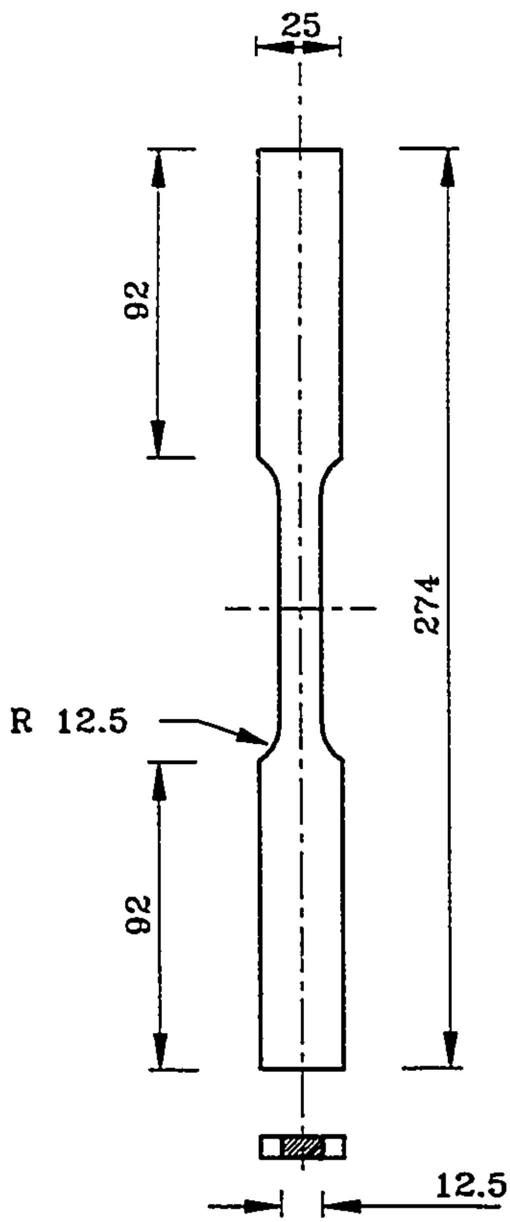

THE TENSION TEST SPECIMEN

FIGURE 3.18

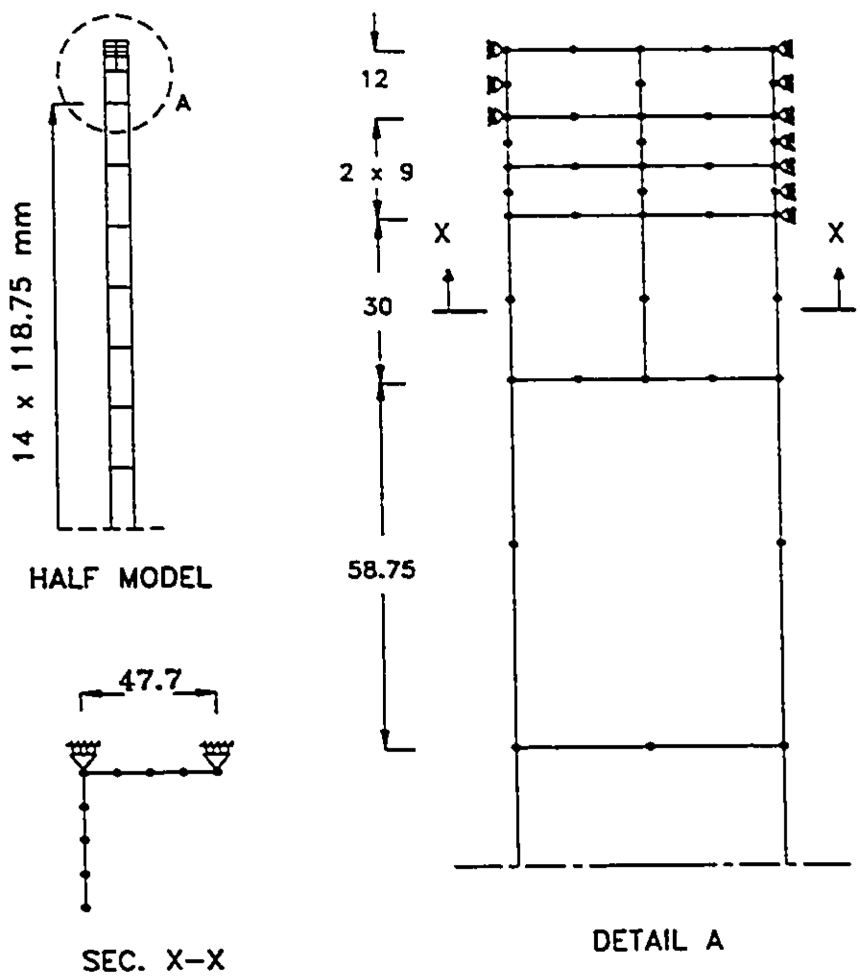

FINITE ELEMENT MODEL FOR SLENDER SPECIMENS

HINGED AT THE WELDED NODES (UNBALANCED CASE)

FIGURE 4.1

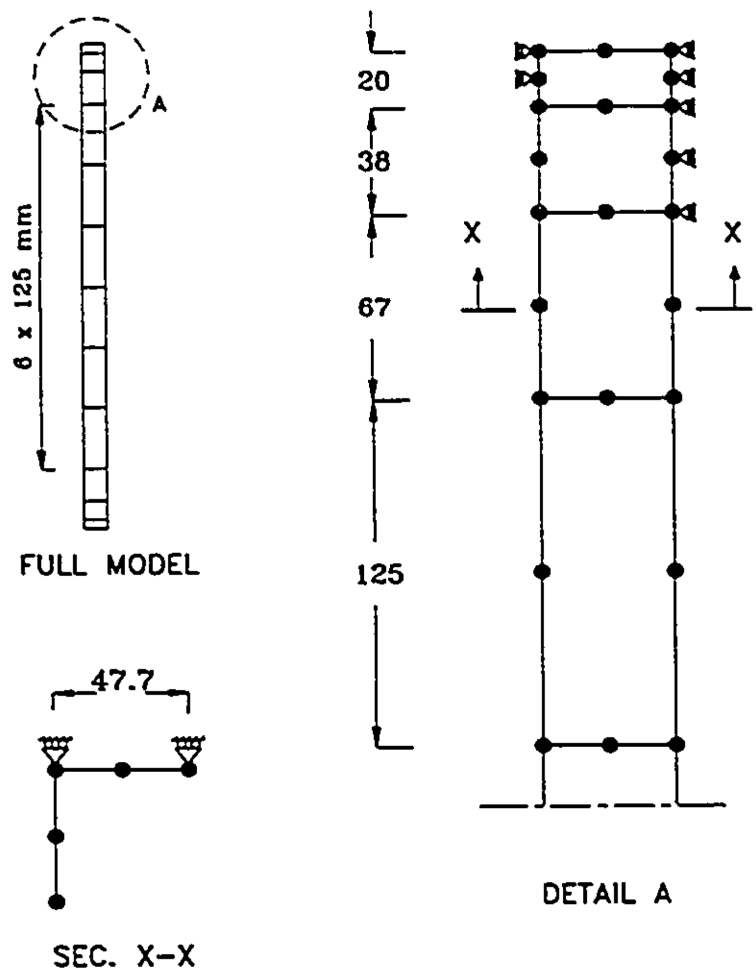

FINITE ELEMENT MODEL FOR INTERMEDIATE LENGTH SPECIMENS

HINGED AT THE WELDED NODES (UNBALANCED CASE)

FIGURE 4.2

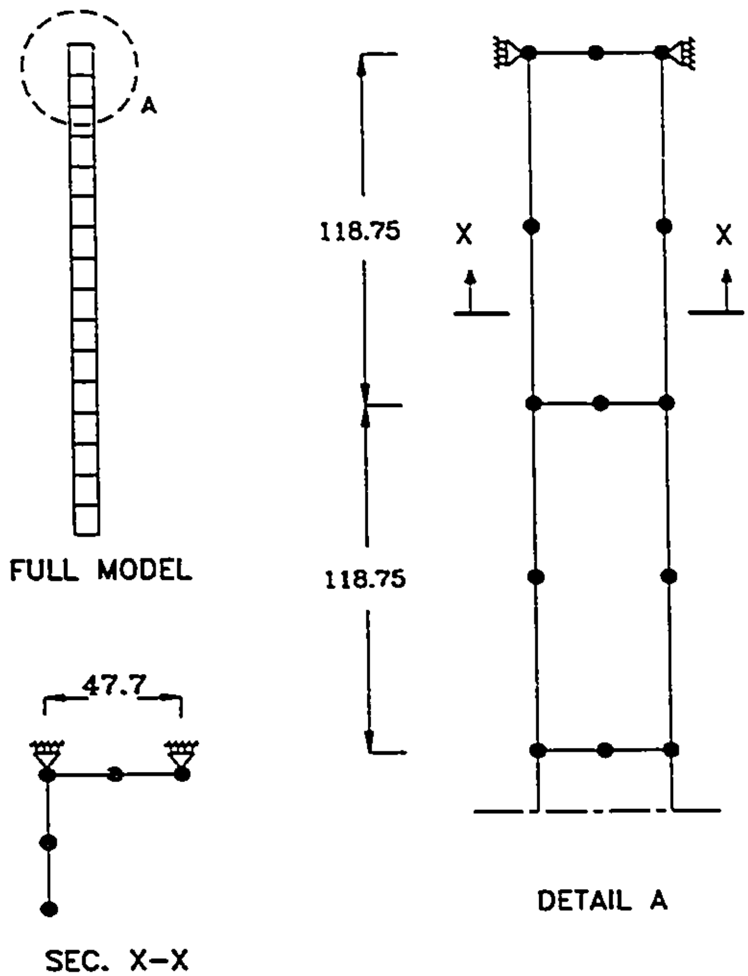

FINITE ELEMENT MODEL FOR SLENDER SPECIMENS

HINGED AT THE END POINTS OF THE EDGE OF THE WELDED LEG

FIGURE 4.3

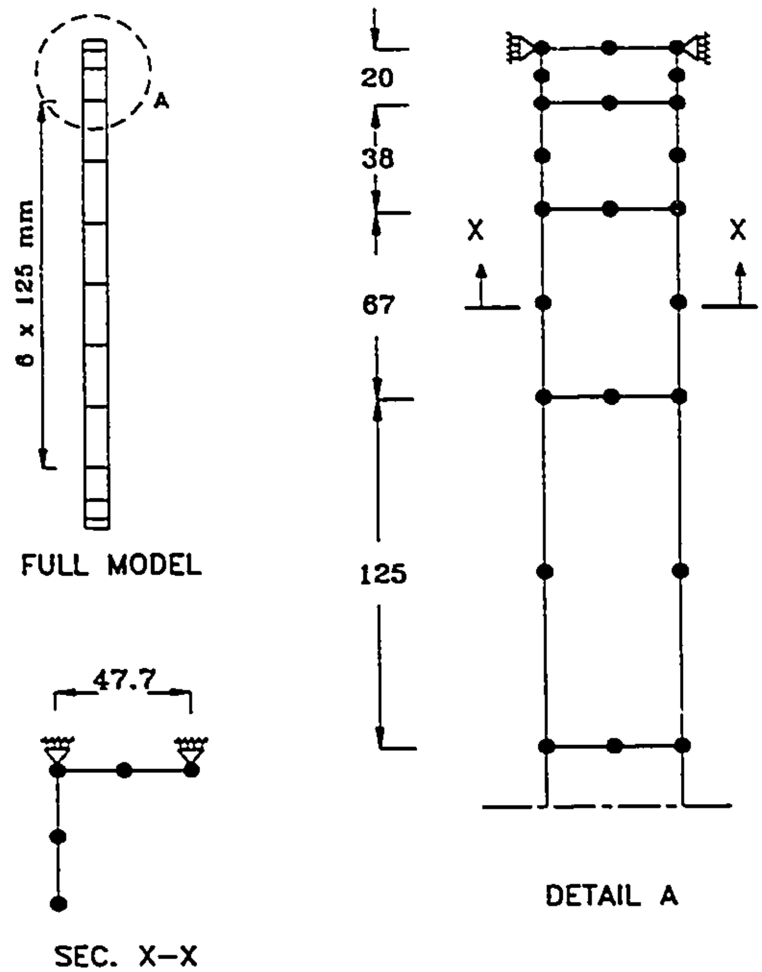

FINITE ELEMENT MODEL FOR INTERMEDIATE LENGTH SPECIMENS

HINGED AT THE END POINTS OF THE EDGE OF THE WELDED LEG

FIGURE 4.4

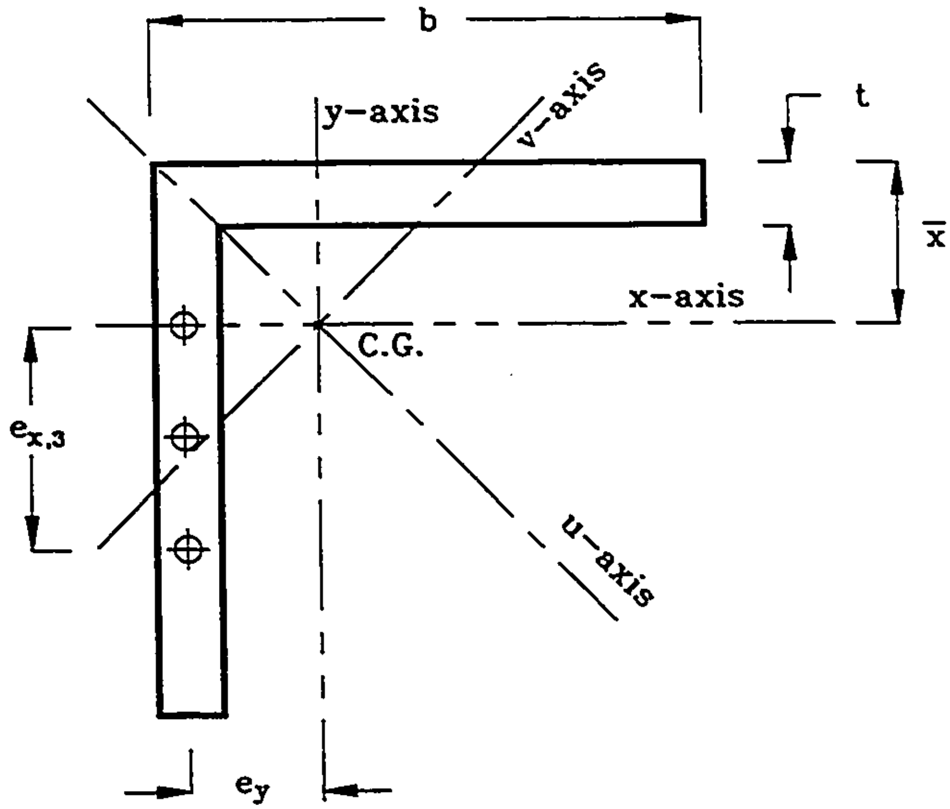

IDEALIZED RECTANGULAR CROSS−SECTION

FIGURE 4.5

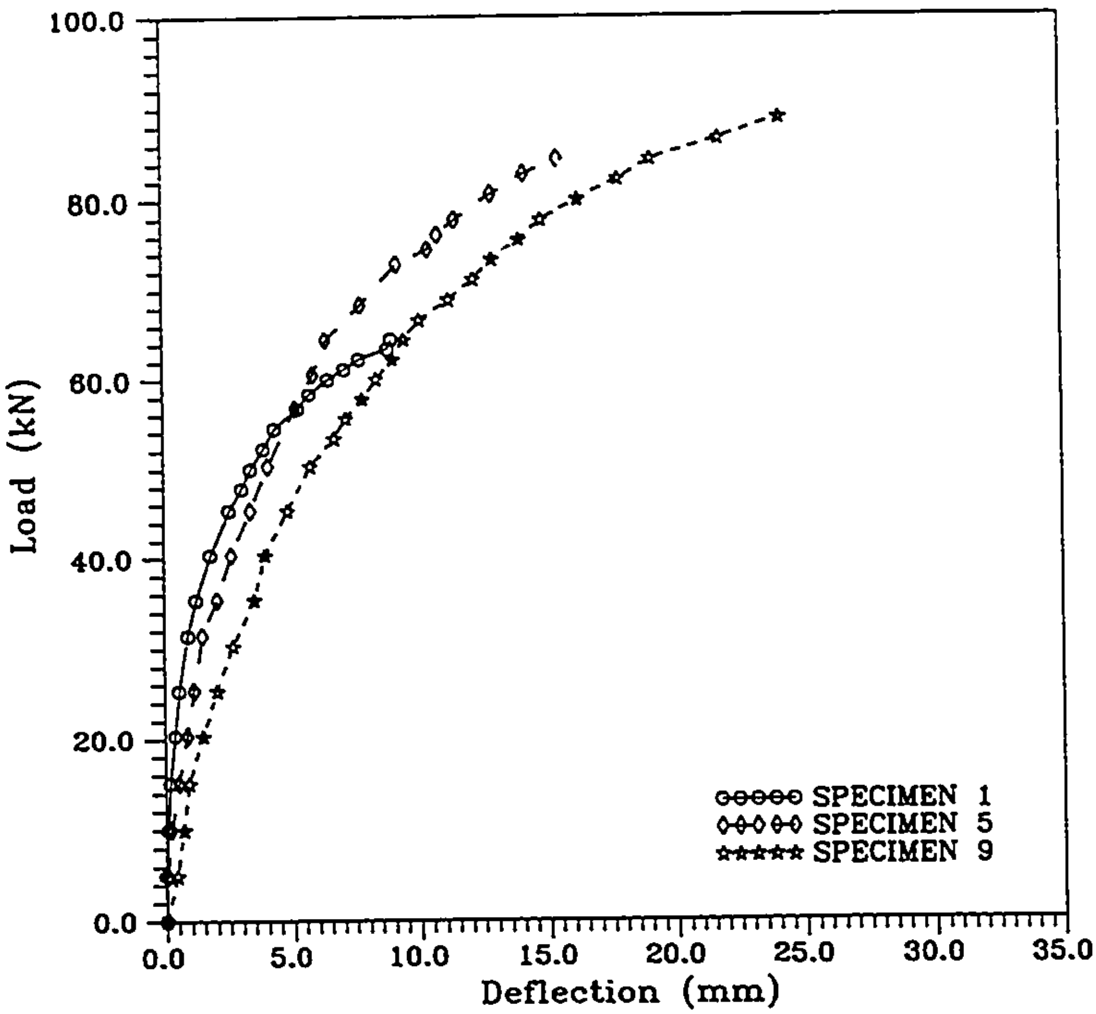

COMPARISON BETWEEN THE
LOAD-DEFLECTION CURVES FOR
SPECIMENS 1, 5, AND 9
SLENDER SPECIMENS – DIAL GAUGE D

FIGURE 5.1

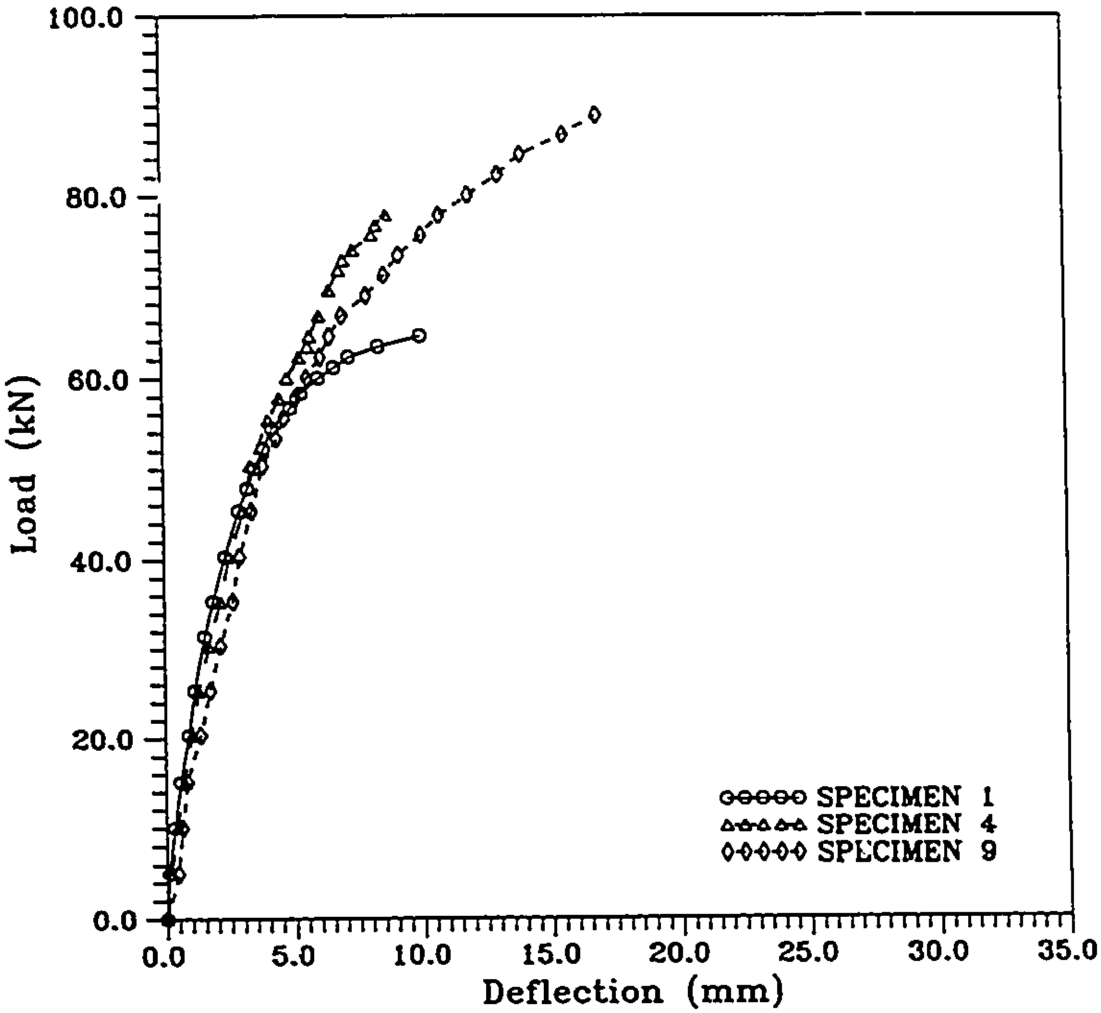

COMPARISON BETWEEN THE
LOAD-DEFLECTION CURVES FOR
SPECIMENS 1, 4, AND 9
SLENDER SPECIMENS - DIAL GAUGE C

FIGURE 5.2

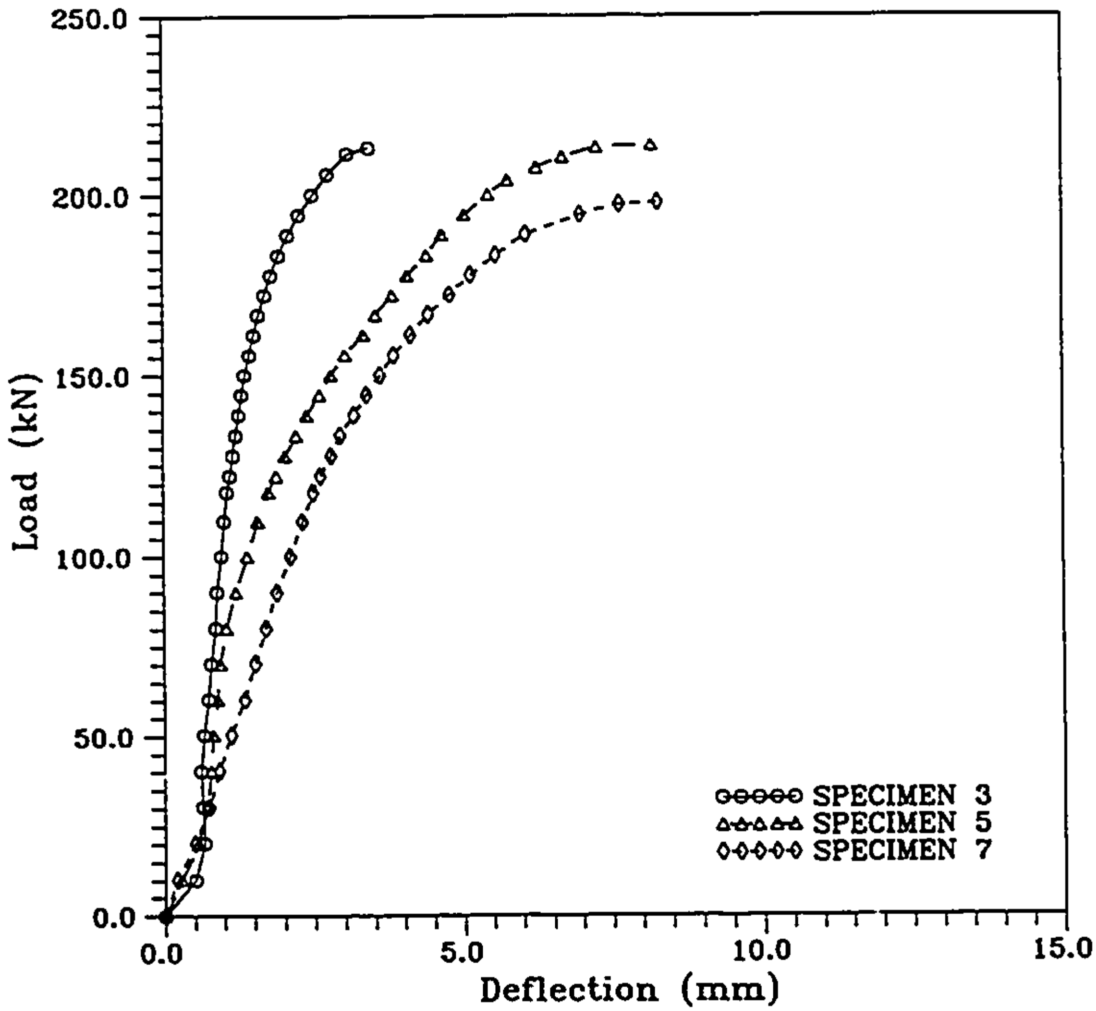

COMPARISON BETWEEN THE LOAD-DEFLECTION CURVES FOR SPECIMENS 3, 5, AND 7 INTERMEDIATE LENGTH SPECIMENS DIAL GAUGE D

FIGURE 5.3

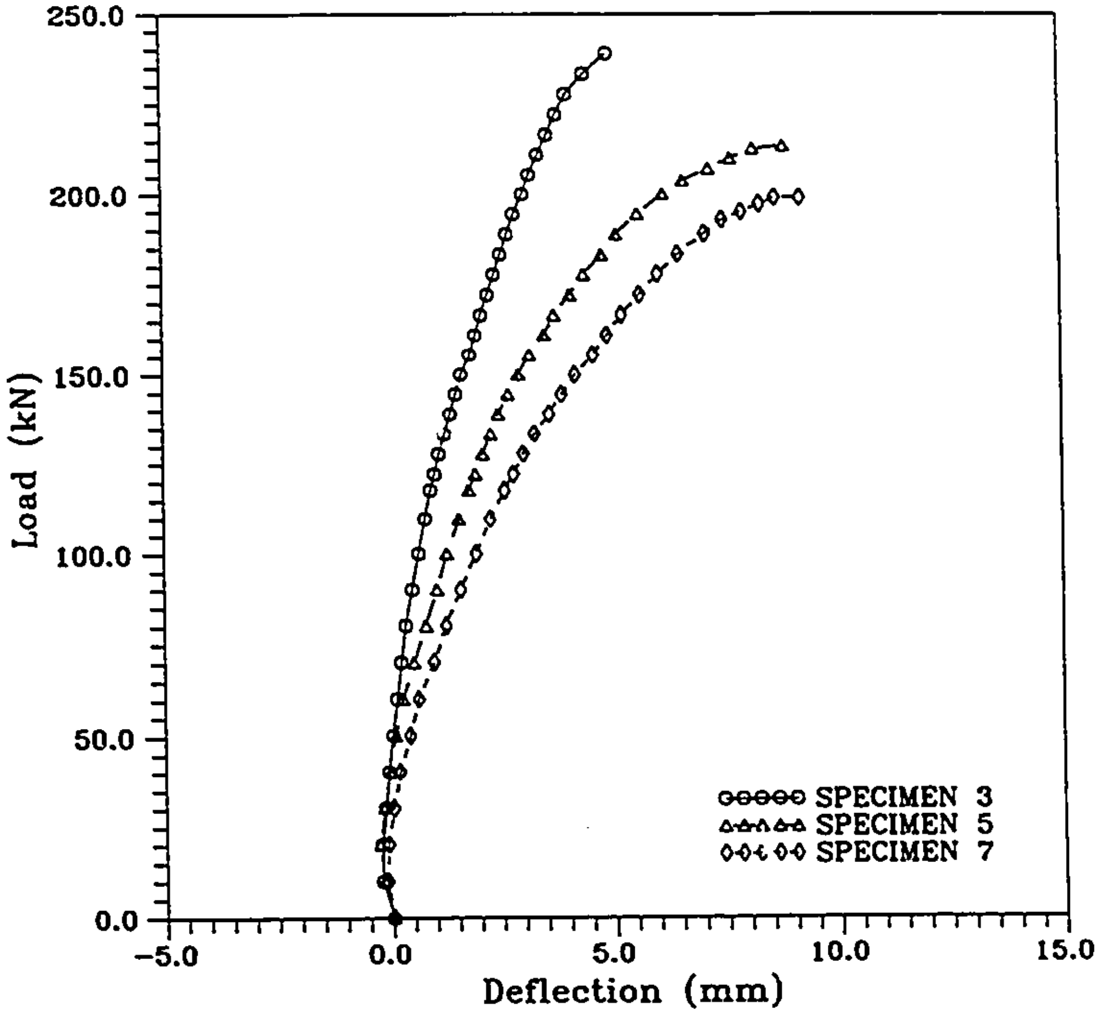

COMPARISON BETWEEN THE LOAD-DEFLECTION CURVES FOR SPECIMENS 2, 5, AND 9 INTERMEDIATE LENGTH SPECIMENS DIAL GAUGE C

FIGURE 5.4

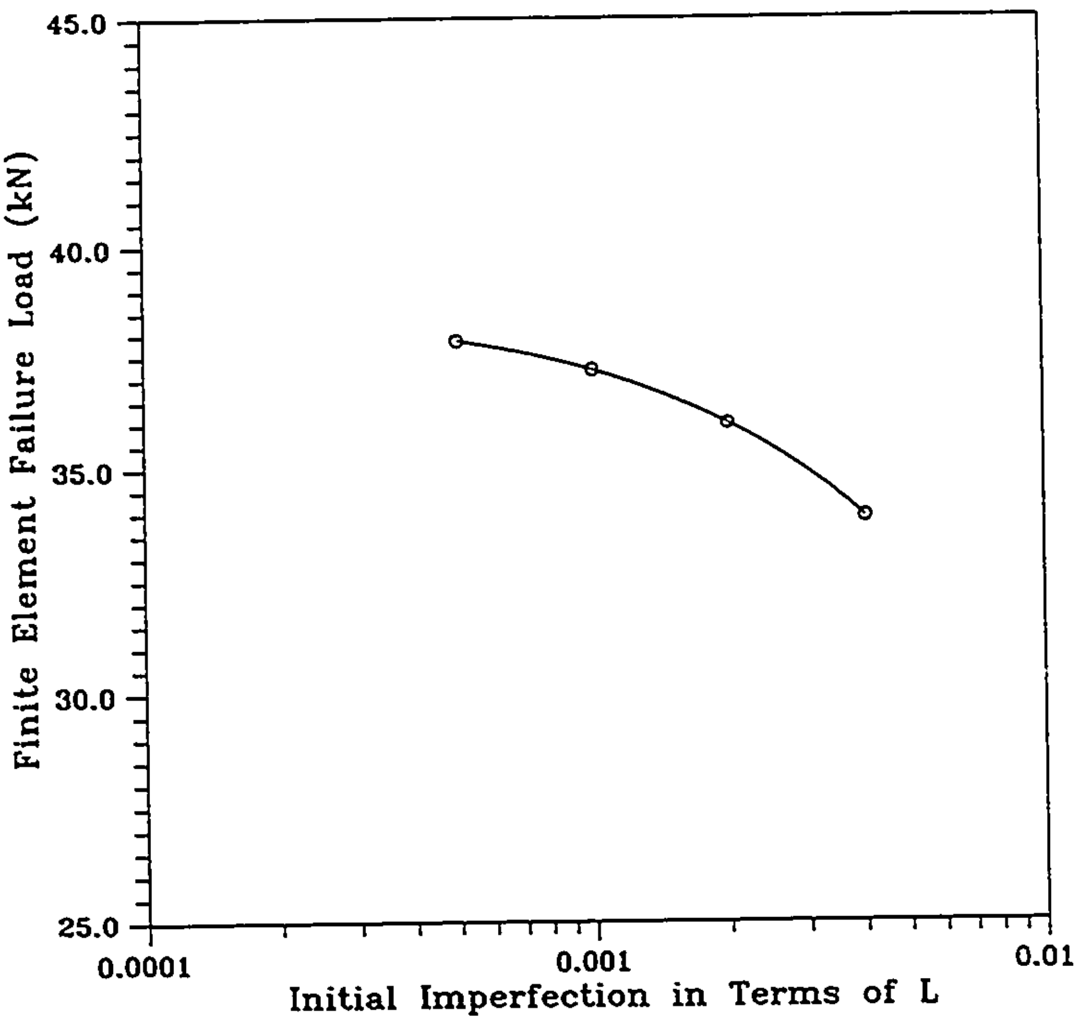

EFFECT OF INITIAL IMPERFECTION
ON FINITE ELEMENT FAILURE LOADS
SLENDER SPECIMENS

FIGURE 5.5

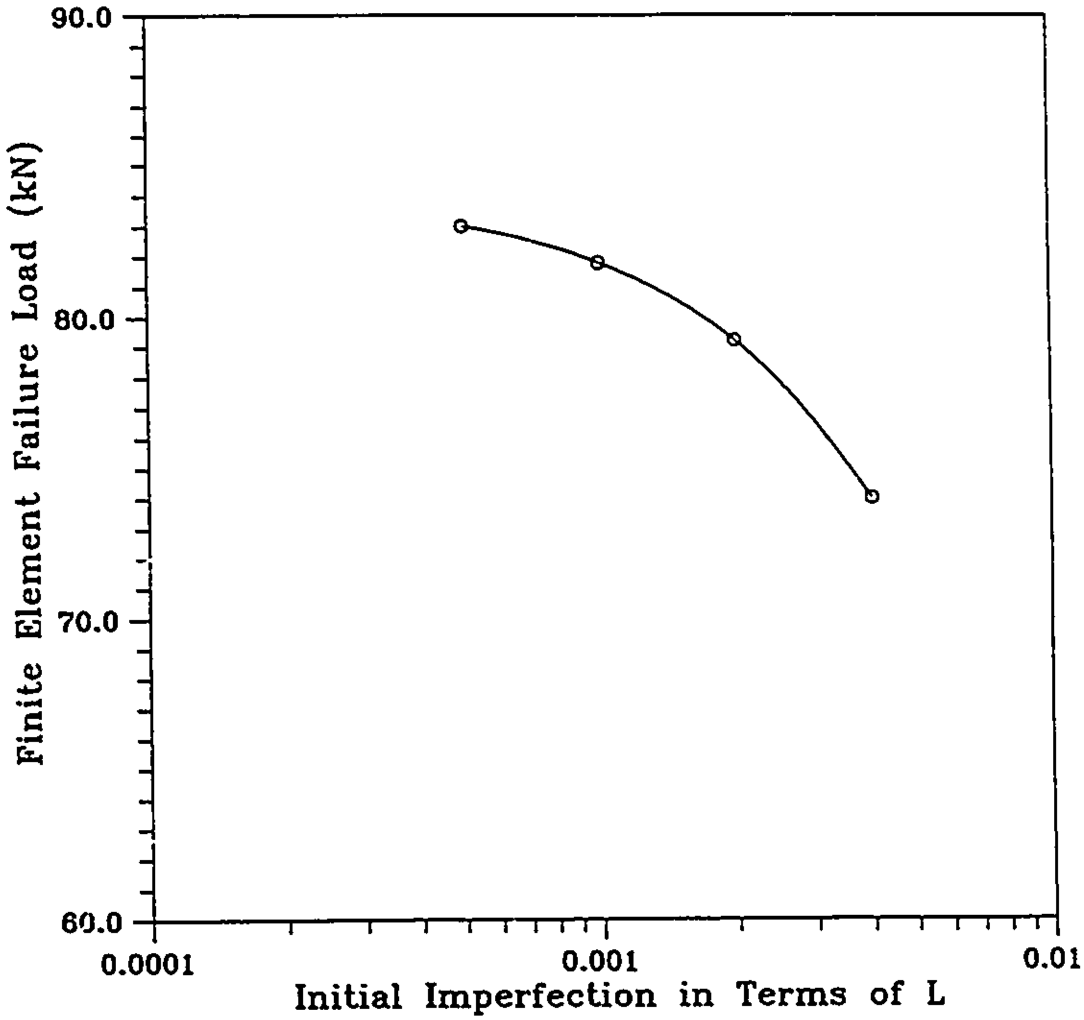

EFFECT OF INITIAL IMPERFECTION
ON FINITE ELEMENT FAILURE LOADS
INTERMEDIATE LENGTH SPECIMENS

FIGURE 5.6

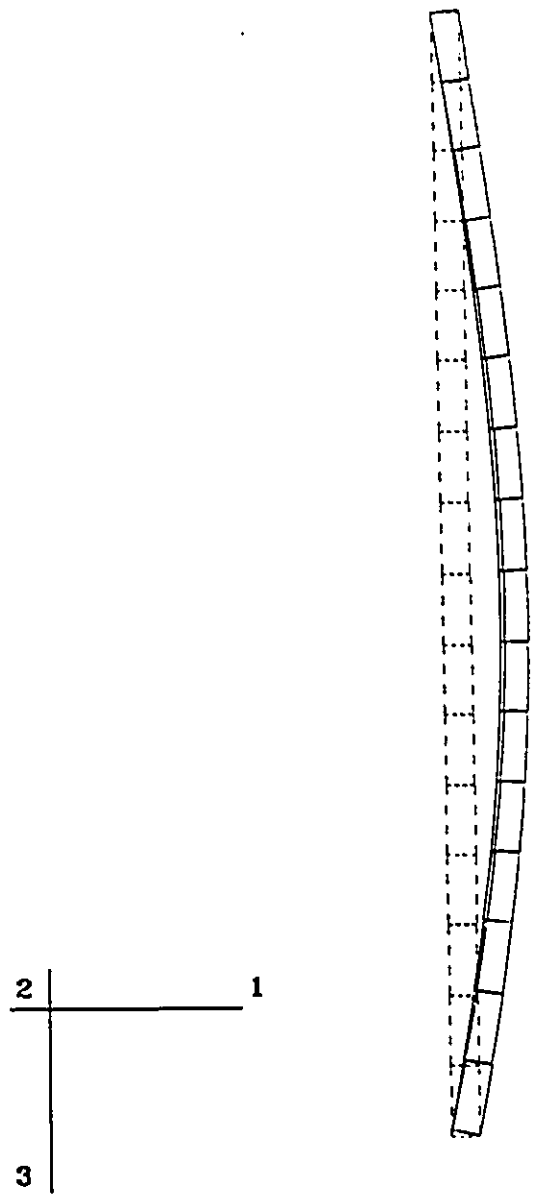

TYPICAL DEFORMED SHAPE
FOR A SLENDER SPECIMEN

FIGURE 5.7

TABLE 1. NOMINAL CROSS-SECTIONAL PROPERTIES

Properties	Units	Nominal Values
b	mm	50.8
t	mm	6.35
x or y	mm	15.1
A	mm^2	612.0
I_x or I_y	mm^4	147 000
r_x or r_y	mm	15.5
I_u	mm^4	233 650
r_u	mm	19.54
I_v	mm^4	60 350
r_v	mm	9.93

TABLE 2. MECHANICAL PROPERTIES OF STEEL

Properties	Specimens 1	Specimens 2	Specimens 3	Average
Cross Section Area (mm^2)	75.88	76.50	76.51	---
Yield Load (kN)	28.0	27.6	28.2	---
Yield Stress (MPa)	369.0	360.8	368.6	366.1
Modulus of Elasticity (MPa)	196 300	196 600	190 800	194 600

TABLE 3. EXPERIMENTAL RESULTS

FOR SLENDER SPECIMENS

* C_r= 31.0 kN (from CAN/CSA-S16.1-M89 for K=1.0)

No.	Failure Load (kN)	Average Failure Load (kN)	Average Length Factor K	Type of Weld	Ratio With Respect to Balanced Weld
1	32.2				
2	34.5	33.9	0.936	Balanced	1.00
3	35.0				
4	38.9				
5	42.2	42.6	0.830	Equal	1.25
6	46.7				
7	45.0				
8	46.1	45.2	0.803	Unbalanced	1.33
9	44.5				

TABLE 4. EXPERIMENTAL RESULTS

FOR INTERMEDIATE LENGTH SPECIMENS

* C_r= 89.0 kN (from CAN/CSA-S16.1-M89 for K=1.0)

No.	Failure Load (kN)	Average Failure Load (kN)	Average Length Factor K	Type of Weld	Ratio With Respect to Balanced Weld
1	107.8				
2	119.5	111.2	0.835	Balanced	1.00
3	106.4				
4	98.5				
5	106.7	105.0	0.871	Equal	0.95
6	110.0				
7	98.9				
8	101.4	99.9	0.91	Unbalanced	0.90
9	99.5				

TABLE 5. EXPERIMENTAL DEFLECTIONS CORRESPONDING TO THE COMPRESSIVE RESISTANCE AS GIVEN BY CAN/CSA-S16.1-M89 FOR K=1.0 FOR SLENDER SPECIMENS

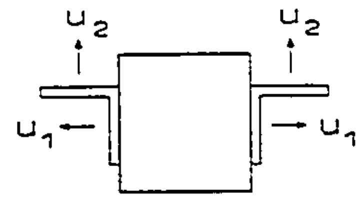

* C_r= 31.0 kN (from CAN/CSA-S16.1-M89 for K=1.0)

No.	Displacement mm		Type	Average Displacement mm	
	Avg. u_1	Avg. u_2		u_1	u_2
1	6.5	3.0	Balanced	4.9	2.0
2	4.5	2.0			
3	3.8	1.0			
4	5.6	0.5	Equal	4.9	1.0
5	6.0	2.0			
6	3.0	0.5			
7	5.5	1.0	Unbalanced	6.5	1.7
8	6.5	1.0			
9	7.5	3.0			

TABLE 6. EXPERIMENTAL DEFLECTIONS CORRESPONDING TO THE COMPRESSIVE RESISTANCE AS GIVEN BY CAN/CSA-S16.1-M89 FOR K=1.0 FOR INTERMEDIATE LENGTH SPECIMENS

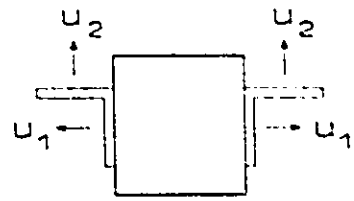

* C_r= 89.0 kN (from CAN/CSA-S16.1-M89 for K=1.0)

No.	Displacement mm		Type	Average Displacement mm	
	Avg. u_1	Avg. u_2		u_1	u_2
1	1.7	0.3	Balanced	1.8	0.6
2	1.6	0.4			
3	2.2	1.2			
4	6.0	2.5	Equal	4.7	2.0
5	4.5	2.0			
6	3.5	1.5			
7	5.0	2.0	Unbalanced	5.7	2.5
8	6.0	2.5			
9	6.0	3.0			

TABLE 7. INITIAL IMPERFECTION FOR SLENDER SPECIMENS AT MID-HEIGHT

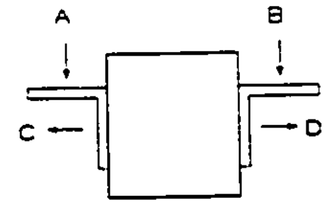

Type of Weld	Specimen No.	A	B	C	D	Failure Load (kN)
Balanced Weld	1	2.34	2.90	1.30	0.80	32.2
	2	4.30	1.50	3.40	2.50	35.0
	3	2.16	2.28	2.50	2.36	33.3
Equal Weld	4	2.45	2.45	3.00	2.32	38.9
	5	1.96	1.78	1.26	1.12	42.2
	6	1.08	0.91	1.14	1.18	46.7
Unbalanced Weld	7	2.32	1.38	2.65	0.60	45.0
	8	1.48	2.14	2.08	1.80	46.1
	9	1.25	1.40	0.65	1.96	44.4

TABLE 8. INITIAL IMPERFECTION FOR INTERMEDIATE LENGTH SPECIMENS AT MID-HEIGHT

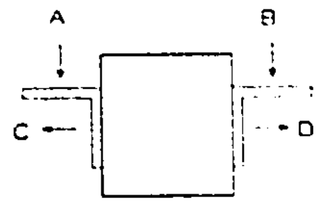

Type of Weld	Specimen No.	A	B	C	D	Failure Load (kN)
Balanced Weld	1	1.02	1.10	0.96	1.50	107.8
	2	1.72	1.00	3.00	0.35	119.4
	3	0.60	0.70	0.90	1.50	106.4
Equal Weld	4	0.85	1.20	1.30	1.40	98.4
	5	0.70	0.80	0.90	1.00	106.7
	6	0.70	0.70	1.00	1.10	110.0
Unbalanced Weld	7	1.00	0.70	1.02	0.75	98.9
	8	0.60	0.75	1.00	0.95	101.4
	9	0.40	0.65	0.65	0.88	99.4

TABLE 9. COMPARISON BETWEEN FINITE ELEMENT MODELLING RESULTS AND THE EXPERIMENTAL RESULTS FOR SLENDER SPECIMENS

	Balanced	Equal	Unbalanced
Finite Element Failure Loads (kN)	37.2	39.4	42.0
Ratio with Respect to the Balanced Case	1.00	1.06	1.13
Experimental Failure Loads (kN)	34.0	42.6	45.2
Ratio with Respect to the Balanced Case	1.00	1.25	1.33
Finite Element Displacement Ratio u_1:u_2	2.62 : 1	3.47 : 1	5.92 : 1
Experimental Displacement Ratio u_1:u_2	2.45 : 1	4.86 : 1	3.82 : 1

TABLE 10. COMPARISON BETWEEN FINITE ELEMENT MODELLING RESULTS AND THE EXPERIMENTAL RESULTS FOR INTERMEDIATE LENGTH SPECIMENS

	Balanced	Equal	Unbalanced
Finite Element Failure Loads Model 1 (kN)	84.0	96.0	68.0
Finite Element Failure Loads Model 2 (kN)	201.2	197.0	152.0
Experimental Failure Loads (kN)	111.2	105.0	99.9

* Model 1 : angle is assumed to have double hinges at the ends of the welded leg.

* Model 2 : the displacements are assigned to zero at all the welded nodes.

TABLE 11. CALCULATED COMPRESSIVE RESISTANCE FOR SLENDER SPECIMENS BASED ON THE EXPERIMENTAL FAILURE AXIS

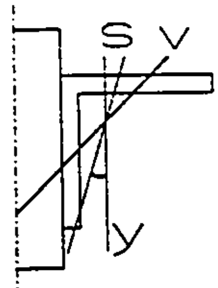

	Balanced	Equal	Unbalanced
$u_1:u_2$ mm	4.9 : 2.0	4.86 : 1	6.5 : 1.7
θ°	22.2	11.6	14.6
I_s mm^4	84 860	111 070	103 020
r_s mm	11.8	13.6	13.0
C_r kN	42.6	54.4	51.0
Experimental Results (kN)	33.9	42.6	45.2

Remarks :

1- C_r is calculated according to CAN/CSA-S16.1-M89 with ϕ=1.0

2- The inertia about the failure axis can be calculated as follows:

$$I_s = I_x - I_{xy} \cdot \sin 2\alpha$$

$$= 144\ 850 - 85{,}740 \sin 2\alpha$$

TABLE 12. CALCULATED COMPRESSIVE RESISTANCE FOR INTERMEDIATE LENGTH SPECIMENS BASED ON THE EXPERIMENTAL FAILURE AXIS

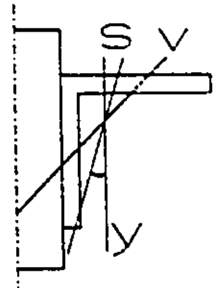

	Balanced	Equal	Unbalanced
$u_1 . u_2$ mm	1.8 : 0.6	4.67 : 2	5.7 : 2.5
θ°	18.4	23.2	23.7
I_s mm^4	93 490	82 750	81 730
r_s mm	12.4	11.7	11.6
C_r kN	120.0	110.6	109.6
Experimental Results (kN)	111.2	105.0	99.9

Remarks :

1- C_r is calculated according to CAN/CSA-S16.1-M89 with ϕ=1.0

2- The inertia about the failure axis can be calculated as follows:

$$I_s = I_x - I_{xy} \cdot \sin 2\alpha$$

$$= 144\ 850 - 85\ 740 \sin 2\alpha$$

TABLE 13. COMPARISON BETWEEN ALL RESULTS OBTAINED FOR THE LOAD CARRYING CAPACITIES OF SLENDER SPECIMENS

	Balanced	Equal	Unbalanced
Experimental Results (kN)	33.9	42.6	45.2
Finite Element Results (kN)	37.2	39.4	42.0
Beam Column Analysis (kN)	18.3	22.9	17.7
Hinged-hinged Column with K =1.0 (kN)	31.0	31.0	31.0

TABLE 14. COMPARISON BETWEEN ALL RESULTS OBTAINED FOR THE LOAD CARRYING CAPACITIES OF INTERMEDIATE LENGTH SPECIMENS

	Balanced	Equal	Unbalanced
Experimental Results (kN)	111.2	105.0	99.9
Finite Element Results Model 1 (kN)	84.0	96.0	68.0
Beam Column Analysis (kN)	37.2	50.0	33.2
Hinged-hinged Column with K =1.0 (kN)	89.0	89.0	89.0

* Model 1 : angle is assumed to have double hinges at the ends of the welded leg.

Appendix A

LOAD-DEFLECTION CURVES

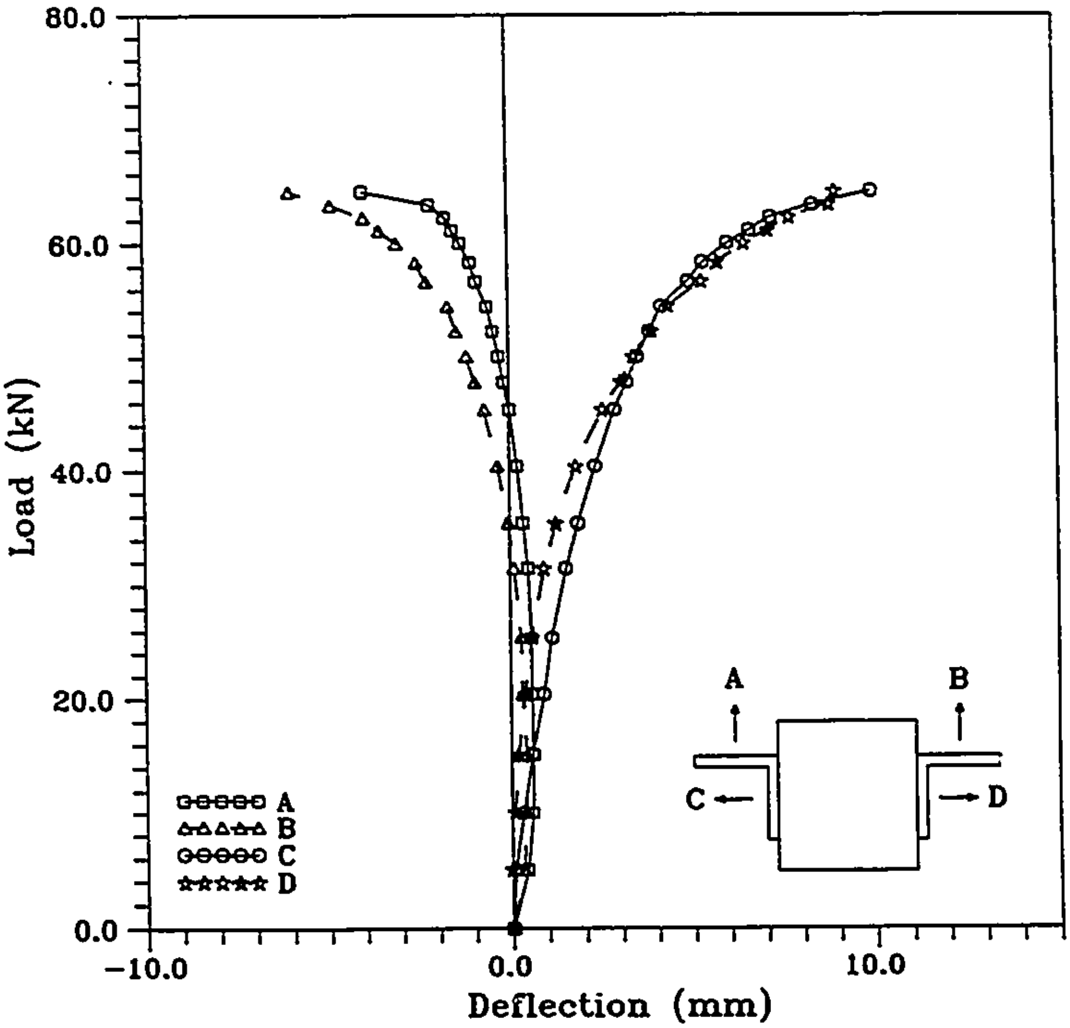

LOAD-DEFLECTION CURVES FOR SPECIMEN 1 - SLENDER SPECIMENS BALANCED WELD

FIGURE A.1

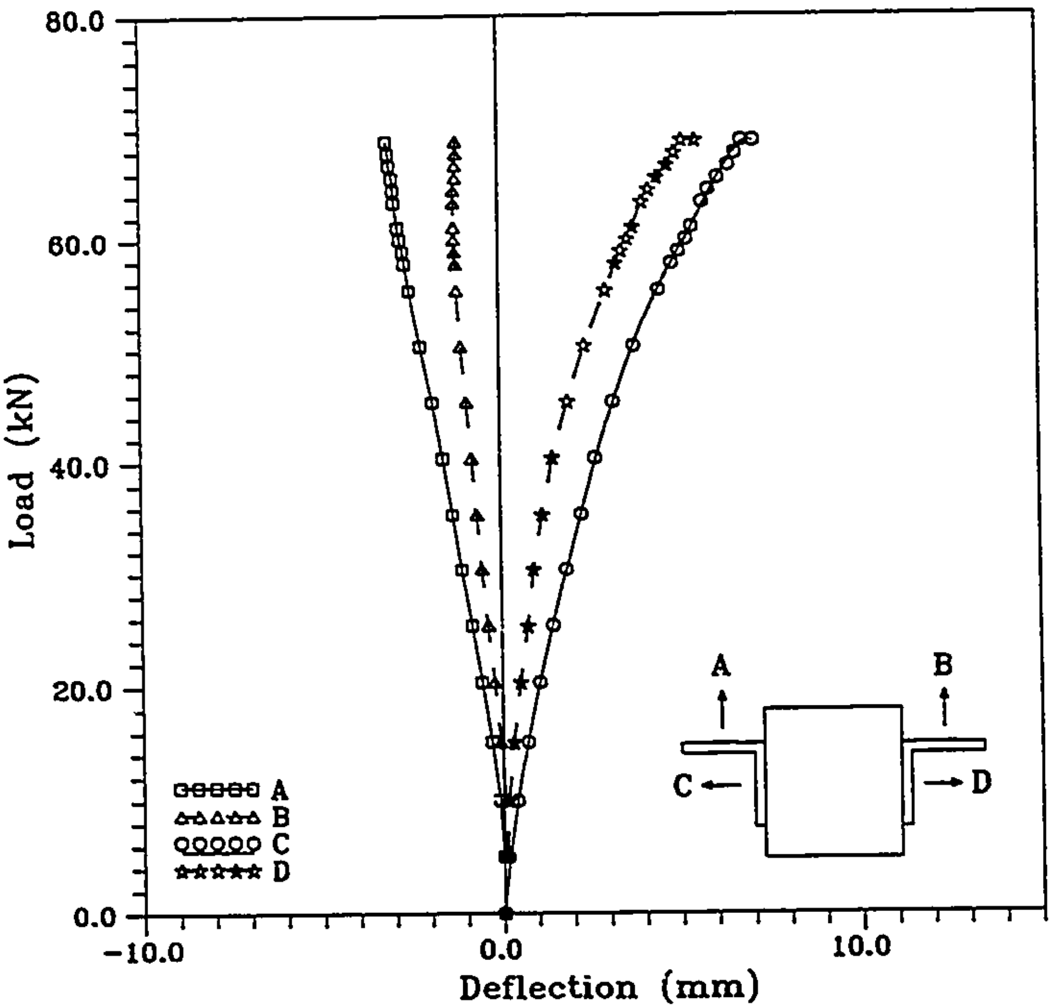

LOAD-DEFLECTION CURVES FOR SPECIMEN 2 - SLENDER SPECIMENS BALANCED WELD

FIGURE A.2

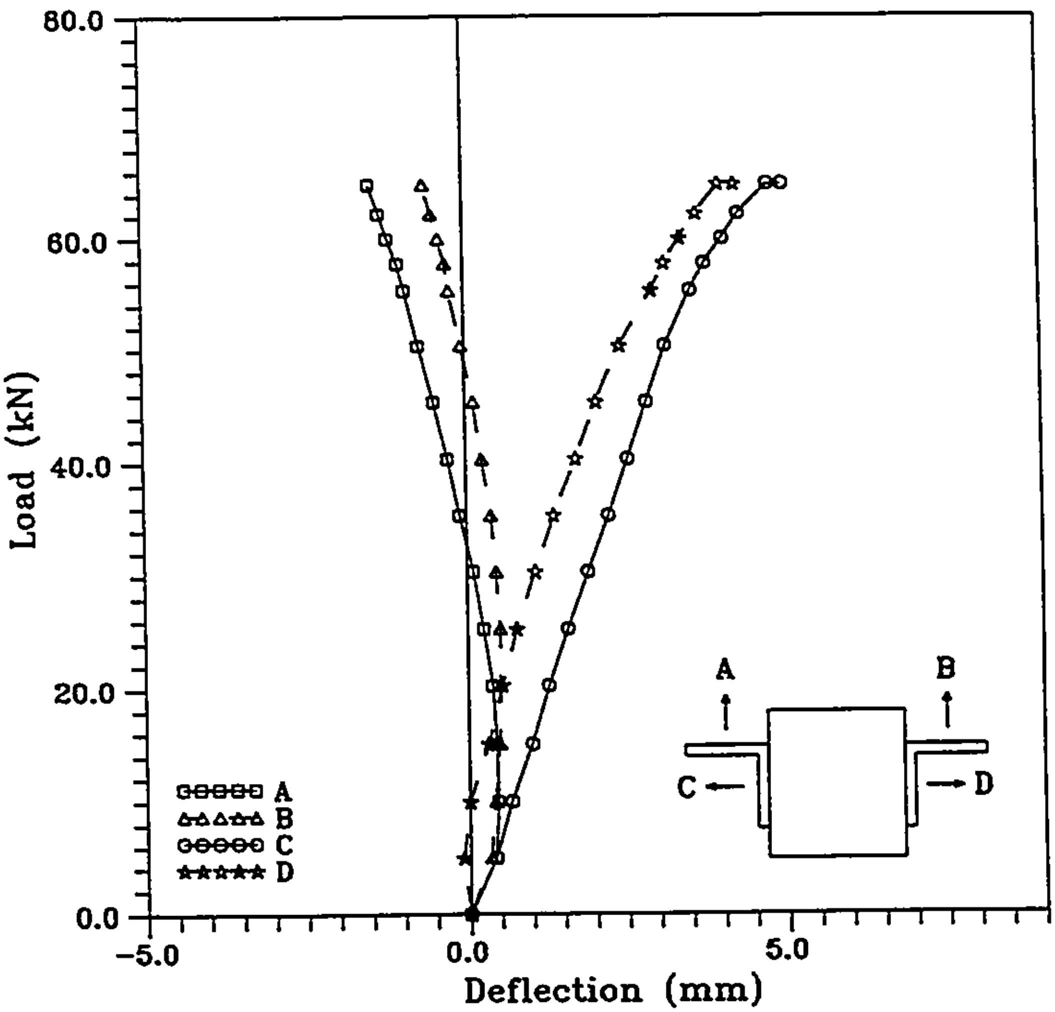

LOAD-DEFLECTION CURVES FOR SPECIMEN 3 - SLENDER SPECIMENS BALANCED WELD

FIGURE A.3

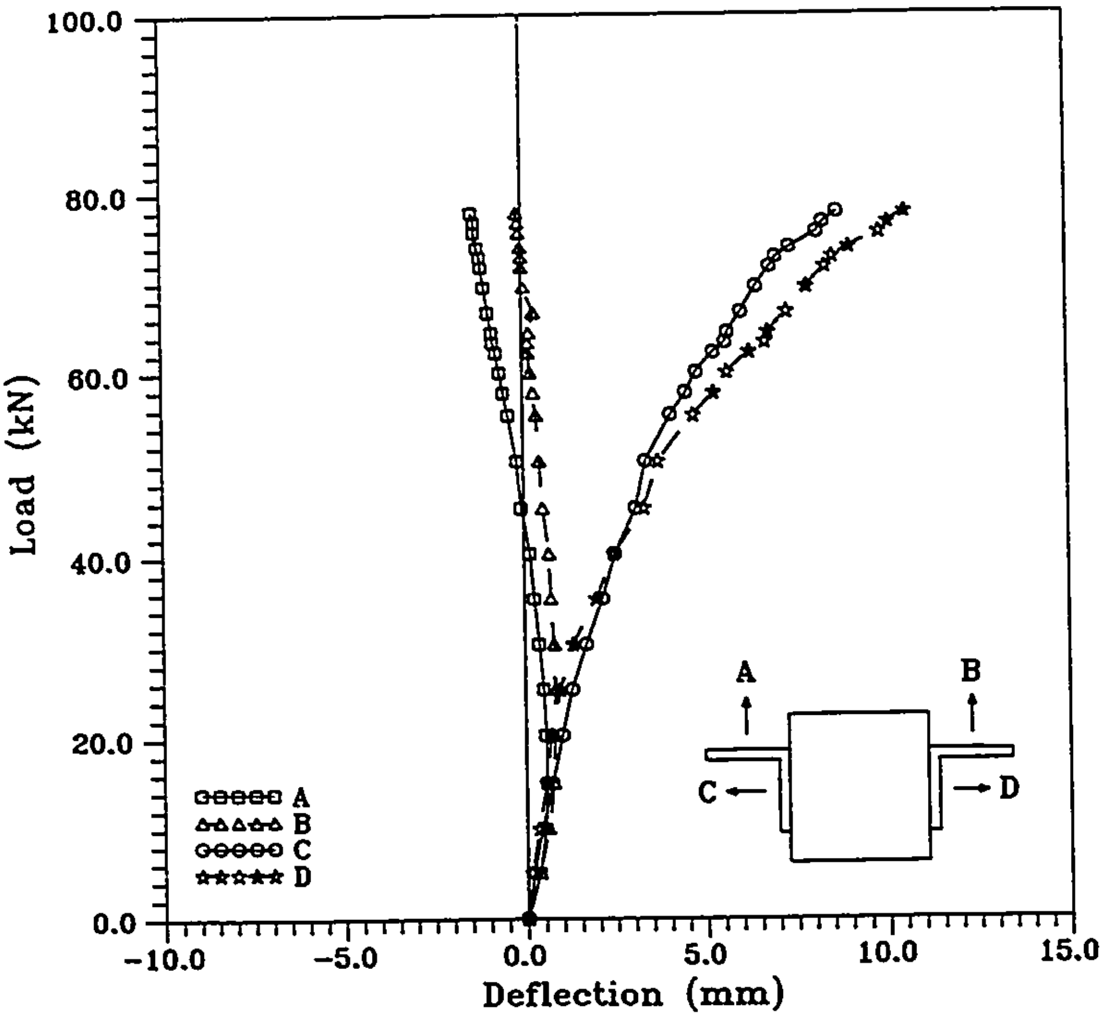

LOAD-DEFLECTION CURVES FOR SPECIMEN 4 - SLENDER SPECIMENS EQUAL WELD

FIGURE A.4

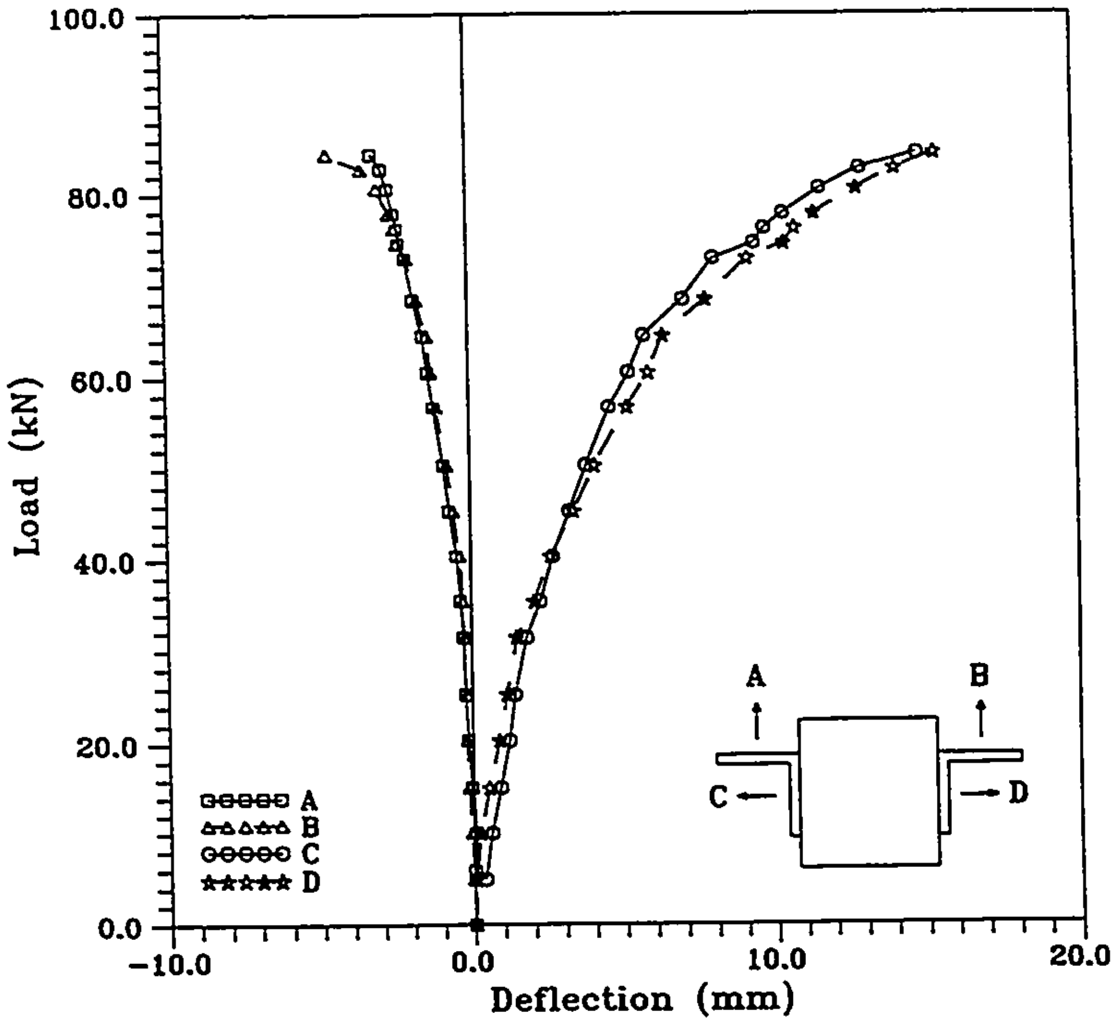

LOAD-DEFLECTION CURVES FOR SPECIMEN 5 - SLENDER SPECIMENS EQUAL WELD

FIGURE A.5

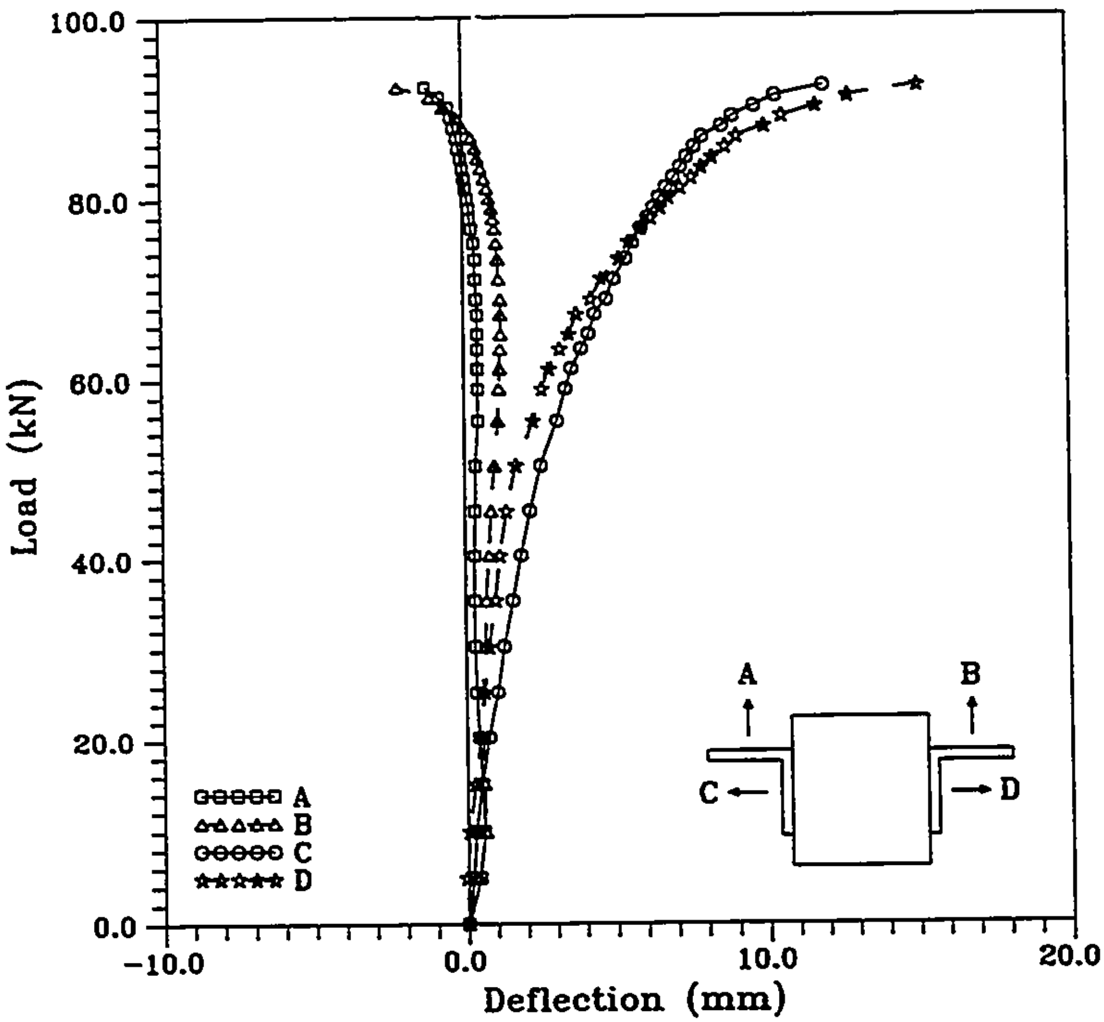

LOAD-DEFLECTION CURVES FOR SPECIMEN 6 - SLENDER SPECIMENS EQUAL WELD

FIGURE A.6

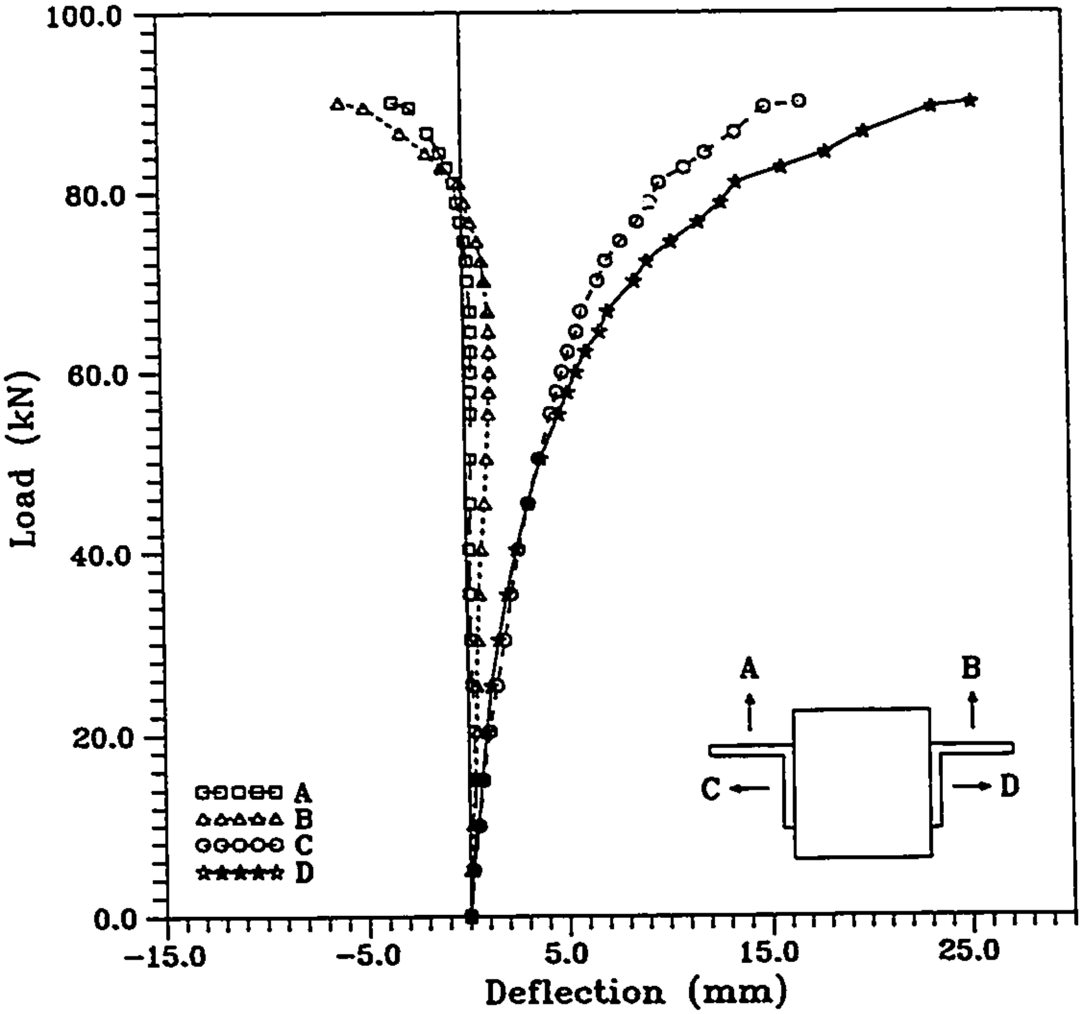

LOAD-DEFLECTION CURVES FOR SPECIMEN 7 - SLENDER SPECIMENS UNBALANCED WELD

FIGURE A.7

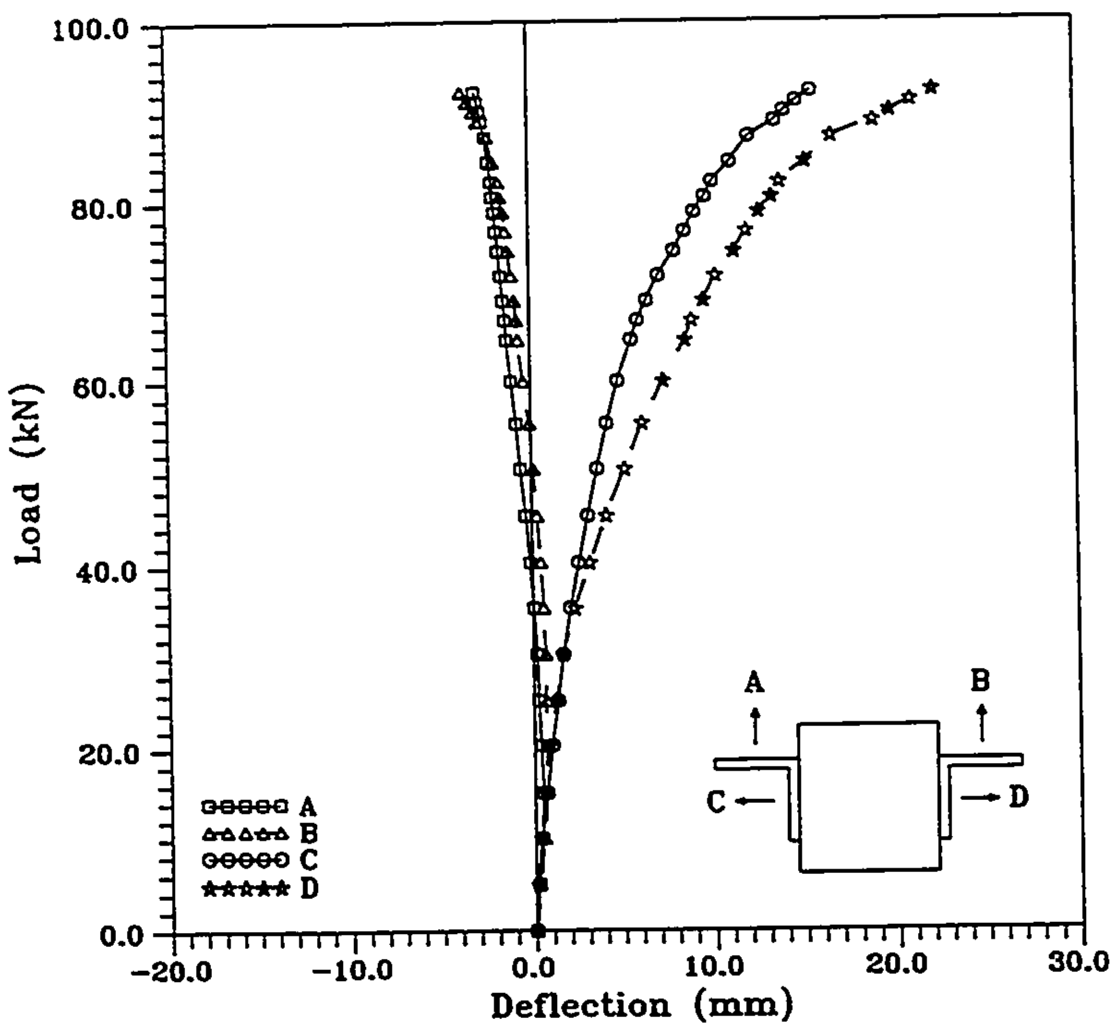

LOAD-DEFLECTION CURVES FOR SPECIMEN 8 - SLENDER SPECIMENS UNBALANCED WELD

FIGURE A.8

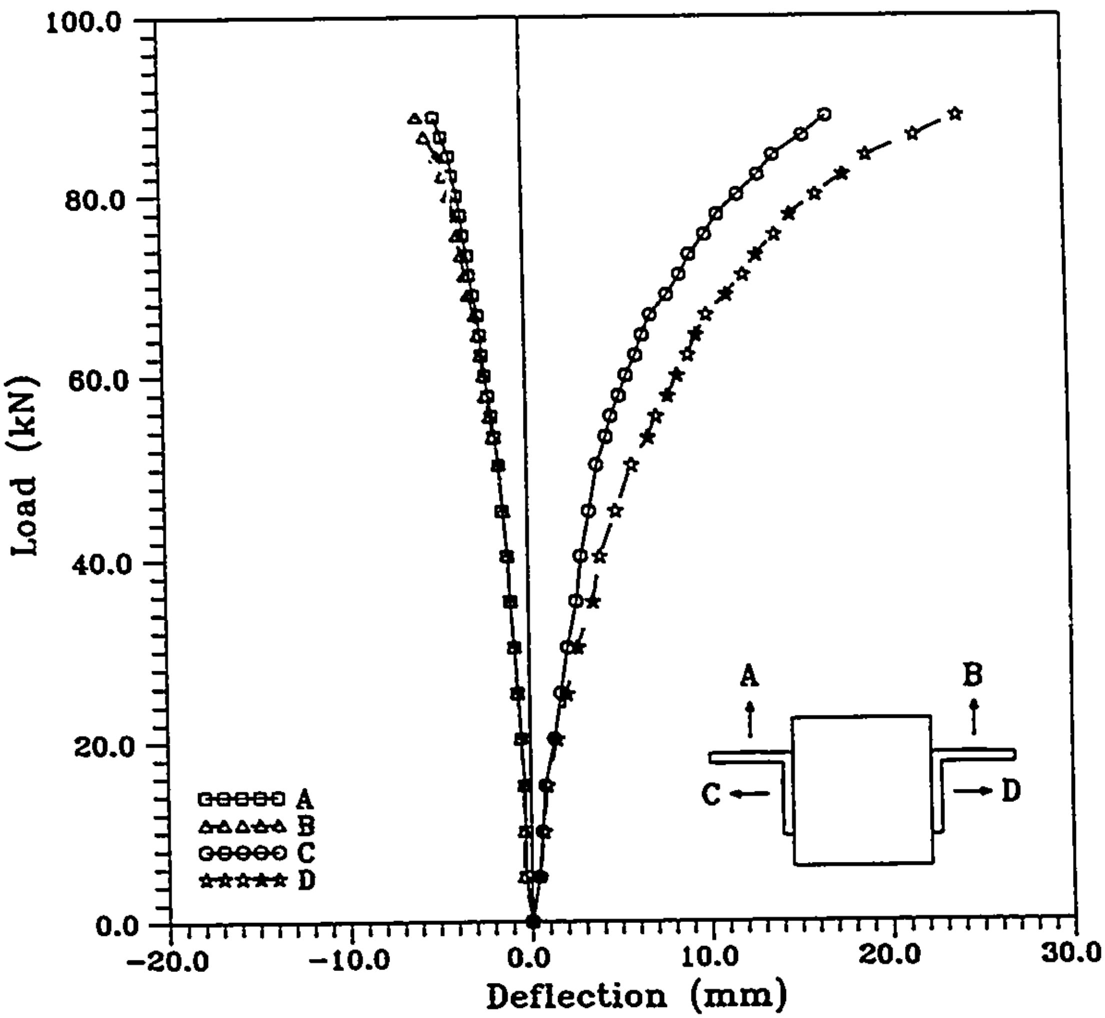

LOAD-DEFLECTION CURVES FOR SPECIMEN 9 - SLENDER SPECIMENS UNBALANCED WELD

FIGURE A.9

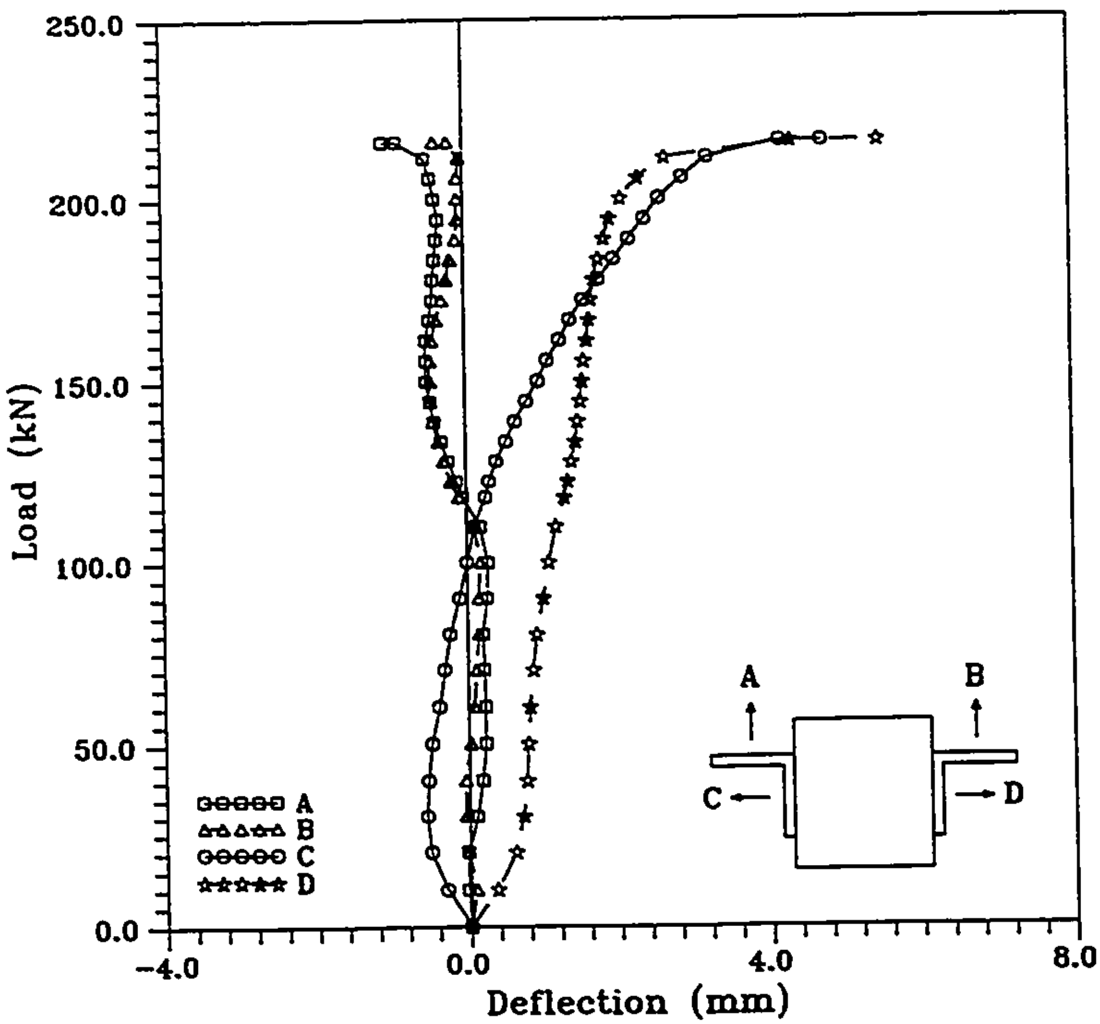

LOAD-DEFLECTION CURVES FOR SPECIMEN 1 - INTERMEDIATE LENGTH SPECIMENS BALANCED WELD

FIGURE A.10

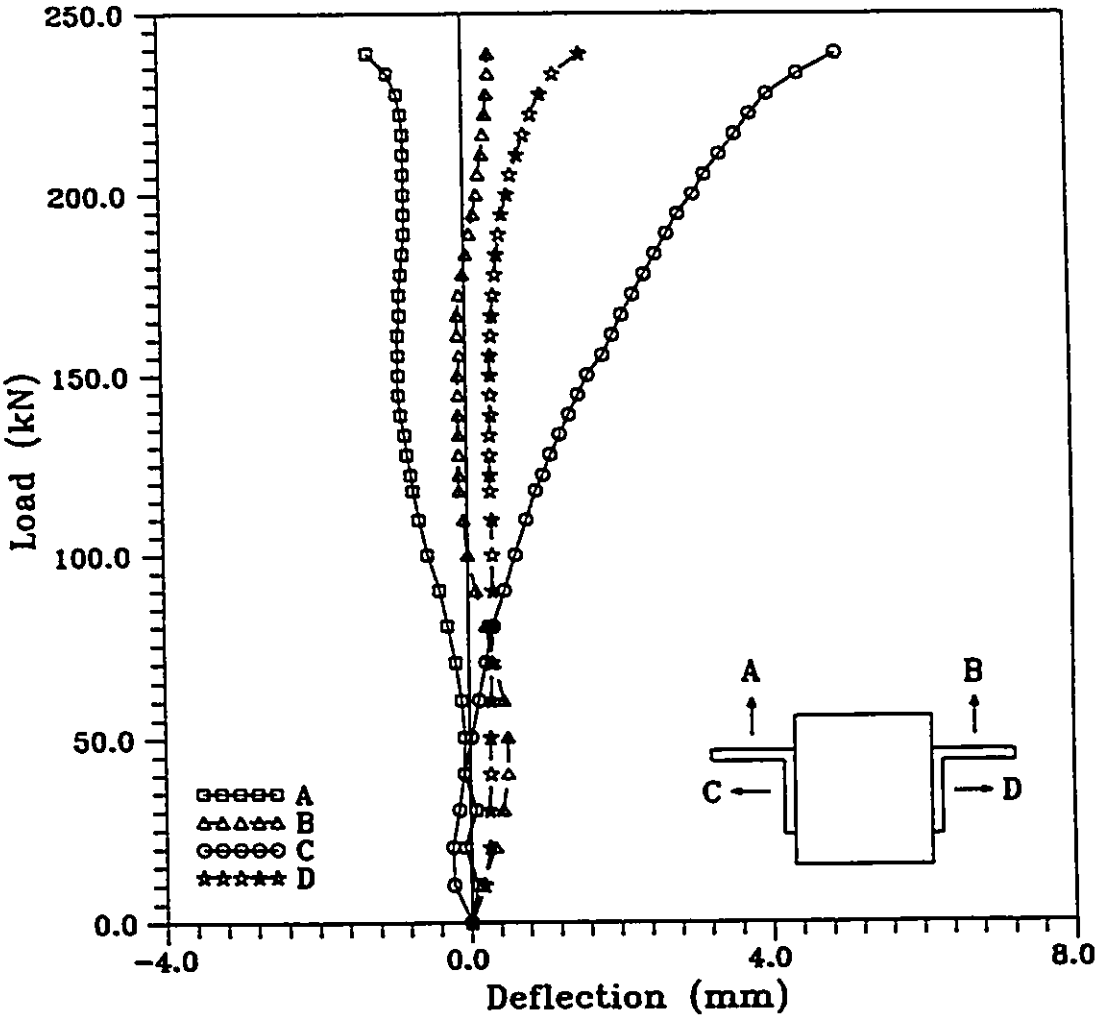

LOAD-DEFLECTION CURVES FOR SPECIMEN 2 - INTERMEDIATE LENGTH SPECIMENS BALANCED WELD

FIGURE A.11

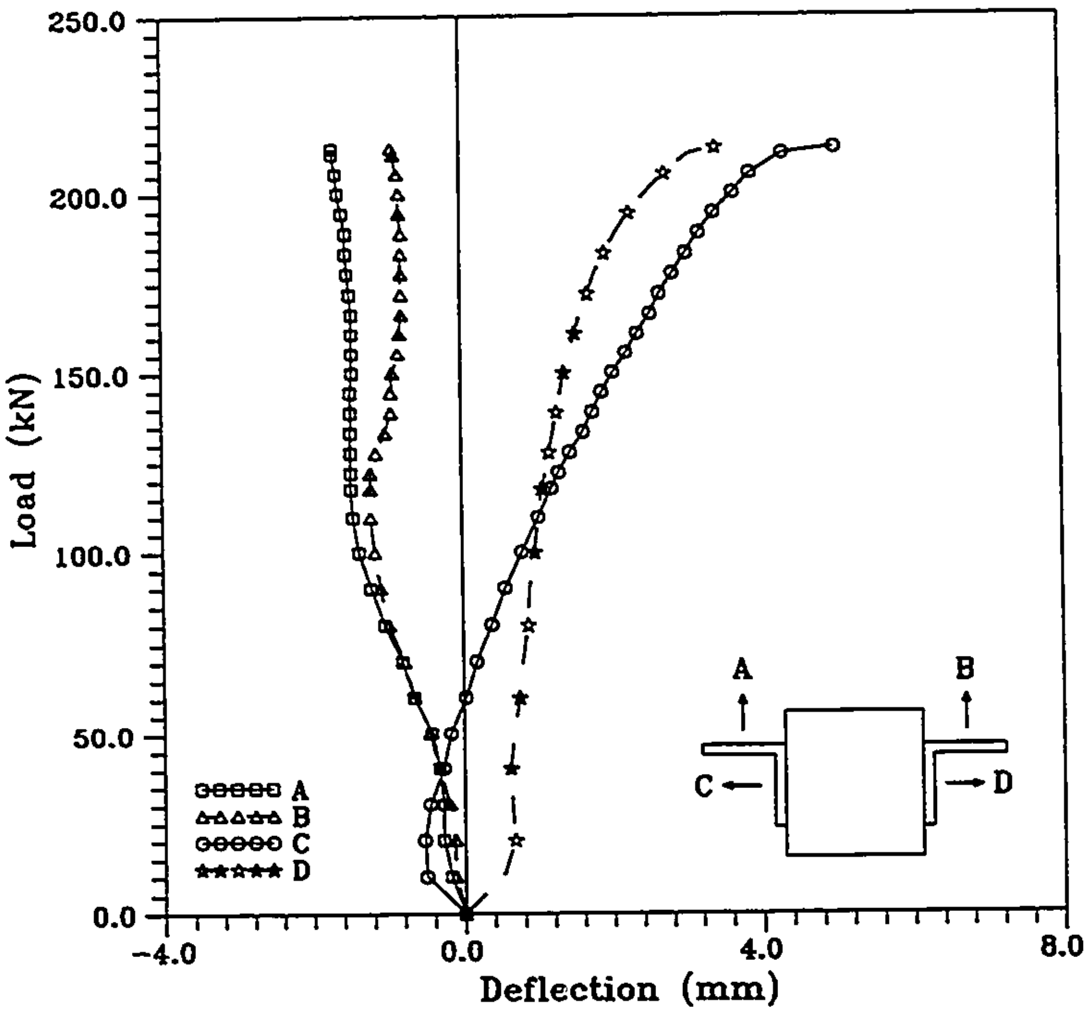

LOAD-DEFLECTION CURVES FOR SPECIMEN 3 - INTERMEDIATE LENGTH SPECIMENS BALANCED WELD

FIGURE A.12

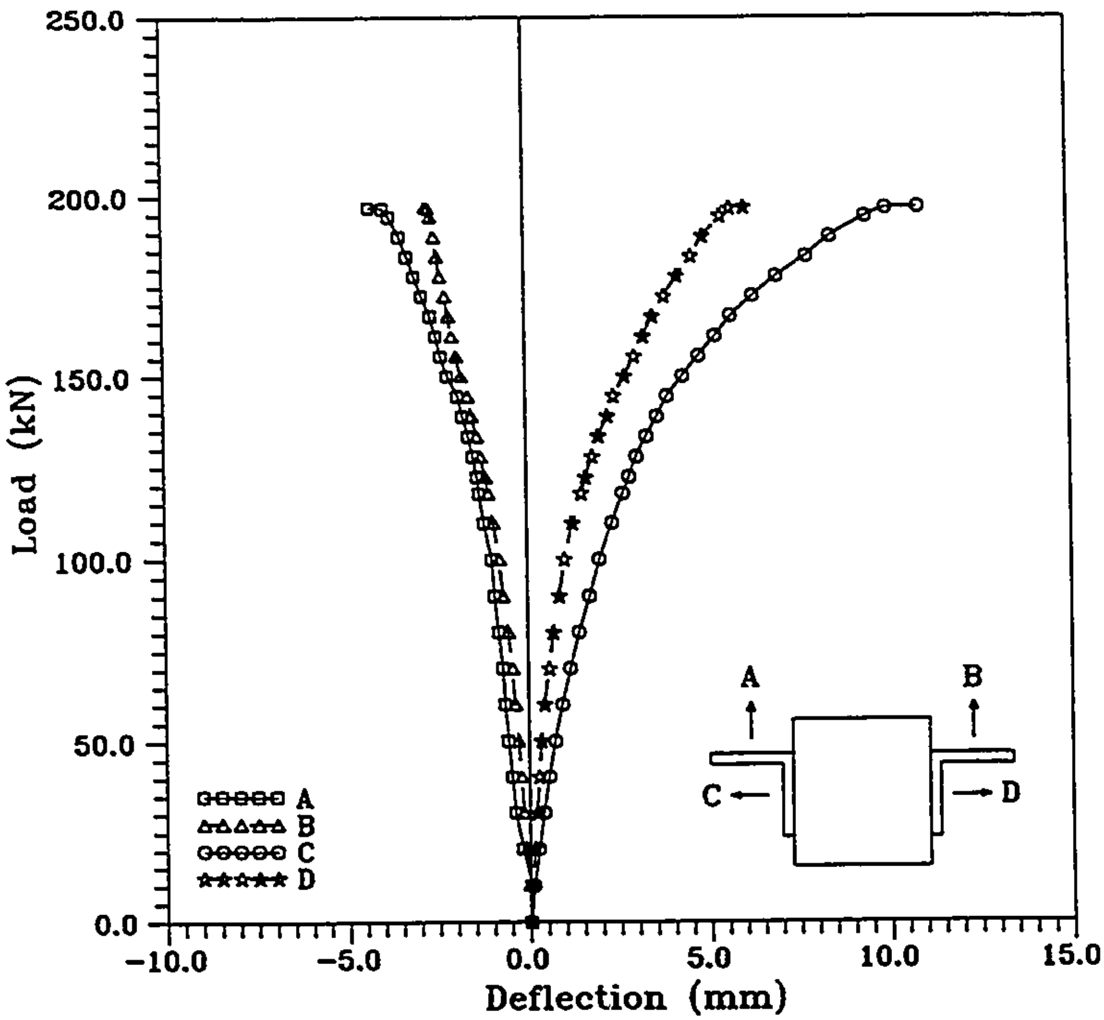

LOAD-DEFLECTION CURVES FOR SPECIMEN 4 - INTERMEDIATE LENGTH SPECIMENS EQUAL WELD

FIGURE A.13

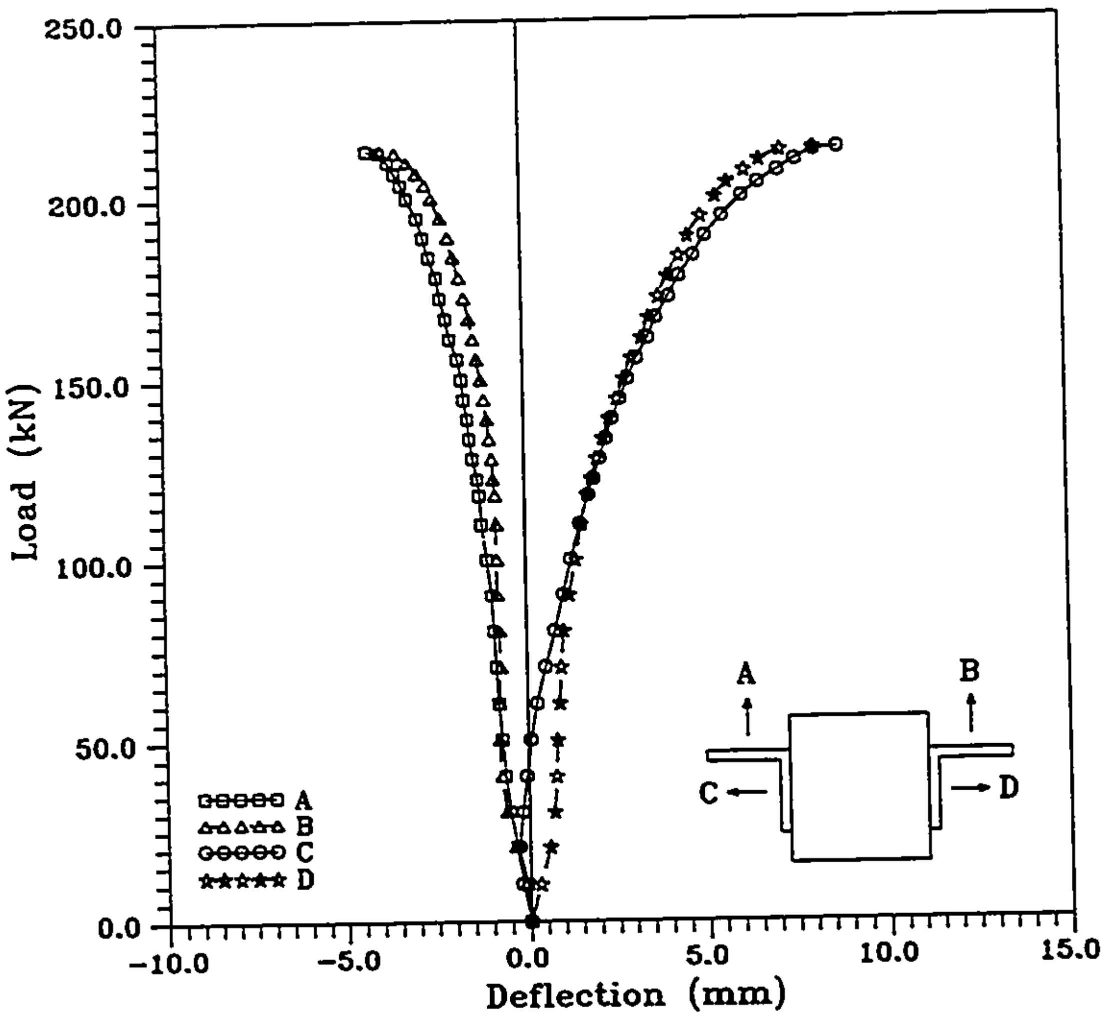

LOAD-DEFLECTION CURVES FOR
SPECIMEN 5 - INTERMEDUIATE LENGTH SPECIMENS
EQUAL WELD

FIGURE A.14

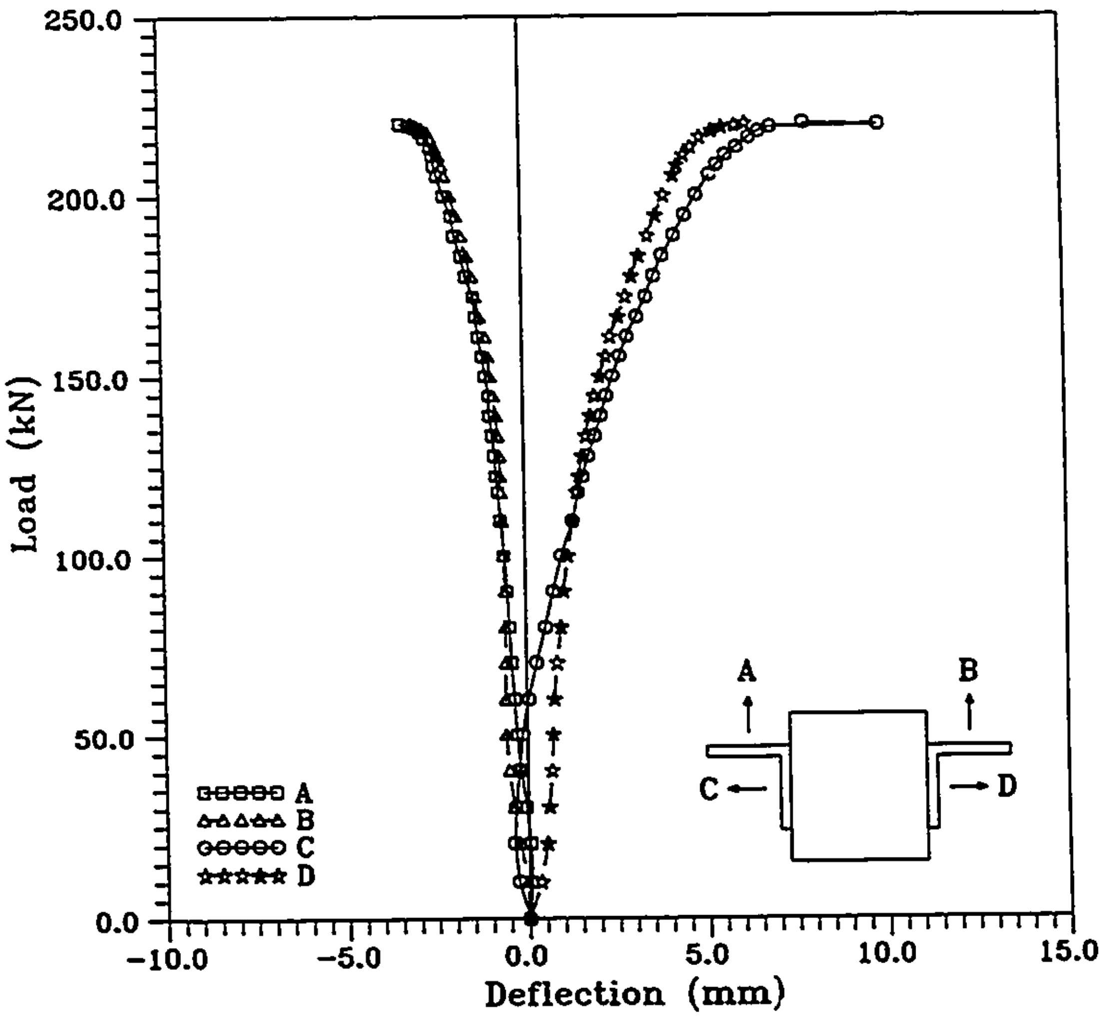

LOAD-DEFLECTION CURVES FOR SPECIMEN 6 - INTERMEDIATE LENGTH SPECIMENS EQUAL WELD

FIGURE A.15

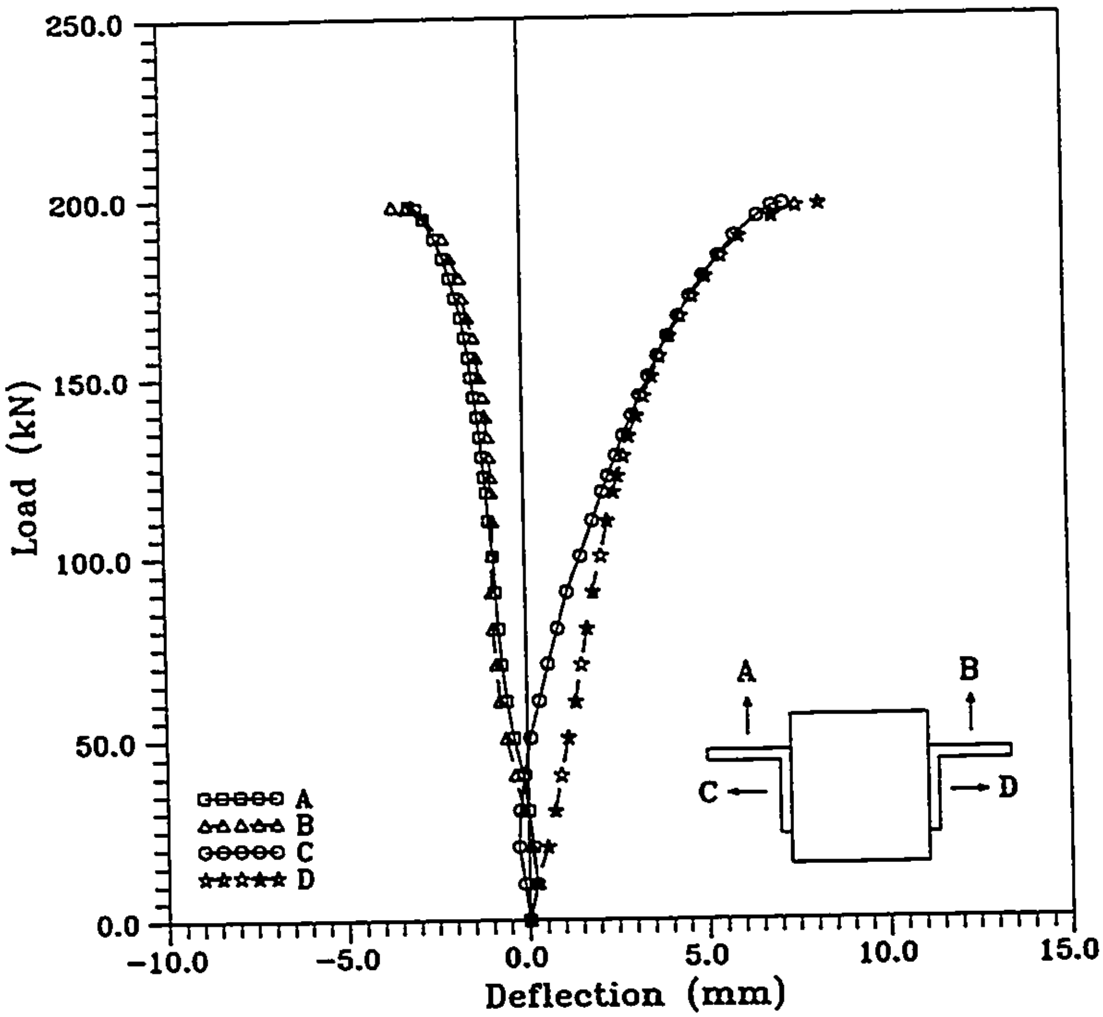

LOAD-DEFLECTION CURVES FOR SPECIMEN 7 - INTERMEDIATE LENGTH SPECIMENS UNBALANCED WELD

FIGURE A.16

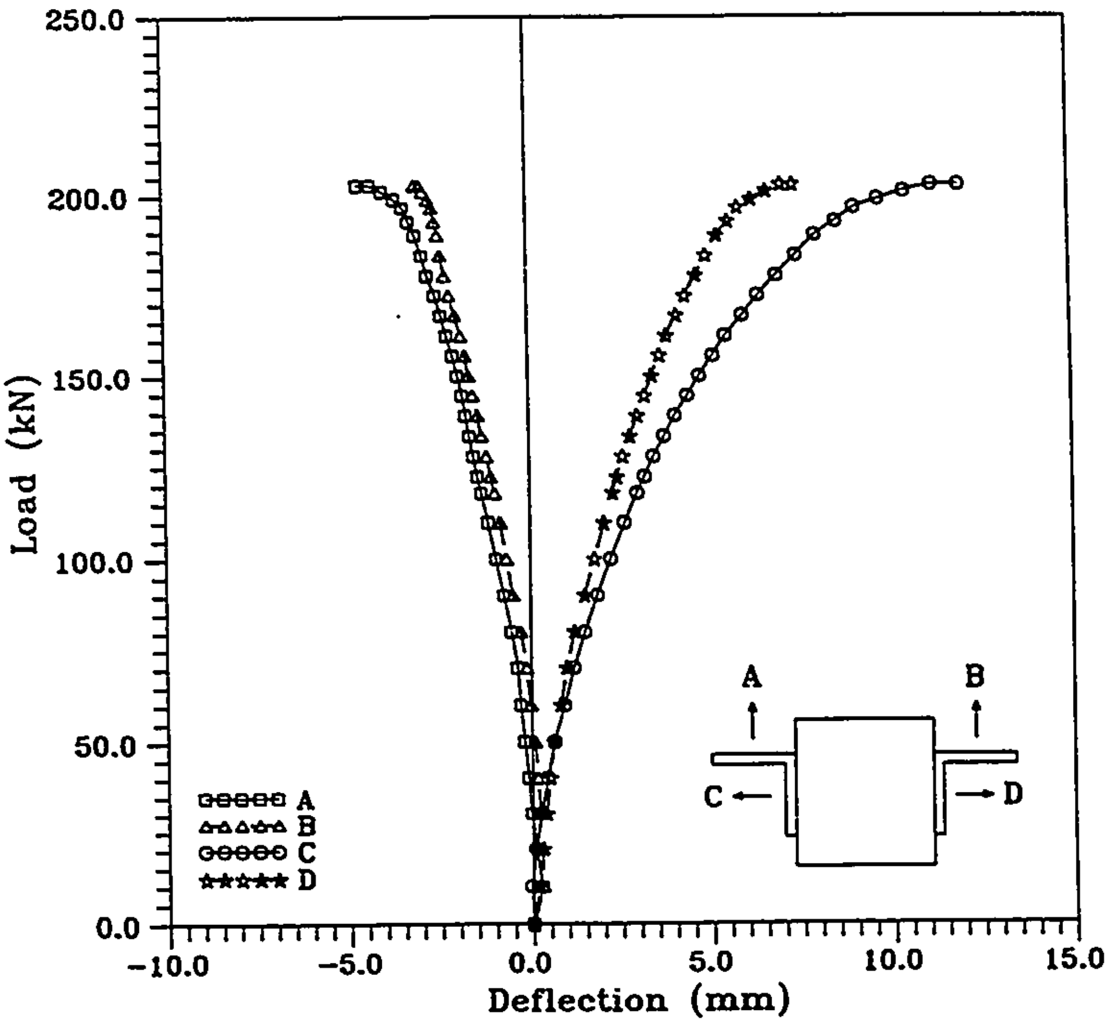

LOAD-DEFLECTION CURVES FOR SPECIMEN 8 - INTERMEDIATE LENGTH SPECIMENS UNBALANCED WELD

FIGURE A.17

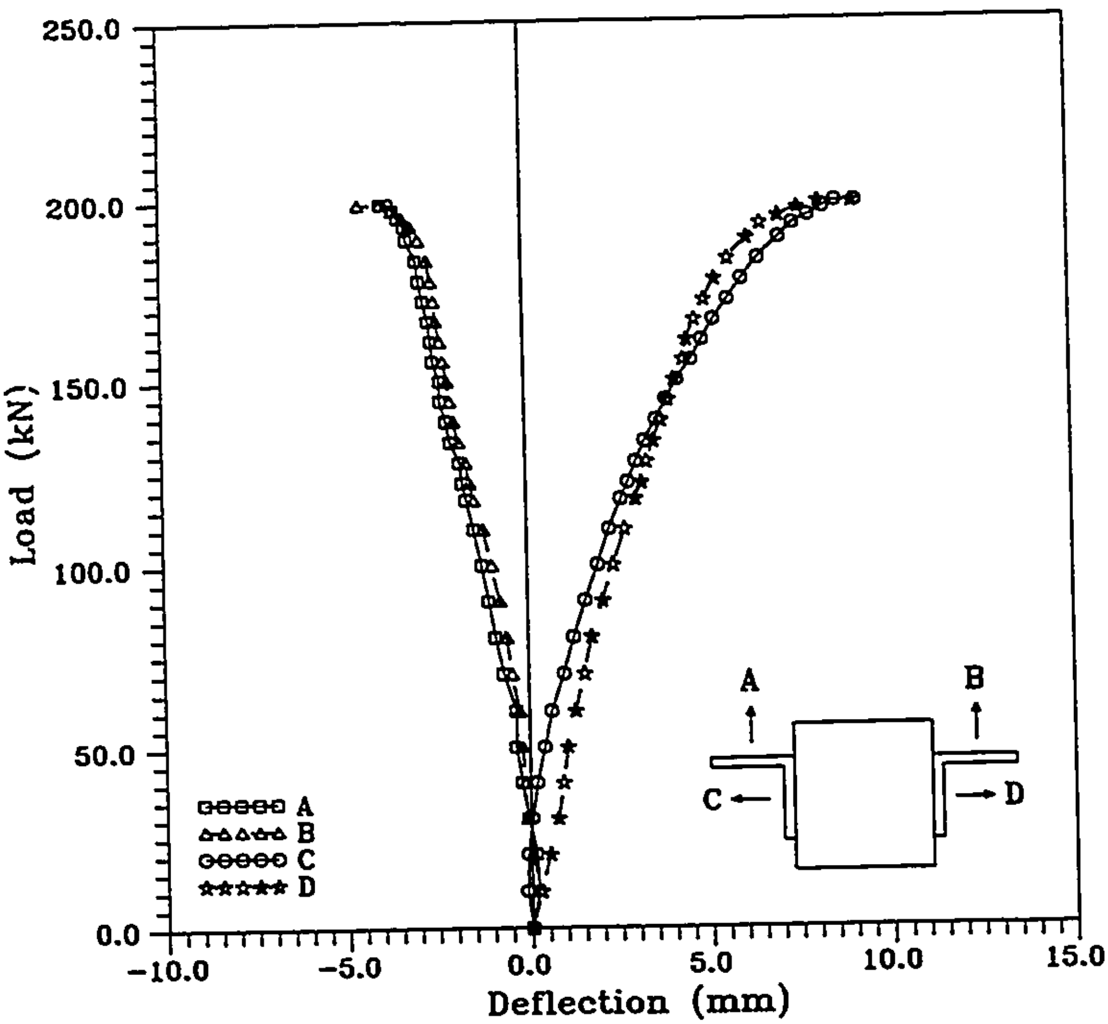

LOAD-DEFLECTION CURVES FOR
SPECIMEN 9 - INTERMEDIATE LENGTH SPECIMENS
UNBALANCED WELD

FIGURE A.18

Appendix B

BEAM-COLUMN ANALYSIS

Beam-Column Analysis

In this appendix, the ultimate compressive resistances of the tested angles are calculated according to CAN/CSA-S16.1-M89, Clause 13.8. The change of the weld pattern from balanced to unbalanced weld condition is modelled as an eccentricity in the applied load. Both short and long columns are analyzed in this appendix.

1- Long Columns

Data:

The properties of the cross section of the angle are as follows:

$A = 612\ mm^2$, $b = 51\ mm$, $t = 6.3\ mm$

$I_v = 60{,}346\ mm^4$, $r_v = 9.93\ mm$, $S_v = 2826\ mm^3$

$I_u = 233{,}654\ mm^4$, $r_u = 15.54\ mm$, $S_u = 6479\ mm^3$

$F_y = 367\ MPa$

From Figure 4.5, it can be seen that

$e_u = 8.43\ mm$, $e_v = 8.43\ mm$ (balanced weld)

$e_u = 15.79\ mm$, $e_v = 1.08\ mm$ (equal weld)

$e_u = 23.07\ mm$, $e_v = 6.27\ mm$ (unbalanced weld)

where: $e_u = (e_x + e_y) \cos 45$

$$e_v = (e_x - e_y) \cos 45$$

The eccentric load can be replaced by a concentric load and two end moments as follows:

$$M_{fu} = P.\ e_u \quad \text{and} \quad M_{fv} = P.\ e_v$$

Where:

C_f, M_{fu}, M_{fv} = the factored axial compressive resistance and moment resistances which are defined in Clause 13.8.

In these calculations, ϕ (the resistance factor), will be taken equal to 1.0 because the ultimate load is required from the equations.

Solution:

To determine the ultimate bearing capacities of the beam-column angle, three conditions have to be satisfied.

a) Local Buckling Requirement

The class of the angle has to be determined before taking any step in the calculations. From Table (1) of CSA-S16.1-M89 :

$$\frac{b}{t} = 8 < \frac{200}{\sqrt{200}} = 10.4$$

The angles used in this research can be classified as Class 3 section which means that the local buckling will not occur at stresses up to and including yield stresses.

b) Cross Sectional Strength Requirement

The cross-sectional strength of the beam-column angle cannot be exceeded. Assuming the beam-column to fail by yielding in the extreme fibres of the cross section. From Clause 13.8.1.(a)

$$\frac{C_f}{C_r} + \frac{M_{fu}}{M_{ru}} + \frac{M_{fv}}{M_{rv}} \leq 1.0 \tag{B-1}$$

in which:

$C_r = \phi\ A\ F_y = (1.0)(612)(367) = 244.6$ kN.

$M_{ru} = \phi\ S_u\ F_y = (1.0)(6476)(367) = 2377$ kN.mm

$M_{rv} = \phi\ S_v\ F_y = (1.0)(2826)(367) = 1037$ kN.mm

C_f can be calculated from (B-1) as follows:

$$\frac{C_f}{244.6} + \frac{C_f\ e_u}{2377} + \frac{C_f\ e_v}{1037} = 1.0$$

from which we obtain:

$C_f = 63.4$ kN (balanced weld)

$C_f = 85.0$ kN (equal weld)

$C_f = 50.4$ kN (unbalanced weld) (B-2)

c) Overall Member Strength Requirement

The overall strength of a member depends on its slenderness. This section checks the overall member failure caused by excessive stresses due to the second-order effects from moment amplifications. From Clause 13.8.1.(b) :

$$\frac{C_f}{C_r} + \frac{\omega_u \, M_{fu}}{M_{ru}\,(1-\frac{C_f}{C_{eu}})} + \frac{\omega_v \, M_{fv}}{M_{rv}\,(1-\frac{C_f}{C_{ev}})} \leq 1.0 \qquad \text{(B-3)}$$

$w_u = w_v$ = 1.0 (equal end moments causing single curvature in the member)

C_{eu}, C_{ev} = Euler's load about u and v axes, respectively.

C_r = as defined in Clause 13.3.1.(d)

M_{ru}, M_{rv} = as defined in Clause 13.5.(b)

C_r = 31 kN

C_{eu} = 127.76 kN, C_{ev} = 33 kN

M_{ru} = 2.377 kN.m, M_{rv} = 1.037 kN.m

Hence equation (B-3) becomes:

$$\frac{C_f}{31} + \frac{e_u \, C_f}{2377\,(1-\frac{C_f}{127.76})} + \frac{e_v \, C_f}{1037\,(1-\frac{C_f}{33})} = 1.0$$

After solving the above equation :

C_f = 18.3 kN (balanced weld)

C_f = 22.9 kN (equal weld)

C_f = 17.7 kN (unbalanced weld) (B-4)

Comparing (B-2) and (B-4), it can be seen that (B-4) will govern the analysis. Thus, the ultimate load carrying capacity of the angle under the three weld patterns are 18.3 kN, 22.9 kN and 17.7 kN respectively.

2- Short Columns

a) Local Buckling and Cross-Sectional Strength are the same as long columns because they are independent of the angle length.

b) Overall Member Strength Requirement

C_r = 89.3 kN, C_{eu}= 461.2 kN, C_{ev}= 119.1 kN

Equation (B-3) becomes

$$\frac{C_f}{89.3} + \frac{e_u\, C_f}{2377\ (1-\frac{C_f}{461.2})} + \frac{e_v\, C_f}{1037\ (1-\frac{C_f}{119.1})} = 1.0$$

After solving the above equation :

C_f = 37.2 kN (balanced weld)

C_f = 50.0 kN (equal weld)

C_f = 33.2 kN (unbalanced weld) (B-5)

Appendix C

ABAQUS INPUT

TYPICAL FINITE ELEMENT INPUT
FOR LONG SPECIMENS

```
*HEADING
ANGLE 51 X 51 X 6.35 X 1900 mm.
** S8R SHELL ELEMENTS, ASPECT RATIO 2.5:1, MESH 16 X 1 ELEMENTS
** WITH DOUBLE HINGES AT THE WELDED LEG
** BALANCED WELD
*NODE
**************************** LEVEL 1
6000,79.,0.,0.
5000,79.,48.,0.
4000,127.,48.,0.
**************************** LEVEL 2
6032,79.95,-0.95,475.
5032,79.95,47.05,475.
4032,127.95,47.05,475.
**************************** LEVEL 3
6064,80.34,-1.34,950.
5064,80.34,46.66,950.
4064,128.34,46.66,950.
**************************** LEVEL 4
6096,79.95,-0.95,1425.
5096,79.95,47.05,1425.
4096,127.95,47.05,1425.
**************************** LEVEL 5
6128,79.,0.,1900.
5128,79.,48.,1900.
4128,127.,48.,1900.
************************** END OF NODE COORDINATES
*NGEN, NSET=R1-UP
4128,5128,500
*NGEN, NSET=R1-1/4
4032,5032,500
*NGEN, NSET=R1-1/2
4064,5064,500
```

```
*NGEN, NSET=R1-3/4
4096,5096,500
*NGEN, NSET=R1-LOW
4000,5000,500
*NFILL, NSET=R1-1
R1-LOW,R1-1/4,8,4
*NFILL, NSET=R1-2
R1-1/4,R1-1/2,8,4
*NFILL, NSET=R1-3
R1-1/2,R1-3/4,8,4
*NFILL, NSET=R1-4
R1-3/4,R1-UP,8,4
********************* END OF CREATING R1 LEG NODES
*NGEN, NSET=R2-UP
5128,6128,500
*NGEN, NSET=R2-1/4
5032,6032,500
*NGEN, NSET=R2-1/2
5064,6064,500
*NGEN, NSET=R2-3/4
5096,6096,500
*NGEN, NSET=R2-LOW
5000,6000,500
*NFILL, NSET=R2-1
R2-LOW,R2-1/4,8,4
*NFILL, NSET=R2-2
R2-1/4,R2-1/2,8,4
*NFILL, NSET=R2-3
R2-1/2,R2-3/4,8,4
*NFILL, NSET=R1-4
R2-3/4,R2-UP,8,4
*NSET, NSET=MID-R
4064,4564,5064,5564,6064
********************* END OF CREATING R2 LEG NODES
*ELEMENT , TYPE =S8R
5000,5000,4000,4008,5008,4500,4004,4508,5004
6000,6000,5000,5008,6008,5500,5004,5508,6004
*ELGEN, ELSET=R1
5000,16,8,8
** END OF CREATING R1 LEG ELEMENTS
*ELGEN, ELSET=R2
6000,16,8,8
*ELSET, ELSET=MID-R
```

```
5064,6064
** END OF CREATING R2 LEG ELEMENTS
**********************************
*SHELL SECTION  , MATERIAL = ST
6.35
*MATERIAL , NAME=ST
*ELASTIC
196.E3 ,.3
*PLASTIC
366.
*BOUNDARY
5128,1,2
6128,1,2
5000,1,3
6000,1,3
************************************ END OF BOUNDARY CONDITIONS
*STEP, NLGEOM, INC=50, CYCLES=15, SUBMAX
*STATIC, PTOL=100., MTOL=5000.
0.1,1.0,,0.8
*CLOAD
**BALANCED
5128,3,-45000.
6128,3,-15000.
****EQUAL
**5128,3,-30000.
**6128,3,-30000.
****UNBALANCED
**5128,3,-15000.
**6128,3,-45000.
************************************ END OF LOAD INPUT
*NODE PRINT, NSET=MID-R, FREQ=1
U1,U2,U3
*ELPRINT, ELSET=MID-R, FREQ=5, POSITION = AVERAGED AT NODES
S
*PLOT, FREQ=2
*VIEWPOINT , DEFINITION= MODEL AXIS ROTATION
90.,0.,0.
*DISPLACED
U
*END STEP
```

TYPICAL FINITE ELEMENT INPUT
FOR SHORT SPECIMENS
MODEL 1

```
*HEADING
ANGLE 51 X 51 X 6.35 X 1000 mm.
** S8R SHELL ELEMENTS, ASPECT RATIO 2.5:1, BALANCED WELD
** THIS MODEL IS SHOWN IN FIGURE 4.4
** WITH DOUBLE HINGES AT THE WELDED LEG
** END ELEMENTS ARE ASSUMED TO BE FULLY ELASTIC
** LOADS ARE CONCENTRATED AT THE UPPER NODES ONLY
*NODE
**************************** LEVEL 1 (BASE)
6000,79.,0.,0.
5000,79.,48.,0.
4000,127.,48.,0.
**************************** LEVEL 2
6008,79.02,-0.02,10.
5008,79.02,47.98,10.
4008,127.02,47.98,10.
**************************** LEVEL 3 (END OF 10 MM WELD)
6016,79.045,-0.045,20.
5016,79.045,47.955,20.
4016,127.045,47.955,20.
**************************** LEVEL 4
6024,79.086,-0.086,39.
5024,79.086,47.913,39.
4024,127.086,47.913,39.
**************************** LEVEL 5 (END OF 58 MM WELD)
6032,79.13,-0.87,58.
5032,79.13,47.87,58.
4032,127.13,47.87,58.
**************************** LEVEL 6
6040,79.2,-0.2,91.5
5040,79.2,47.2,91.5
4040,127.2,47.2,91.5
**************************** LEVEL 7 ( BOTTOM 1/8)
```

6048,79.27,-0.27,125.
5048,79.27,47.73,125.
4048,127.27,47.73,125.
*************************** LEVEL 8 (BOTTOM 1/4)
6064,79.5,-0.5,250.
5064,79.5,47.5,250.
4064,127.5,47.5,250.
*************************** LEVEL -- (MID HEIGHT)
6096,79.71,-0.71,500.
5096,79.71,47.29,500.
4096,127.71,47.29,500.
*************************** LEVEL 8 (TOP 1/4)
6128,79.5,-0.5,750.
5128,79.5,47.5,750.
4128,127.5,47.5,750.
*************************** LEVEL 7 (TOP 1/8)
6144,79.27,-0.27,875.
5144,79.27,47.73,875.
4144,127.27,47.73,875.
*************************** LEVEL 6
6152,79.2,-0.2,908.5
5152,79.2,47.2,908.5
4152,127.2,47.2,908.5
*************************** LEVEL 5 (END OF 58 MM WELD)
6160,79.13,-0.13,942.
5160,79.13,47.87,942.
4160,127.13,47.87,942.
*************************** LEVEL 4
6168,79.086,-0.086,961.
5168,79.086,47.913,961.
4168,127.086,47.913,961.
*************************** LEVEL 3 (END OF 10 MM WELD)
6176,79.045,-0.045,980.
5176,79.045,47.955,980.
4176,127.045,47.955,980.
*************************** LEVEL 2
6184,79.02,-0.02,990.
5184,79.02,47.98,990.
4184,127.02,47.98,990.
*************************** LEVEL 1 (TOP)
6192,79.,0.,1000.
5192,79.,48.,1000.
4192,127.,48.,1000.

```
************************* END OF NODE COORDINATES
*NSET, NSET=U4
4144,4152,4160,4168,4176,4184,4192
*NSET, NSET=U5
5144,5152,5160,5168,5176,5184,5192
*NSET, NSET=U6
6144,6152,6160,6168,6176,6184,6192
*NSET, NSET=L4
4000,4008,4016,4024,4032,4040,4048
*NSET, NSET=L5
5000,5008,5016,5024,5032,5040,5048
*NSET, NSET=L6
6000,6008,6016,6024,6032,6040,6048
*NFILL, NSET=NL
L4,L5,4,250
*NFILL, NSET=NU
U4,U5,4,250
*NFILL, NSET=WL
L5,L6,4,250
*NFILL, NSET=WU
U5,U6,4,250
*********************** NON WELDED LEG
*NGEN, NSET=N-1/8
4048,5048,500
*NGEN, NSET=N-1/4
4064,5064,500
*NGEN, NSET=N-1/2
4096,5096,500
*NGEN, NSET=N-3/4
4128,5128,500
*NGEN, NSET=N-7/8
4144,5144,500
*NFILL, NSET =N1
N-1/8,N-1/4,2,8
*NFILL, NSET =N2
N-1/4,N-1/2,4,8
*NFILL, NSET =N3
N-1/2,N-3/4,4,8
*NFILL, NSET =N4
N-3/4,N-7/8,2,8
************************** WELDED LEG
*NGEN, NSET=W-1/8
5048,6048,500
```

```
*NGEN, NSET=W-1/4
5064,6064,500
*NGEN, NSET=W-1/2
5096,6096,500
*NGEN, NSET=W-3/4
5128,6128,500
*NGEN, NSET=W-7/8
5144,6144,500
*NFILL, NSET =W1
W-1/8,W-1/4,2,8
*NFILL, NSET =W2
W-1/4,W-1/2,4,8
*NFILL, NSET =W3
W-1/2,W-3/4,4,8
*NFILL, NSET =W4
W-3/4,W-7/8,2,8
*NSET, NSET=MID-R
4096,4596,5096,5596,6096
*NSET, NSET=LBOUND
5000,6000
*NSET, NSET=UBOUND
5192,6192
******************** END OF CREATING R2 LEG NODES
*ELEMENT , TYPE =S8R
5032,5032,4032,4048,5048,4532,4040,4548,5040
5000,5000,4000,4016,5016,4500,4008,4516,5008
5160,5160,4160,4176,5176,4660,4168,4676,5168
6032,6032,5032,5048,6048,5532,5040,5548,6040
*ELGEN, ELSET=LM
5000,2,16,16,2,1000,1000
*ELGEN, ELSET=UM
5160,2,16,16,2,1000,1000
*ELGEN, ELSET=R1
5032,8,16,16
********************** END OF CREATING R1 LEG ELEMENTS
*ELGEN, ELSET=R2
6032,8,16,16
*ELSET, ELSET=ENDS
LM,UM
*ELSET, ELSET=BODY
R1,R2
*ELSET, ELSET=MID-R
5096,6096
```

```
*** END OF CREATING R2 LEG ELEMENTS
****************************************
*SHELL SECTION , MATERIAL = ST, ELSET= BODY
6.35
*MATERIAL , NAME=ST
*ELASTIC
196.E3 ,.3
*PLASTIC
366.
****************************************
*SHELL SECTION , MATERIAL = ST1, ELSET= ENDS
6.35
*MATERIAL , NAME=ST1
*ELASTIC
196.E3 ,.3
****************************************
*BOUNDARY
UBOUND,1,2
LBOUND,1,3
************************************* END BOUNDARY
*STEP, NLGEOM, INC=50, CYCLES=15, SUBMAX
*STATIC, PTOL=400., MTOL=15000.
0.1,1.0,,,0.8
*CLOAD
5192,3,-237825.
5692,3,-85720.
6192,3,-76465.
*NODE PRINT, NSET=MID-R, FREQ=1
U1,U2,U3
*NODE PRINT, NSET=UBOUND, FREQ=1
U1,U2,U3
RF
*NODE PRINT, NSET=LBOUND, FREQ=1
U1,U2,U3
RF
*ELPRINT, ELSET=MID-R, FREQ=5, POSITION = AVERAGED AT NODES
S
*PLOT, FREQ=2
*VIEWPOINT , DEFINITION= MODEL AXIS ROTATION
90.,0.,0.
*DISPLACED
U
*END STEP
```

TYPICAL FINITE ELEMENT INPUT
FOR SHORT SPECIMENS
MODEL 2

```
*HEADING
ANGLE 51 X 51 X 6.35 X 1000 mm.
** S8R SHELL ELEMENTS, ASPECT RATIO 2.5:1, BALANCED WELD
** THIS MODEL IS SHOWN IN FIGURE 4.2
** HINGED AT THE WELD POINTS OF THE WELDED LEG ** END ELEMENTS
ARE ASSUMED TO BE FULLY ELASTIC
** LOADS ARE CONCENTRATED AT THE UPPER NODES ONLY
*NODE
**************************** LEVEL 1 (BASE)
6000,79.,0.,0.
5000,79.,48.,0.
4000,127.,48.,0.
**************************** LEVEL 2
6008,79.02,-0.02,10.
5008,79.02,47.98,10.
4008,127.02,47.98,10.
**************************** LEVEL 3  (END OF 10 MM WELD)
6016,79.045,-0.045,20.
5016,79.045,47.955,20.
4016,127.045,47.955,20.
**************************** LEVEL 4
6024,79.086,-0.086,39.
5024,79.086,47.913,39.
4024,127.086,47.913,39.
**************************** LEVEL 5 (END OF 58 MM WELD)
6032,79.13,-0.87,58.
5032,79.13,47.87,58.
4032,127.13,47.87,58.
**************************** LEVEL 6
6040,79.2,-0.2,91.5
5040,79.2,47.2,91.5
4040,127.2,47.2,91.5
**************************** LEVEL 7   ( BOTTOM 1/8)
6048,79.27,-0.27.125.
```

```
5048,79.27,47.73,125.
4048,127.27,47.73,125.
**************************** LEVEL 8   (BOTTOM 1/4)
6064,79.5,-0.5,250.
5064,79.5,47.5,250.
4064,127.5,47.5,250.
**************************** LEVEL --  (MID HEIGHT)
6096,79.71,-0.71,500.
5096,79.71,47.29,500.
4096,127.71,47.29,500.
**************************** LEVEL 8 (TOP 1/4)
6128,79.5,-0.5,750.
5128,79.5,47.5,750.
4128,127.5,47.5,750.
**************************** LEVEL 7  ( TOP 1/8)
6144,79.27,-0.27,875.
5144,79.27,47.73,875.
4144,127.27,47.73,875.
**************************** LEVEL 6
6152,79.2,-0.2,908.5
5152,79.2,47.2,908.5
4152,127.2,47.2,908.5
**************************** LEVEL 5 (END OF 58 MM WELD)
6160,79.13,-0.13,942.
5160,79.13,47.87,942.
4160,127.13,47.87,942.
**************************** LEVEL 4
6168,79.086,-0.086,961.
5168,79.086,47.913,961.
4168,127.086,47.913,961.
**************************** LEVEL 3  (END OF 10 MM WELD)
6176,79.045,-0.045,980.
5176,79.045,47.955,980.
4176,127.045,47.955,980.
**************************** LEVEL 2
6184,79.02,-0.02,990.
5184,79.02,47.98,990.
4184,127.02,47.98,990.
**************************** LEVEL 1  (TOP)
6192,79.,0.,1000.
5192,79.,48.,1000.
4192,127.,48.,1000.
************************* END OF NODE COORDINATES
```

```
*NSET, NSET=U4
4144,4152,4160,4168,4176,4184,4192
*NSET, NSET=U5
5144,5152,5160,5168,5176,5184,5192
*NSET, NSET=U6
6144,6152,6160,6168,6176,6184,6192
*NSET, NSET=L4
4000,4008,4016,4024,4032,4040,4048
*NSET, NSET=L5
5000,5008,5016,5024,5032,5040,5048
*NSET, NSET=L6
6000,6008,6016,6024,6032,6040,6048
*NFILL, NSET=NL
L4,L5,4,250
*NFILL, NSET=NU
U4,U5,4,250
*NFILL, NSET=WL
L5,L6,4,250
*NFILL, NSET=WU
U5,U6,4,250
*********************** NON WELDED LEG
*NGEN, NSET=N-1/8
4048,5048,500
*NGEN, NSET=N-1/4
4064,5064,500
*NGEN, NSET=N-1/2
4096,5096,500
*NGEN, NSET=N-3/4
4128,5128,500
*NGEN, NSET=N-7/8
4144,5144,500
*NFILL, NSET =N1
N-1/8,N-1/4,2,8
*NFILL, NSET =N2
N-1/4,N-1/2,4,8
*NFILL, NSET =N3
N-1/2,N-3/4,4,8
*NFILL, NSET =N4
N-3/4,N-7/8,2,8
************************** WELDED LEG
*NGEN, NSET=W-1/8
5048,6048,500
*NGEN, NSET=W-1/4
```

```
5064,6064,500
*NGEN, NSET=W-1/2
5096,6096,500
*NGEN, NSET=W-3/4
5128,6128,500
*NGEN, NSET=W-7/8
5144,6144,500
*NFILL, NSET =W1
W-1/8,W-1/4,2,8
*NFILL, NSET =W2
W-1/4,W-1/2,4,8
*NFILL, NSET =W3
W-1/2,W-3/4,4,8
*NFILL, NSET =W4
W-3/4,W-7/8,2,8
*NSET, NSET=MID-R
4096,4596,5096,5596,6096
*NSET, NSET=LBOUND
5032,5024,5016,5008,5000,5500,6000,6008
*NSET, NSET=UBOUND
5160,5168,5176,5184,5192,5692,6192,6184
******************** END OF CREATING R2 LEG NODES
*ELEMENT , TYPE =S8R
5032,5032,4032,4048,5048,4532,4040,4548,5040
5000,5000,4000,4016,5016,4500,4008,4516,5008
5160,5160,4160,4176,5176,4660,4168,4676,5168
6032,6032,5032,5048,6048,5532,5040,5548,6040
*ELGEN, ELSET=LM
5000,2,16,16,2,1000,1000
*ELGEN, ELSET=UM
5160,2,16,16,2,1000,1000
*ELGEN, ELSET=R1
5032,8,16,16
********************** END OF CREATING R1 LEG ELEMENTS
*ELGEN, ELSET=R2
6032,8,16,16
*ELSET, ELSET=ENDS
LM,UM
*ELSET, ELSET=BODY
R1,R2
*ELSET, ELSET=MID-R
5096,6096
*** END OF CREATING R2 LEG ELEMENTS
```

```
****************************************
*SHELL SECTION  , MATERIAL = ST, ELSET= BODY
6.35
*MATERIAL , NAME=ST
*ELASTIC
196.E3 ,.3
*PLASTIC
366.
****************************************
*SHELL SECTION  , MATERIAL = ST1, ELSET= ENDS
6.35
*MATERIAL , NAME=ST1
*ELASTIC
196.E3 ,.3
****************************************
*BOUNDARY
UBOUND,1,2
LBOUND,1,3
************************************** END BOUNDARY
*STEP, NLGEOM, INC=50, CYCLES=15, SUBMAX
*STATIC, PTOL=400., MTOL=15000.
0.1,1.0,,,0.8
*CLOAD
5192,3,-237825.
5692,3,-85720.
6192,3,-76465.
*NODE PRINT, NSET=MID-R, FREQ=1
U1,U2,U3
*NODE PRINT, NSET=UBOUND, FREQ=1
U1,U2,U3
RF
*NODE PRINT, NSET=LBOUND, FREQ=1
U1,U2,U3
RF
*ELPRINT, ELSET=MID-R, FREQ=5, POSITION = AVERAGED AT NODES
S
*PLOT, FREQ=2
*VIEWPOINT , DEFINITION= MODEL AXIS ROTATION
90.,0.,0.
*DISPLACED
U
*END STEP
```

REFERENCES

1- ABAQUS, VERSION 4-8, ***Vol. 1:Theory Manual, Vol. 2: Verification Manual, Vol. 3: User's Manual, Vol. 4: Example Problems Manual***, Hibbitt, Karlsson & Sorensen, Inc., 1989.

2- AMERICAN INSTITUTE OF STEEL CONSTRUCTION, ***Manual of Steel Construction, "Load and Resistance Factor Design"***, First Edition, Chicago, Illinois, 1986.

3- AMERICAN SOCIETY FOR TESTING AND MATERIALS, Section 3: ***"Metals Test Methods and Analytical Procedures"***, Vol. 03.01, Philadelphia, 1989, pp.131-161.

4- BLODGETT, O. W., ***"Design of Welded Structures"***, Fifth Edition, The James F. Lincoln Arc Welding Foundation, Ohio, USA, 1966.

5- BRITISH STANDARDS INSTITUTION, ***"Structural Use of Steelwork in Building"***, British Standard, BS 5950: Part 1: 1985.

6- CANADIAN INSTITUTE OF STEEL CONSTRUCTION, ***"Handbook of Steel Construction"***, Fourth Edition, CISC, Willowdale, Ontario, 1991.

7- CANADIAN STANDARDS ASSOCIATION, ***"Limit States Design of Steel Structures"***, CAN/CSA-S16.1-M89, Rexdale, Ontario.

8- CANADIAN STANDARDS ASSOCIATION, *"Welded Steel Construction (Metal Arc Welding)"*, CAN/CSA-W59-M1989, Rexdale, Ontario.

9- GIBSON, G. J. and WAKE, B. T., *"An Investigation of Welded Connections for Angle Tension Members"*, Welding Journal, January 1942.

10- Lipson, S. L. and Haque, M. I., *"Elast-Plastic Analysis of Single-Angle Bolted-Welded Connections Using the Finite Element Method"*, Computers & Structures, Vol. 9, 1978, pp. 533-545.

11- SHAN, L., *"Ultimate Strength of Angle Members or Subassemblies in steel Lattice Towers"*, Ph.D. Thesis, 1988, University of Wisconson-Madison.

BIBLIOGRAPHY

1- AMERICAN SOCIETY FOR METALS, ***Metals Handbook, "Properties and Selection: Irons and Steel"***, Vol. 1, Ninth Edition, Ohio, 1978, pp. 117-151.

2- Bergan, P. G., Horrigmoe, G., Krakeland, B. and Soreide, T. H., ***"Solution Techniques for Non-Linear Finite Element Problems"***, International Journal for Numerical Methods in Engineering, Vol. 12, 1978, pp. 1677-1696.

3- ELMAHDY, G., ***"The Buckling of Built-Up Compression Members in the Plane of the Connectors"***, M.A.Sc. Thesis, University of Windsor, Windsor, Ontario, 1991.

4- MADUGULA, M. K. S. and KENNEDY, J. B., ***"Single and Compound Angle Members : Structural Analysis and Design"***, Elsevier Applied Science Publishers Ltd., England, 1982.

5- McGUIRE, W., ***"Steel Structures"***, Prectice Hall, Inc., Englewood Cliffs, New Jersey, 1968.

6- NARAYANAN, R., ***"Axially Compressed structures : Stability and Strength"***, Applied Science Publishers Ltd., England, 1982.

7- Powell, G. and Simons, J., ***"Improved Iteration Strategy for Nonlinear Structures"***, International Journal for Numerical Methods in Engineering, Vol.

17, 1981, pp. 1455-1467.

8- SALMON, C. G. and JOHNSON, J. E., *"Steel Structures : Design and Behaviour"*, Secon Edition, Harper & Row Publishers, New York, 1980.

9- TAN, J. C., *"The Interconnection of Widely Spaced Angles"*, M.A.Sc. Thesis, University of Windsor, Windsor, Ontario, 1987.

10- YANG, T. Y., *"Finite Element Structural Analysis"*, Prentice Hall, 1986.

VITA AUCTORIS

1967	Born on November 20th in Assiout, Egypt
1984	Graduated from El-Malek El-Kamel High School, El-Mansourah, Egypt.
1989	Graduated from El-Mansourah University, El-Mansourah, Egypt, with the degree of Bachelor of Applied Science in Civil Engineering.
1990	Accepted into the Faculty of Graduate Studies and Research, University of Windsor, Windsor, Ontario, Canada, in a programme leading to the degree of Master of Applied Science in Civil Engineering.